1982

Behaviour of prestressed concrete-filled tubular column.

Mokkarala Venkata. Prakash
University of Windsor

BEHAVIOUR OF PRESTRESSED CONCRETE-FILLED TUBULAR COLUMN

by

© Mokkarala Venkata Prakash

A Thesis
Submitted to the Faculty of Graduate Studies
through the Department of
Civil Engineering in Partial Fulfillment
of the requirements for the Degree
of Master of Applied Science at
The University of Windsor

Windsor, Ontario, Canada
1981

ABSTRACT

Concrete-filled tubular columns represent a class of structures in which the best properties of steel and concrete are used to their maximum advantage. Filling the tube with concrete increases the load carrying capacity without increasing the size of the member. Prestressing these concrete-filled tubular columns further enhances their load carrying capacity and greater economies can be achieved.

In this investigation, the behaviour of prestressed concrete-filled tubular column was predicted throughout its loading range. A uniaxial stress-strain curve was used for the steel tube and the concrete. Effects of the confinement of a circular steel tube on concrete, if any, were neglected. The change of stress in an unbonded prestressed tendon was evaluated by numerically integrating the deflection curve. The deflection of the column was obtained by using a finite-difference method. A computer program was written to carry out the entire analysis. The deflection was checked with Newmark's integration method. The results of prestressed concrete-filled tubular columns were compared with similar nonprestressed members.

The experimental study was carried out using five prestressed concrete-filled tubular columns and one non-prestressed. The main variable was the amount of prestressing although in two columns including the nonprestressed column, the axial load was varied. The columns were tested up to the collapse load. The strains and deflections obtained from the tests are found to be in satisfactory agreement with the theoretically predicted results. The experimental moment-curvature relationship shows good agreement with the theoretical results. The comparison between nonprestressed and prestressed concrete-filled tubular column reveals an increase in the strength with the amount of prestress up to an optimum level of prestressing.

ACKNOWLEDGEMENTS

The author wishes to express his sincere gratitude to his advisor, Dr. M.C. Temple, for his guidance, suggestions and continuous encouragement throughout the preparation of this thesis.

The author would like to thank the structural engineering staff members for their valuable discussions. Thanks are due to Mr. F. Kiss and Mr. P. Feimer for their help in the experimental work. Thanks are also due to the Computer Center at the University of Windsor for running the computer programs.

The financial assistance given by the Natural Sciences and Engineering Research Council of Canada under Grant No. A7611 is greatly appreciated.

TABLE OF CONTENTS

LIST OF FIGURES

LIST OF TABLES

LIST OF APPENDICES

NOTATION

A_{si}, A_{ci} = areas of steel and concrete strips, respectively

D_i = distance from the centre of the tendon to centroid of the section

D = diameter of the column

d = diameter of the outer steel tube

E_s = Young's modulus of prestressing steel

EI = flexural stiffness of the column

e = eccentricity of load

F_i = net prestressed force

f = stress corresponding to moment M

f_s = average stress in the prestressing tendon

f_c = concrete stress corresponding to ε_c

f_c' = the 28 day compressive strength of concrete

f_c'' = 0.85 times f_c'

G_i = distance from the centre of the strip to centroid of the section

h = length of each segment

j = number of steel strips

k = number of concrete strips

kd = neutral axis depth from extreme compression fiber

L = length of the column

ℓ = number of prestressed tendons

M = bending moment at a section

M_{er} = external moment at the rth point

M_{io} = moment at the mid-height

P = external applied axial load

P_i = internal axial force

R_i = equivalent concentrated angle change

r = radius of gyration of the cross-section

r_s = radius of the steel tube

${}_{i-1}S_i$ = average slopes between node positions

t = thickness of the steel tube

u_i = deflection at ith station

x = distance along the length of the column

Y_o = distance of neutral axis from the centroid of the section at mid-height

y = deflection of the column

y_o = total deflection, $(y+e)$

y_p = distance of the tendon from the neutral axis

y_r = deflection along the column length

y_i' = linear correction to deflection

Greek letters:

$\delta\phi$ = increment of curvature

$\delta\varepsilon_4$ = increment of extreme compressive fibre

$\partial P/\partial\phi$ = rate of change of load with curvature

$\partial P/\partial\varepsilon_4$ = rate of change of load with ε_4

$\partial M/\partial\phi$ = rate of change of moment with curvature

$\partial M/\partial\varepsilon_4$ = rate of change of moment with ε_4

ε_c = strain of concrete at a particular section

ε_o = maximum concrete strain under which maximum stress occurs

ε_T = total strain change along the length of the column

$\bar{\varepsilon}_4$ = extreme compressive fibre strain corresponding to $\bar{\phi}$

μ_{conc} = Poisson's ratio of concrete

μ_{steel} = Poisson's ratio of steel

ρ_o = curvature at mid-height

σ_{si}, σ_{ci} = stresses of steel and concrete strips respectively

σ_{trans} = transverse stress

σ_{radial} = radial stress

σ_{conc} = augmented strength of concrete

σ_{sl} = longitudinal stress in steel

σ_{sh} = hoop stress in steel

σ_3 = radial stress in steel

$\bar{\phi}$ = curvature at any section

Chapter 1

INTRODUCTION

1.1 General

A circular hollow cross-section possesses many inherent advantages which make it attractive as a structural section. These include an aesthetically pleasing shape, the radii of gyration about orthogonal axes which are equal, thereby ensuring excellent compression strength for long slender columns, bracing and truss chords, a high torsional strength, etc. These have proven to be economical to be used in large aircraft hangars, auditoriums, heavy industrial buildings, offshore drilling rigs, etc. The main advantages of concrete-filled steel tubular sections are much higher strength than hollow section at little extra cost, high capacity columns with a minimum of space, increase in the speed of construction, etc. In many compression members, there is bending either due to load eccentricity, or due to transverse loads and each tends to produce tension in the concrete or to make the column unstable. Prestressing in the foregoing becomes a practical solution. It might also be justifiable on the basis of economy, construction advantages, transportation and erection stresses. Precast uniformly prestressed columns offer distinct advantages for multi-storey construction, the most important of which is saving in cost with these concrete-filled tubular columns.

The external axial-load carrying capacity of a column is clearly reduced by a uniform prestress, but for members also subject to large moment, the moment capacity may be increased by the application of uniform or eccentric pre-compression.

1.2 Objective

The primary objective of this investigation is to determine the behaviour of prestressed concrete-filled tubular columns throughout its loading range up to collapse. Prestressing of columns is beneficial particularly in the region where bending moments are large. One of the objectives of this study was to determine this region. Since this region varies with the amount of prestressing, this was chosen as main variable. Beyond a particular value of pre-stress, increase in prestress results in a reduction of load-carrying capacity. It was also the objective of this study to find out this optimum level of prestressing for a particular cross-section. Another objective of the study, although minor, was to determine the effect of axial load. As the axial load increases, the section is less cracked and thus confinement of concrete can occur by the steel tube, which, when combined with prestressing, may be advantageous. To establish an accurate analysis for prestressed concrete-filled tubular columns was another main objective of this study. The analysis for an unbonded post-tensioned system includes the determination of the change of stress in the tendon, which in turn depends on the cracked stiffness of the cross-section.

Finally, to check the validity of the above analytical procedures, several prestressed concrete-filled tubular columns were tested under similar conditions to what have been assumed in the analysis.

CHAPTER 2

LITERATURE SURVEY

2.1 General

Research work on prestressed concrete-filled tubular columns is non-existent. However, research data is available for concrete-filled tubular columns and prestressed concrete columns separately. The literature survey herein will give some insight into these topics.

2.2 Concrete-Filled Tubular Columns

In 1957, Kloppel and Goder (1) presented a table of allowable working stresses to predict the working loads of pipe columns for the two cases of mild steel and high strength steel pipe. An important conclusion by Kloppel was that the modulus of elasticity of tube with contained concrete can be determined with sufficient accuracy from the uniaxial stress condition. Kloppel also examined the effects of creep of concrete on the behaviour of pipe columns and found that "permanent loading caused at least no vital reduction in the carrying capacity."

In 1967, Gardner and Jacobson (2), tested concrete-filled steel tubes as axially loaded compression members. Both stub and long columns were tested and the experimental results were compared with theoretical results. Long column buckling loads were estimated by the tangent modulus method and for the stub columns confinement effects were considered with maximum shear stress theory. It was proved that a lateral restraint factor of 4.1 can be used for stub columns as suggested for spiral columns by Richart et al in 1928 (3).

In 1967, Furlong (4) reported on tests performed on round and square concrete-filled tubular columns subjected to different amounts of axial load and bending moments. The lower limit value for pure bending moment capacity was taken simply as the plastic moment capacity of the steel tube. An elliptical interaction equation was suggested as a lower bound estimate. In another paper, in 1968 (5), it was stated that there was no effect of bond between steel pipe and concrete. An equation for critical load of a long column was given. The tests conducted were of cold rolled and welded steel tubing which contain extensive residual stresses.

In 1968, Gardner (6) reported on an experimental investigation of spirally welded steel tubes filled with concrete and concluded that they behave in a similar manner as seamless pipe columns.

In 1969, Neogi et al (7) reported on an extensive theoretical and experimental investigation of concrete-filled tubular columns under concentric and eccentric loading. The elasto-plastic behaviour was studied numerically. The eccentrically loaded column was analysed, both by determining the exact deflected shape by finite difference method and by the cosine wave method. Good agreement was reported between the experimental and theoretical behaviour of the columns for L/D ratios greater than 15, (in which L = length of the column; D = Diameter of the column). It was also stated that for L/D ratios less than 15, triaxial effects give some gain in the strength for smaller eccentricities.

In 1969, Knowles and Park (8) predicted the buckling loads for long columns accurately by summing the tangent modulus loads for the steel tube and the concrete core acting as independent columns. A straight line interaction formula was fitted, approximately, which is unsafe for slender columns and conservative for short columns. In 1970 (9), the same authors presented a method for calculating the limits of slenderness ratio which determines whether an increase in concrete strength due to triaxial confinement is likely. An equation was derived to determine the ultimate load of axially loaded concrete-filled column.

In 1970, Gardner (10) presented a design method for concrete-filled tubular column by using non-dimensional ultimate axial load-moment-length interaction curves. It was also suggested that the ultimate axial short column load, taken from the interaction curves should be multiplied by the square root of the ratio between the short column load and the long column load at the same eccentricity.

In 1973, Chen and Rentschler (11) developed a simplified method for calculating the ultimate strength of concrete-filled tubular columns without using computer facilities and can be divided into two distinct computations. The first one deals with cross-section properties and the second one is concerned with particular beam-column loading condition, end condition and the length. It has also been shown that the moment-magnification factor given by ACI is a very acceptable and safe method of obtaining the maximum beam-column moment given the end moment. In 1973, Chen, in another paper (12) presented a theoretical investigation of the elastic-plastic behaviour of pin-ended, concrete-filled steel tubular columns loaded either symmetrically or unsymmetrically about either of the axes by a column-curvature method. Three types of concrete stress-strain relationships involving uniaxial and triaxial states of stress have been used to obtain interaction curves relating the axial force, end moment and the slenderness ratio.

In 1973, Tomii, Matsui, Sakino (13) reported on the behaviour of concrete-filled tubular columns subjected to combined stresses of axial load, bending moment and shear force. Studies of panel zones of connections and types of connections were discussed.

In 1973, Yamada (14) concluded that this structural member has an extraordinary large ductility and suggested that this is the most effective seismic structural member.

In 1976, Bridge (15) presented a theoretical and experimental investigation of the behaviour of pin-ended concrete-filled square steel tubes eccentrically loaded to bend about any required axis. The principal variables examined were eccentricity of loading, slenderness and inclination of the loading axis. The analysis is shown to accurately predict the observed results.

In 1977, Ghosh (16) reported two tests on long concrete-filled tubular columns of slenderness ratio as high as 129 and confirmed that although the Canadian Standard does not allow for the contribution of concrete to be considered in the design of concrete-filled tubular columns, concrete does increase the load and moment-carrying capacity.

In 1977, Tomii, Yoshimura and Moroshita (17) reported on 270 stub column tests under concentric axial load, to investigate the increase in strength and ductility due to confinement. They have also investigated the effects of shape and size of steel tube and mechanical properties of concrete.

In 1977, Huart (18) summarized the design procedures for the design of concrete-filled HSS columns. He gave guidelines for concrete filling and joints to transfer moments.

In 1978, Ramamurty and Srinivasan (19) reported tests on typical connections and suggested that the "beam-to-column" type of connection will not lead to proper exploitation of infilled tubular columns, particularly in the case of square and rectangular sections. It is stated that "flat slab-to-column" type of connection could be a preferable arrangement. It is also stated that service load and ultimate load behaviour are governed by different parameters and the former is not a mere scaled down version of the latter.

In 1980, Virdi and Dowling (20) reported tests on several concrete-filled tubular columns for establishing the strength of bond between the concrete core and the steel tube. Several parameters were investigated including concrete compressive strength, length-to-diameter ratio for the interface, tube diameter-to-thickness ratio, etc. The tests show the importance of imperfections in the manufacture of the tubes in contributing to the overall bond strength. A characteristic bond strength that may be used in design is recommended on the basis of these tests and the value has, in fact, been adopted by the joint ECCS-CEB-FIP-IABSE committee drafting the European code for composite construction.

In 1981, Brady, Cran and Keen (21) recommended guidelines for concrete-filled columns in which the length of HSS section to be filled should not exceed the smaller of 30 times the diameter or side of the member or 12 meters. They also stated that most of the connections used with concrete-filled HSS are very similar to those for standard HSS connections.

In 1981, Stelco Inc., (22) released a design manual for concrete-filled HSS columns which is a Canadian edition of CIDECT Monograph #5, in which concrete subjected to triaxial state of stress and steel to a biaxial state of stress have been used in arriving at the ultimate load of a concrete-filled HSS stub column. Design charts and design examples were presented for various sections.

2.3 Prestressed Concrete Columns

In 1953, Breckenridge (23) reported on a theoretical and experimental investigation of concentrically loaded prestressed columns. It was concluded that prestressing a slender column does not decrease the concentric load that will cause the column to buckle and the column will fail in compression if the prestressing stresses exceed the difference between the buckling stress and ultimate strength of the concrete.

Breckenridge's findings were disputed in 1956, when Ozell and Jernigan (24) published results of tests on 41 pretensioned columns. They found that prestress had a marked effect on the ultimate strength of axially loaded slender columns.

In 1957, Zia (25) attempted to explain the action of slender hinged-ended columns with axial prestress by applying the ultimate strength theory of reinforced concrete. He assumed, however, that the failure would be essentially a flexure failure and that it would be governed by a critical strain of the same magnitude as that found for failure in pure flexure. In fact, long concrete columns present a true instability phenomenon and can sustain loads in excess of those suggested by Zia.

In 1957, Lin and Itaya (26) presented an analysis of a prestressed concrete column subjected to axial load and bending.

In 1965, Brown (27) reported the results of 73 prestressed concrete columns, experimental and theoretical. A general theoretical inelastic analysis is developed to determine the ultimate load carrying capacity of pin-ended prestressed concrete columns under short-term loading, which includes the effects of slenderness, magnitude and position of prestressing tendons, and eccentricity of loading. A close agreement was obtained between theory and experiments.

In 1963, Hall (28) reported that prestressing produces a marked increase in load carrying capacity for eccentricities greater than 0.1D, where D is overall thickness of the column (in the direction of eccentricity). With fairly large eccentricities bending predominates and the maximum load is to a large extent independent of the amount of prestress. For large eccentricities, the failure is a bending failure and depends on the yield strength of the prestressing steel. The failure is usually called a material failure. No beneficial effect can be gained by a prestress less than $0.2f_c'$ where f_c' is the compressive strength of concrete. For an eccentricity of 0.25D the load carrying capacity was increased by 60% by prestressing.

In 1965, Itaya (29) summarized the knowledge to that date and presented a rational analysis and outlined an approach to the design of prestressed concrete columns.

In 1968, Aroni (30) reported the results of a theoretical investigation of the strength of slender, axially prestressed, eccentrically loaded columns. The effects of prestress, eccentricity, slenderness, concrete compressive strength, concrete tensile strength, initial curvature and the area of steel were presented and discussed. For small eccentricity, a maximum critical load was reached at a low prestress ratio. For medium eccentricity, a maximum critical load was observed in the region of medium prestress. For the largest eccentricity, the effect of prestress on critical load was very small. It was also concluded that for a particular value of prestress, the maximum critical load decreases sharply with increase in eccentricity.

In 1966, Zia and Moreadith (31) reported on some tests for columns with different prestressing levels. It was concluded that for columns with zero eccentricity heavy prestressing is detrimental to the load carrying capacity of the column, especially for short columns. Prestressed columns of low strength concrete and subjected to eccentric loads (e = 0.5D) showed considerable advantage when compared with conventional reinforced concrete columns ranging from short columns (L/D = 10) to slender columns (L/D = 70). The effect was most pronounced in the short columns.

In 1967, Zia and Guillermo (32) presented interaction curves for prestressed concrete columns for full prestressing and partial prestressing. Full prestressing reduces the ultimate strength of the column as compared to 50% partial prestressing and reduction in load carrying capacity is nearly constant regardless of applied bending moment. For columns subjected to large axial loads, a reduction of 50% prestressing produces a significant increase in the bending moment capacity of the column, where as for columns subjected to a small axial load, a reduction of 50% prestressing would cause a slight reduction in the bending capacity of the column.

In 1970, Anderson and Moustafa (33) published a computer program which was used to construct interaction diagram for prestressed concrete piles.

In 1972, Mikhailov (34) reported on a method of predicting the ultimate capacity of long slender prestressed concrete columns subject to an axial load with a small eccentricity. This method allows the selection of the most economical or most suitable shape from a variety of different shapes and prestress configurations. It shows that heavy prestressing is the best precaution against growing curvature and thereby against buckling.

In 1972, Nathan (35) considered the effects of slenderness on the load carrying capacity of prestressed concrete sections with irregular shapes, such as might be used in load-bearing walls, using a mathematical model embodying a minimum of simplification. The moment-rotation curves for the section were developed at various load levels. The column deflection curve was then deduced and magnification and instability effects were computed.

In 1972, Rawi (36) tested 17 circular prestressed concrete columns with L/r = 80, where L = length of the column and r = radius of gyration of the cross-section, under pure torsion, concentric load, bending moment and all combinations of such, and predicted the cracking load of an eccentrically loaded column closely by the usual elastic theory. The ultimate load was also predicted by taking into consideration, the effect of cracking of concrete on column deflections. The non-dimensional interaction curve of a prestressed concrete column under bending moment and an axial load resembles the interaction curve for the conventionally reinforced column, except that the prestressed diagram lacks a definite yield point which accounts for the absence of a definite balance point.

All the above-mentioned references consider bonded prestressed construction except Breckenridge, who tested unbonded post-tensioned axially loaded columns.

CHAPTER 3

THEORETICAL FORMULATION

3.1 General Behaviour

The aim of the analytical study was to develop computational procedures which would enable the load-deformation behaviour of prestressed concrete-filled steel tubes to be studied over the entire range of loading.

When a concrete-filled tubular column is subjected to an axial compressive load, all elements of the cross-section should undergo the same longitudinal strain. If the average strain on a section is known, the stress in the concrete and the steel could be established from the stress-strain characteristics. The longitudinal stress-strain characteristics of steel and concrete might be affected if any transverse confining pressure was exerted on the concrete by a steel encasement. The modulus of elasticity or stiffness of commercial grades of steel remains virtually constant until strains of 0.001 to 0.0012 are reached, but the stiffness of plain concrete (even concrete with some lateral confining pressure) tends to decrease for strains in excess of 0.001 for high strength concretes and 0.0005 for low strength concretes. The stiffness of unconfined concrete tends toward zero at strains near 0.0018 to 0.0020. Since the stiffness of steel does not tend to decrease as much as the stiffness of concrete when strains increase, the proportion of total load carried by steel increases as the strains increase (4).

In the absence of any transverse pressure exerted by steel on encased concrete, a lower limit to the capacity of steel-encased composite columns could be established as the force necessary to yield the steel plus the force on the concrete at the strain required to yield the steel. Any transverse confinement of steel on concrete would tend to increase the effective stress developed in the concrete before the steel yields longitudinally. Unless the longitudinal yield stress of steel exceeds 50 ksi (at a corresponding strain near 0.002), steel should yield longitudinally before the encased concrete begins to "soften" enough to reach a stress as high as f'_c. For steel with a yield strength higher than 60 ksi, encased concrete might be expected to begin to crush before the steel yield strength is developed.

Any transverse confinement of concrete provided by steel encasement should be more effective in round cross-sections than in sections with flat sides. The unit cost of steel tubing is considerably higher than the cost of concrete, and the material efficiency of composite columns tends to increase as the percentage of steel in a cross-section decreases. Lower limits to amount of steel in a cross-section are established by the possibility of local buckling of thin steel walls. For round tubes, concrete core forces the local buckling of steel into a post-yield mode of transverse outward ripples (4). By forcing the steel to buckle outward, the concrete stabilizes steel in the elastic range, thereby insuring the development of the longitudinal yield strength of round steel tubes. The plastic moment of the steel section alone is a lower limit to the pure bending capacity of steel encased beam-columns. If a very thin-walled tube is used with high strength concrete, the ultimate moment could be appreciably higher than the plastic moment of the steel alone.

At strains less than 0.001, Poisson's ratio of plain concrete is probably one-half to two-thirds that of steel, and the consequent differences in the rate of lateral expansion tends to separate the steel encasement from the concrete core. Apparently, at strains above 0.001, after microcracking of concrete begins, the effective Poisson's ratio of the concrete approaches that of steel. After the unconfined cylinder strength is attained, the concrete would tend to spall and disintegrate in the absence of a confining steel jacket. If the jacket buckles before strains large enough to develop f'_c are attained, the full strength of concrete cannot be utilized to maximum load.

Structural members under compression forces can fail in combination of three basic modes; crushing, general buckling, or local buckling. Short columns are columns which fail by crushing rather than general buckling.

For low strains the value of Poisson's ratio of concrete is in the range of 0.15 to 0.25, but for large strains, the value can rise to approximately 0.60. As concrete is not a linear material (or even elastic) its Poisson's ratio need not be less than 0.5. Even larger values of Poisson's ratio can be measured for triaxially loaded concrete (7).

In the initial stages of loading of concrete-filled tubes, Poisson's ratio for the concrete is lower than that for steel, and thus the steel does not restrain the concrete core. The initial circumferential steel hoop stresses are compressive and the lateral stresses are tensile (Fig. 1). The concrete will be under a lateral tension at this stage, provided the bond between the steel and concrete does not break down. As the load is increased the lateral deformations of the concrete catch up to those of the steel. For a further increase in load the tube restrains the concrete and hoop stress in the steel becomes tensile. At this stage, the steel tubing is subjected to an internal pressure (Fig. 2). Therefore,

$$\sigma_{trans.} = \sigma_{radial} \left(\frac{r_s}{t}\right) \tag{3.1.1}$$

where, $\sigma_{trans.}$ = transverse stress;

σ_{radial} = radial stress;

r_s = radius of the steel tube;

t = thickness of steel tube.

As the steel tube restrains the concrete at failure, then the longitudinal compressive strength of the concrete will be augmented and has been found to be (2):

$$\sigma_{conc.} = f_c' + k\,(\sigma_{radial}) \tag{3.1.2}$$

where, $k = 4$.

The increase in failure load due to triaxial confinement of concrete depends, among other factors, on the magnitude of the strain at failure load and consequently varies inversely with length and eccentricity. Short columns with relatively large eccentricity and all slender columns, fail before the strain at the concave side is sufficiently large for the increase in failure load to be appreciable. Moreover, the triaxial augmentation of strength of concrete on the convex side is either reduced or absent. It transpires therefore that for many practical columns it is unnecessary to take triaxial effects into account (7). To include triaxial effects is difficult because under eccentric loading, both the longitudinal and the hoop stress vary across the section. At present, there is no theory available for the inelastic deformation of concrete under three unequal principal stresses.

The behaviour of an axially loaded steel tube filled with concrete will vary according to the method in which the ends of the member are loaded. Essentially there are three different methods of applying the loading:

1) Load the steel but not the concrete - This may not increase the axial load capacity of the column above that of the steel tube alone, because the load on the tube causes it to increase in diameter (due to Poisson's effect) and to separate from the concrete when the adhesive bond between concrete and steel is exceeded. Thus the column fails at the maximum load which the steel tube alone can carry, but the concrete core may tend to delay the local buckling of steel and thus increase the bending resistance. The previous investigator's tests show that loading the

steel alone did not increase the failure load above that of a hollow tube;

2) Load the concrete but not the steel - This is the Lohr (37) column principle, with the steel acting as an encasement. Ideally this is the best method as the steel does not resist axial load but only provides a confining stress to the concrete as in a spirally reinforced concrete column. Steel used this way is approximately twice as effective as longitudinal steel at ultimate load. However, any bond between the steel and the concrete will cause some longitudinal strain (and hence axial load) in the steel. If the steel is axially stressed in compression as well as circumferentially stressed in tension, it will be in a state of biaxial state of stress which, as theories of failure show, will reduce the yield stress in the circumferential direction. This will lower the confining pressure on the concrete and thus reduce the maximum load even though there is some contribution from the longitudinal stress in the steel. Some bond is probable, expecially when the steel is exerting a high lateral pressure on the concrete, and therefore ideal behaviour seems unlikely. In fact, the previous investigations proved that loading the concrete alone did not increase the failure load to above that obtained from loading both the concrete and steel together;

3) Load the steel and the concrete so that the longitudinal strain is the same in both materials - This is the probable method which would be used in construction. To

be able to predict accurately the performance of such columns underload, the behaviour of concrete when subjected to compressive longitudinal stress and lateral pressure must be known.

If there is a breakage of bond, there is a possibility of overloading the concrete before any lateral pressure is exerted on the steel tube. When such a thing happens there is a possibility of the concrete column failing by buckling. However if, before the concrete core fails by column buckling, the longitudinal concrete strain exceeds the strain at which volume increase begins, the failure will be delayed.

Compared with hollow steel tubes, concrete-filled steel tubes will have a higher fire resistance and they need less fire-proof material around the steel tube, because concrete has a larger thermal capacity than the air which is enclosed in the hollow steel tube. Even if the sustained loads carried by steel tubes are decreased by the heat, the columns will not be crushed during the fire if the columns are designed so as to sustain the dead and live loads only by their concrete cores. So the structure will not suffer great damage.

The concrete core and steel shell do not act together until the load is considerably greater than half the ultimate load. Thus service load behaviour of these columns have to take into account the independent action of these two constituent materials. Thus service load behaviour is not just a scaled down version of ultimate load behaviour. Capacity interaction formula derived from methods applicable to reinforced concrete give a reasonable first approximation under eccentric loading.

The bond strength between steel tube and concrete is not affected to any measurable extent by factors such as contact length, tube size, tube thickness, and concrete strength. There is sufficient evidence (20) to indicate that the most important factor is the mechanical keying of the concrete core with the irregularities in the steel tube. This mechanical keying could, however, arise due to two different types of irregularities. The first type occurs due to the roughness of the steel surface. Before the concrete core as a whole can begin to move, it is this interlocking that must first be broken. For this reason, this type of interlocking may be thought to contribute mainly to ultimate bond strength. The rupture of this primary interlocking may then be related to the local crushing of concrete near the interface. This lends substance to the adoption of 0.0035 strain as the critical value for the definition of ultimate bond strength. The second type of bond resistance occurs due to manufacturing tolerances associated with the internal diameter of the tube. This type of interlocking contributes in essence to the frictional resistance associated with the latter. A value of 150 to 160 psi may be used for ultimate bond strength (20).

For normal prestressed concrete columns of central prestress which are subjected to eccentric loading before the load eccentricity equals half the section depth, the loss in ultimate axial load carrying capacity was offset by the additional flexural resistance developed in the concrete. For a loading eccentricity of greater than 3/7 of the column depth, the benefits from uniform prestressing were obtained without loss of its axial load carrying capacity (27).

Prestressing transforms a cracked section into an uncracked one, thus increasing its strength and stiffness. If the tube is in hoop tension, longitudinal prestressing may indirectly help the whole structure to be in a triaxial prestressed condition. The previous investigations show that triaxial prestressing will help to increase the load-carrying capacity of the member.

A prestressed concrete-filled tubular member may fail in a different mode of failure than a nonprestressed member because prestressing increases the strength of the column.

3.2 Theory

The calculation of the ultimate load carrying capacity of a column depends entirely upon an accurate knowledge of the stress-strain behaviour of the materials throughout the period of loading.

Assumptions made in the analysis:

(1) A plane cross-section remains plane after bending;

(2) Hognestad's parabola was used for concrete until it reached the peak and then constant f_c'' was assumed beyond ε_o (ε_o was taken as 0.0025); (Fig. 3);

(3) Complete interaction takes place between steel tube and

concrete core, i.e., there is no longitudinal or circumferential slip;

(4) Failure due to local buckling or shearing does not occur;

(5) Concrete takes no tension.

The exact stress-strain values obtained from tensile coupons for steel tube and the prestressing steel were used in the analysis. (Figs. 4 and 5)

The first assumption is usual in normal analysis. The second assumption is justified on the grounds that the concrete is laterally confined. This has been used by Stelco Inc., (22) for its design tables. The value of ε_o has been taken as 0.0025 after Barnard's (38) tests. The parabolic equation of Hognestad (39) is given as:

$$f_c = f_c'' \left[\frac{2\,\varepsilon_c}{\varepsilon_o} - \left(\frac{\varepsilon_c}{\varepsilon_o}\right)^2 \right], \quad \varepsilon_o < 0.0025 \qquad (3.2.1)$$

in which f_c' = ultimate compression strength of standard concrete cylinders;

f_c'' = $0.85\ f_c'$;

ε_c = strain at a particular section;

ε_o = the maximum strain at which f_c'' occurs;

f_c = concrete stress corresponding to ε_c.

There is a considerable variation in concrete strength down the height of the individual column, with the highest strength at the bottom of the column and lowest at the top. This is probably due to the water gain at the top during casting. That is why f_c'' was taken as 0.85 f_c'.

The differential equation governing the bent equilibrium configuration of an eccentrically loaded column is derived by equating the internal and external forces and moments in a deformed section. The external moment is equal to the applied load times the total deflection which includes the eccentricity. Equating the external and internal moments of a deformed column gives:

$$EI \frac{d^2y}{dx^2} + Py = 0 \qquad (3.2.2)$$

in which, EI = flexural stiffness of the column;

y = deflection of the column;

x = distance along the length of the column;

P = external axial load.

Since the flexural stiffness EI is not a constant, but a complicated function of load, deflection and distance along the length of the column, analytical integration of Eq. (3.2.2) is not possible, and numerical integration has to be used.

The linear strain distribution of a cross-section may be specified by the curvature ρ and the distance Y of the neutral axis from the centroidal axis. The internal axial force and moment can be calculated from the strain distribution by the following equations:

$$P_i = \int_A \sigma \, dA = \sum_{i=1}^{j} \sigma_{si} A_{si} + \sum_{i=1}^{k} \sigma_{ci} A_{ci} + \sum_{i=1}^{\ell} F_i$$

$$= f_1(\rho, Y) \qquad (3.2.3)$$

$$M_i = \int_A \sigma G_i dA = \sum_{i=1}^{j} \sigma_{si} G_i A_{si} + \sum_{i=1}^{k} \sigma_{ci} G_i A_{ci} + \sum_{i=1}^{\ell} F_i D_i$$

$$= f_2(\rho, Y) \qquad (3.2.4)$$

where, j = number of strips of steel;

k = number of strips of concrete;

ℓ = number of prestressed tendons;

σ_{si}, σ_{ci} = stresses of steel and concrete strip, respectively;

A_{si}, A_{ci} = areas of steel and concrete strip, respectively;

G_i = distance from the center of the strip to centroid of the section;

F_i = net prestressed force (tension has been taken as negative);

D_i = distance from the center of tendon to centroid of the section.

Using Eqs. (3.2.3) and (3.2.4) the bending moment and corresponding axial load for any given strain distribution can be evaluated.

When the prestressing tendon is unbonded, upon loading, the steel slips with respect to the concrete. Due to this slip the strain in the tendon will be different from that of the neighboring concrete. Any change of strain in the unbonded tendon will be distributed throughout its entire length. To compute the average strain for the cable, it is necessary to determine the total change in length of the tendon due to the moments in the column. This can be done by integrating the strain along its entire length neglecting friction along tendon.

If M is the moment at any section, the unit strain ε in the concrete at any point is given by:

$$\varepsilon = \frac{f}{E} = \frac{My_p}{EI} \qquad (3.2.5)$$

where, y_p = distance of the tendon from the neutral axis;

f = stress corresponding to moment M.

The total strain along the cable is then:

$$\varepsilon_T = \int_0^L \varepsilon \cdot dx = \int_0^L \frac{My_p}{EI}\, dx \qquad (3.2.6)$$

where, L = length of the column.

The average strain is:

$$\frac{\varepsilon_T}{L} = \int_0^L \frac{My_p}{LEI}\, dx \qquad (3.2.7)$$

The average stress is:

$$f_s = E_s\left(\frac{\varepsilon_T}{L}\right) = \int_0^L \frac{My_pE_s}{LEI}\, dx \qquad (3.2.8)$$

where, E_s = Young's modulus of prestressing steel.

In Eq. (3.2.8), M, EI, y vary along the column length, where y is the deflection along the column. To evaluate these three quantities the deflected shape must be determined first. The deflected shape, however varies with the applied load and hence a trial and error procedure will be used to solve Eqs. (3.2.3) and (3.2.4). The procedure can be summarised as follows:

Steps

(1) Choose an initial value for the curvature ρ at mid-height;

(2) Select a trial value of Kd, the neutral axis depth;

(3) Calculate the values of P and M_{io} corresponding to ρ_o, Kd;

(4) Find the values of M, EI, and y along the column length corresponding to P and M_{io} by an approximate method. In this case a part cosine wave approach was used:

$$y = y_o \cos\frac{\pi x}{L} \tag{3.2.9}$$

where, y = total deflection at a distance x from the middle of the column;

L = half cosine wave length;

y_o = deflection at mid-height;

(5) Using Eq. (3.2.8) the effect of prestressing was evaluated. The net force for the prestressed column was determined, using Eq. (3.2.3);

(6) If the net force is equal to the applied axial force, which was kept constant, go to Step 7, otherwise go to Step 2 with an improved value of Kd, until the internal and external axial force are the same within acceptable limits;

(7) Calculate the bending moment for the corresponding strain distribution taking into consideration the effect of prestressing;

(8) Find the deflections corresponding to the central moment using the finite difference method. Thus a deflected shape will be obtained;

The improvement of Kd in Step 6 was made by using a modified Newton-Raphson method. The finite difference, used in Step 8 will be discussed in the next section.

(9) Increase the curvature in Step 1 and repeat Steps 2 to 8.

Thus, for different values of curvatures, the bending moments and deflections can be obtained for a constant axial force.

3.3 Finite Difference Approach (7)

The deflected shape is expressed in terms of first order finite difference equations at a number of sections along the length. Since the end eccentricities are equal, the column bends in symmetrical single curvature and only half of the column length need be considered. The length is divided into n segments, each of length h (Fig. 6)

The external moment at the rth point M_{er} is given by:

$$M_{er} = P(y_o - V_r) = M_{io} - PV_r \qquad (3.3.1)$$

where, $V_r = y_o - y_r$;

y_r = deflection along the column length.

Since $V_o = 0$ and by symmetry $V_1 = V_{-1}$:

$$V_1 = \frac{1}{2} h^2 \cdot \rho_o \qquad (3.3.2)$$

where, h = length of each segment;

ρ_o = curvature at mid-height.

The computational procedure for calculating the moment-deflection curve consists of the following steps:

(1) Choose an initial value for the central curvature ρ_o;

(2) Select a trial value of Y_o;

(3) Calculate the values of P and M_{io} corresponding to ρ_o and Y_o; (Fig. 7)

(4) Using Eq. (3.3.2) calculate v_1 from ρ_o. Use this value of v_1 in Eq. (3.3.1) to calculate the external moment M_{er} at section (1);

(5) Solve the cross-sectional Eqs. (3.2.3) and (3.2.4) at section (1), thereby obtaining ρ_1 and Y_1 corresponding to P and M_{e1}. Using the values of v_o, v_1 and ρ_1 in first order central difference equation calculate v_2:

$$-\rho_1 = \frac{v_o - 2v_1 + v_2}{h^2}$$

or,

$$v_2 = 2v_1 - v_o - \rho_1 h^2 \qquad (3.3.3)$$

(6) Repeat Step (5) for the sections along the column length until the offset distance v_n is obtained.

The central deflection corresponding to P and M_{io} is then v_n.

By successive incrementing ρ_o values moment-deflection curve for a particular P can be obtained.

To solve the cross-sectional equations in Step 5, a numerical method has been used. By using a modified Newton-Raphson procedure, a faster convergence has been obtained. This is discussed in the next paragraph.

3.3.1 Strain Distribution in a Section Subjected to Given Longitudinal Load and Bending Moments (40)

The problem of finding the strain distribution in a reinforced concrete section under the combined action of a longitudinal load and bending moment cannot be solved directly, and therefore closed form solutions are not available. The numerical procedure which solves the problem successfully, an extension of Newton-Raphson's method is based on the following considerations.

It can be assumed that for a given section and material properties, P and M can be expressed as functions of ϕ and ε_4 as follows:

$$\begin{aligned} P &= P(\phi, \varepsilon_4) \\ M &= M(\phi, \varepsilon_4) \end{aligned} \tag{3.3.1.1}$$

Let $\bar{\phi}$ and $\bar{\varepsilon}_4$ corresponding to certain $\bar{P}$, $\bar{M}$ be known. An expansion of Eq. (3.3.1.1) and $\bar{P}$ and $\bar{M}$ by using Taylor's theorem and retaining only the linear terms yields:

$$\begin{aligned} P &= \bar{P} + \frac{\partial P}{\partial \phi}\,\delta\phi + \frac{\partial P}{\partial \varepsilon_4}\,\delta\varepsilon_4 \\ M &= \bar{M} + \frac{\partial M}{\partial \phi}\,\delta\phi + \frac{\partial M}{\partial \varepsilon_4}\,\delta\varepsilon_4 \end{aligned} \tag{3.3.1.2}$$

where, $\delta\phi$ = increment of curvature necessary to produce P and M;

$\delta\varepsilon_4$ = increment of extreme compressive fibre (top) strain necessary to produce P and M;

$\partial P/\partial\phi$ = rate of change of load with curvature;

$\partial P/\partial\varepsilon_4$ = rate of change of load with top strain;

$\partial M/\partial \phi$ = rate of change of moment with curvature;

$\partial M/\partial \varepsilon_4$ = rate of change of moment with top strain;

P,M = longitudinal load and bending moment, respectively, for which ϕ and ε_4 are sought.

If the four different rates of change can be determined, $\delta\phi$ and $\delta\varepsilon_4$ are readily available through a simultaneous solution of Eq. (3.3.1.2). The required ϕ and ε_4 would then be:

$$\phi = \bar{\phi} + \delta\phi$$
$$\varepsilon_4 = \bar{\varepsilon}_4 + \delta\varepsilon_4 \qquad (3.3.1.3)$$

Because of the approximation involved in Eq. (3.3.1.2) it is likely that Eq. (3.3.1.3) will not provide a solution with the desired accuracy in the initial trial. The necessary check on the accuracy of solution can be made using Eqs. (3.2.3) and (3.2.4) with ϕ and ε_4 to find a longitudinal load P_1 and bending moment M_1. If the agreement is not satisfactory, a new cycle may be started with ϕ, ε_4, P_1 and M_1 as new initial values. It can be expected that these will be closer to the solution. The process converges rapidly with the number of cycles needed depending on the accuracy desired.

The determination of the rates of change of load and moment with curvature and top strain for each cycle is made in two independent steps. First, an increment of curvature, $\Delta\phi$ is given to the strain distribution in the section while $\bar{\varepsilon}_4$ is maintained constant. This is equivalent to a rotation

$\Delta\phi$ of the strain diagram about ε_4. Using Eqs. (3.2.3) and (3.2.4), a new longitudinal load P_ϕ and bending moment M_ϕ can be calculated. The rates of change $\partial P/\partial\phi$ and $\partial M/\partial\phi$ of longitudinal load and bending moment, with respect to curvature, can be calculated as follows:

$$\frac{\partial P}{\partial \phi} = \frac{P_\phi - \bar{P}}{\Delta\phi} \qquad (3.3.1.4)$$

$$\frac{\partial M}{\partial \phi} = \frac{M_\phi - \bar{M}}{\Delta\phi}$$

Secondly, an increment of top strain $\Delta\varepsilon_4$ is given to the same initial strain distribution in the section while $\bar{\phi}$ is maintained constant. This is equivalent to a parallel translation of the strain diagram for a distance $\Delta\varepsilon_4$. If Eqs. (3.2.3) and (3.2.4) are used again, a new longitudinal load P_{ε_4} and bending moment M_{ε_4} can be calculated. The rates of change $\partial P/\partial\varepsilon_4$ and $\partial M/\partial\varepsilon_4$ of longitudinal load and bending moment with respect to top strain can then be calculated as follows:

$$\frac{\partial P}{\partial \varepsilon_4} = \frac{P_{\varepsilon_4} - \bar{P}}{\Delta\varepsilon_4} \qquad (3.3.1.5)$$

$$\frac{\partial M}{\partial \varepsilon_4} = \frac{M_{\varepsilon_4} - \bar{M}}{\Delta\varepsilon_4}$$

The whole process has a graphical interpretation in a simpler case that makes the character of the process more apparent. For the sake of simplicity consider the one-dimensional determination of the unknown abscissa x for a given ordinate y (see Fig. 8). The relation between x and y is given by $y = y(x)$. The coordinates x_1, y_1 of point 1 are known. If the abscissa x_1 is incremented by Δx, the ordinate y_1 of the new point can be obtained as:

$$y_1 = y(x_1+\Delta x) \qquad (3.3.1.6)$$

The rate of change $\Delta y/\Delta x$ as defined in the process is given by:

$$\left[y\ (x+\Delta x)-y_1\right]/\Delta x \qquad (3.3.1.7)$$

This is the slope of the secant to the curve. The required δx as obtained from:

$$y = y_1 + \frac{\Delta y}{\Delta x}\cdot\delta x \qquad (3.3.1.8)$$

is the increment in the abscissa necessary for the extension of the secant to reach an ordinate equal to y. When the new abscissa $(x+\delta x)$ is substituted in $y = y(x)$ an ordinate y_2 is obtained which differs from y a certain amount. If the desired accuracy has not been obtained, Point 2 (see Fig. 8) is used as the initial point and a new trial is initiated. The process is repeated until the desired accuracy has been attained.

The selection of the increments deserves attention. If the increments are very small, the secant may theoretically become the tangent through the point. In practice, very small increments may lead to small differences between large numbers and to consequent round-off errors. When the initial values of P and M represent a condition close to failure, small increments may be in order. Otherwise, increments should be large enough to prevent oscillation of the process around the solution caused by round-off errors. The following expression

$$\Delta A = \alpha A + \beta \qquad (3.3.1.9)$$

(in which A is either ϕ or ε_4) can be used to determine the necessary increments. The coefficient α can be selected as say 0.001 and β as 0.000001, a positive quantity to prevent increment becoming zero. Normally three to four cycles of iteration are sufficient for convergence. The flowchart for the above method is given in Appendix B . The deflection obtained here will be checked by Newmark's integration procedure. The necessary condition for Newmark's method is a pre-determined moment-curvature relationship for a constant axial load.

3.4 Newmark's Numerical Integration (41)

Consider a column of length L loaded with an axial load P having an end eccentricity e, equal at both ends. The column is divided into n equal parts with 0 to n as node junctions. Initial deflections are assumed approximately by a cosine curve. Then the following steps are followed to obtain the deflections at node points. (Fig. 9)

Step 1

Compute the bending moments at the node points due to the total deflections as given by:

$$M_i = P\,(e+y_i),\quad i = 0,1,\ldots n \qquad (3.4.1)$$

where, e = eccentricity at load;

y_i = deflection of column at i.

Step 2

Refer to the M-ϕ curve for the axial load P, and by interpolation obtain the curvatures at node points ϕ_i $(i=0,1,\ldots n)$ corresponding to the node moments computed above.

Step 3

Compute the equivalent concentrated angle changes (i.e., curvatures) at node points assuming a parabolic angle change diagram, as given by:

$$R_o = -\lambda/(7\phi_o + 6\phi_1 - \phi_2)/24$$
$$R_i = -\lambda(\phi_{i-1} + 10\phi_i + \phi_{i+1})/12 \qquad (3.4.2)$$
$$R_n = -\lambda(7\phi_n + 6\phi_{n-1} - \phi_{n-2})/24$$

where, $i = 1,2,\ldots n-1$.

Step 4

Compute values for the average slopes between node positions as given by:

$${}_iS_{i+1} = {}_{i-1}S_i + R_i,\quad i = 1,2,\ldots n-1 \qquad (3.4.3)$$

where, ${}_oS_1$ is assumed to be equal to R_o.

Step 5

Compute deflections at the node positions from the average slopes as given by:

$$u_o = 0 \tag{3.4.4}$$

$$u_i = u_{i-1} + {}_{i-1}S_i, \quad i=1,2,\ldots n$$

Step 6

Apply a linear correction to these deflections to obtain zero deflection at both ends of the column and therefore a new set of values for the additional deflections due to load as given by:

$$y_i' = u_i - i\, u_n/n, \quad i = 0,1,\ldots n \tag{3.4.5}$$

Step 7

Replace the assumed values for y_i used in Step 1 by the new values y_i' calculated in Step 6 and repeat Steps 1 to 6 until convergence is obtained to the desired limits of accuracy. For the purpose of this work, this condition is assumed satisfied if for all the nodes:

$$0.995 \leqslant y_i/y_i' \leqslant 1.005$$

The complete solution took 5 to 6 cycles for convergence. In the present investigation, 'e', the end eccentricity was varied and the mid-deflections were obtained.

CHAPTER 4

EXPERIMENTAL PROGRAMME

4.1 Scope of the Experimental Work

To verify the analytical work proposed in Chapter 3, tests were carried out on several prestressed concrete tubular columns. Out of 6 columns tested, five of them were prestressed and one was nonprestressed (Fig. 10). The main variable examined was the amount of prestressing. The nonprestressed column was tested to check the accuracy of the existing theories. In one of the five prestressed columns, the axial load was varied to find any benefits due to triaxial confinement combined with prestressing.

4.2 Materials

4.2.1 Concrete

High early strength Portland cement (CSA Type 30) was used in all the columns. This type of cement provides the design strength within one week. A clean sand free of impurities was used. The maximum size of coarse aggregate was restricted to 3/8 inch since it should not exceed 1/6 of the size of the least lateral dimension of the column. The maximum clear distance between any two prestressing tendons, which is 0.5 in., provided enough space for the aggregate and the mortar. The coarse aggregate used was crushed stone with hard, clean and durable properties. Natural water having no impurities was used. Concrete mixing was done in Eirich counter current mixer, model EA2(2W) with 5 cu. ft. charging capacity and electrically operated. One batch of concrete mix was used to cast 3 columns at the same time. With each batch of concrete 4 standard 6-inch diameter cylinders were cast. It is difficult to predict the concrete compressive strength which is enclosed by a steel jacket. So two cylinders were cured in perfect dry condition and the other two were cured with water. The average of the result was taken as the compressive strength of the concrete inside the steel tube. There is a 20% difference of strength between dry and wet cured cylinders. A water-cement ratio of 0.4 was used to get a good workability. The proportioning of the concrete mix is given in Appendix A. The mix was proportioned on the basis of "Design and Control of Concrete Mixtures" by Canadian PCA (42). The designed strength and actual strength were very close. All batching was done by weight.

4.2.2 Hollow Steel Tube

The steel tube consists of high tensile steel with a yield strength of about 80 ksi. The length of each specimen was 36 in. and was kept constant. The diameter of the steel tube was 4.5 in. and the wall thickness was 0.133 in. average. All columns were intended to be short columns with an effective length to diameter ratio of approximately 11.5. All columns were tested under a constant axial load and increasing bending moment.

4.2.2.1 Preparation of the Specimen

The tube was cut to 36 inches and was machined to ensure that the ends were flat. Originally the tubes were to be cast without any additional work done to them. Prior to these six columns which are reported here, four columns were tested with prestressing on the concrete alone. The results are not reported here because the strains measured on the steel tube indicated there might have been a bond failure because of the prestressing. Thus it was decided to improve the bond by providing some bond-connectors (shear-connectors) in the shape of lugs at both ends of the columns as far from the ends as possible.

So the new series of tests which is reported in this investigation was conducted with tubes containing four shear connectors per column, two on each end which are welded to the steel tube. This did not change the stress-strain property of the material very much, but improved the bond characteristics significantly. The connectors are 4 inches in length welded on to sides of the tube and projects $1\frac{1}{2}$ inches into the concrete. This also helped to prevent any end zone failure because of prestressing.

4.2.3 High Tensile Steel for Prestressing

High tensile steel wire of 0.276 inch in diameter, with one side buttoned headed, was used for prestressing the concrete-filled tubular columns. Tensile tests indicated an ultimate stress of 262.5 ksi and a yield stress of 245.0 ksi. The stress-strain curve for the prestressing tendon is given in Fig. 5.

4.2.4 Experimental Equipment

4.2.4.1 Prestressing Equipment

The equipment used in the prestressing of the wires was manufactured by Cable Covers Ltd., England. It consists of a hydraulic jack of 20 kips. capacity which was used for post-tensioning. The mechanical gripping device is an open grip anchorage. Black wax lubricant was applied to the wedges to make it easier to release the grips after completing the prestressing operation.

4.2.4.2 End Bearing Plate

An end bearing plate with a thickness of 1/4 in. was used to distribute the prestressing force to the concrete as uniformly as possible. The bearing plates were either square or rectangular in shape. Holes large enough for the prestressing tendons were provided. Two end bearing plates were used for each column, one at each end.

4.2.4.3 Jacks

A hydraulic jack with a load cell mounted on it was used to apply the constant axial force. The bending moment was applied through a tension jack of 16 ton capacity in compression and 8 ton capacity in tension, with a $6\frac{1}{4}$ in. piston length.

4.2.5 Testing Frame

A sketch of the testing apparatus is shown in Fig. 11 The apparatus consists of two heavy steel I beams which are stiffened with transverse stiffners to prevent any local buckling of the web or the flange. Two heavy end fittings were welded to the I beams. These sleeves prevent the column from flying off its base. These sleeves, 4" in height, rotated about as much as the column, and hence had an insignificant effect on the results. The column was subjected to two equal bending moments in opposite directions which forced it to bend in single curvature. The bending moment was applied by pulling on a 5/8 inch threaded bar at 32.5 inches from the center of column. The heavy end beams were attached to end plates with a bearing surface for a spherical ball which acts as a pin in allowing the column to rotate freely. A three-inch ball at the top and a one-and-half inch ball at the bottom were used respectively. As the column rotates, the beams also rotate an equal amount. To prevent the jack from bending, a knife edge was used at the end of each beam. This allowed the jack to remain straight and put a vertical equal force on both ends of the beams.

4.2.6 Casting of Columns

All tubes were filled in a vertical position and the concrete vibrated with a plate vibrator. During the filling operation the bottom end of the tube was held down on a plexi-glass plate so that the mixing water did not leak out. Two wooden templates were used, one from each end of the column to get a uniform surface for the end bearing plate. The template at the top was located about 2 inches from top, and bottom one about 1 inch from the bottom in order to have enough space for prestressing anchorages and buttonned head. Plastic tubes of 1/2" in diameter stiffened with mild steel rods of 1/2" in diameter, were placed in the column before casting to provide an opening for a 0.276"diameter prestressing tendon with a strain gage attached to it. The plastic tubes were greased so that they could be removed after 24 hours. The concrete was dropped into the tube from the top. It was placed in 6" lifts. Each lift was added as soon as the one below had been vibrated. Considerable care had to be taken while vibrating the concrete to ensure proper compaction. It was necessary to continue the vibration until all the air bubbles entrapped within the concrete had been expelled, but stopped before the concrete began to segregate and water rose to the surface. This could only be done by watching the surface of each lift and judging, from its appearance, the proper moment at which to discontinue the vibration. Occasionally, a portable lamp was used. To prevent any horizontal joints, the upper lift was compacted with a rod. The upper surface was made as smooth as possible so that prestressing will be uniform on the entire surface.

4.2.7 Material Properties

Several tensile tests on the material in the steel tube were done on standard tensile specimen, with a length of 12 in. and a gage length of 2". Tensile coupons were taken from the welded tube at various heights and at various locations around the weld to determine the effect of weld on the yield strength. The results indicated a small change. A stub column with a height of 12 inches was also tested in compression.

The results of both the compression and tension tests are very close in agreement.

Two concrete cylinders were tested after 7 days when the prestressing was applied to the column. The remaining two cylinders were tested at time of testing, usually 14 to 20 days. All cylinders were capped before testing.

A prestressing rod of 0.276 in dia. has been tested to determine its stress-strain properties.

4.3 Instrumentation

4.3.1 Strain guages

On each prestressing rod one electrical resistance strain gauge of type CEA-06-250UW-120 was attached. This is a special strain gauge with copper terminals attached for ease in attaching the lead wires. Each strain gauge is of 1/4 inch gauge length and of 120 ohm resistance. Strain gauges of the same type were attached on the column. Two strain gauges, one inclined at 90° to the other, were attached to each tension and compression face.

This arrangement of strain gauges permits the measurement of the strains in the longitudinal and circumferential directions on both the faces. Before attaching the strain gauges, the surfaces were smoothened using fine silicone carbide paper and acetone. The strain gauge was mounted using Eastman M-Bond 200 adhesive with a 200 catalyst as a bonding agent according to the manufacturer's recommendations. The lead wires were then soldered to the gauges and a dust proofed coat, M coat-5, was applied. After curing for 24 hours at room temperature, a plastic tape was wrapped around for further protection.

4.3.2 Mechanical Dial Gauges

The deflections of the column were measured using mechanical dial gauges having a minimum reading of 0.001 inches. These deflection gauges were mounted, along the length of the column, equally spaced, with one in the center and on a straight rigid angle which was clamped to the base. Lateral deformation of the column with respect to its ends was also measured.

Thus strains and deflections relevant to the overall behaviour of the column were measured along two perpendicular directions on the tension and compression faces. The plane of strain gauges and deflections were made to coincide with the plane of eccentricity. A 25 kips load cell was used to measure the eccentric load.

4.4 Experimental Set-Up and Test Procedure

A sketch of the column is shown in Fig. 12. Before testing, the columns were prestressed to an effective prestress of approximately 170 ksi and then both the ends were grouted with a non-shrink grout. The ends were made flush with the steel tube so that the load will be distributed between the steel tube and concrete. The strain gauge wires from the prestressing tendons were taken through holes provided in heavy arms.

Then the column was mounted in the test frame and an initial load of 1 kip was applied so that column will be held in position. The effective length of the column was taken as the distance between the centers of the two spherical balls. The spherical balls created a nearly pinned-pinned column. This can be seen by comparing the rotation of the heavy beams to the column rotation. They are virtually the same. The axial load, which is kept constant, is applied in 5 kip increments. Then the eccentric load was applied in 200 lbs. increments. The eccentricity of the load is 32.5 inches, which is measured from the centre of the column to the centre of the tension jack. The bending moment at the center of the column is due to the primary bending moment, Mo, caused by the eccentric load, plus the secondary bending moment which is equal to the axial load times the central deflection. The concentric axial force was adjusted for each change in the eccentric force so that the total axial force would remain constant while the moments were increased. After every load and/or moment increment strains and deflections were accurately recorded until the failure load was reached.

Failure was indicated by a rapid drop of load or moment. Sometimes the piston length of the tension jack ran out of travel and then the test had to be stopped. At least in one column, knife edges through which the eccentric load was applied ran out of rotation, and then test had to be stopped because by then enough plasticity was induced in the column. Although prestressed concrete-filled tubular columns are very ductile, cürvature of not more than 0.0031 in^{-1} were reached because of limitations in the equipment. The maximum compressive strain recorded was about 7000-8000 $\mu\varepsilon$. Although all the columns were not tested up to the collapse load, it was assumed that at least 70% of the ultimate load was applied. This figure was arrived from observing the strains.

4.5 Cracks

No cracking was heard during testing. After the testing all the columns were cut open with a grinder around the shear connectors on two planes perpendicular to tension and compression faces. This did not disturb or induce any heat in the concrete. The steel shell was easily removed after cutting. There was no adhesive bond between steel and concrete. Little drops of water were seen on the concrete surface indicating a condition similar to water cured cylinders.

CHAPTER 5

DISCUSSION OF RESULTS

5.1 General

Tests on six concrete-filled tubular columns, five prestressed and one nonprestressed were performed to determine the ultimate strength. The column designations are shown in Table 1. The theoretical and experimental results for deflections, strains and curvatures are compared in Figs. 13 to 44. To observe the affect of plasticity, at which the ratio of transverse to longitudinal strain will be 0.5, longitudinal and transverse strains obtained from experiments are also compared. The experimental and theoretical maximum moments are shown in Table 2.

5.2 Nonprestressed Column NS1

NS1, the nonprestressed concrete-filled column, was tested under a constant axial load of 70.0 kips and the bending moment was increased until collapse. The axial load was applied in increments of 5.0 kips up to 70.0 kips and then the eccentric load was applied in increments of 0.5 kips. The column had a deflection of 0.124 inches at mid-height after the application of all of the axial load. When the moment was applied, the deflection increased in the direction of the moment. This was considered in the calculation of the total moment, which is the applied moment plus the $P\Delta$ effect due to the axial load.

A maximum longitudinal compressive strain of 7540$\mu\varepsilon$ was measured and an ultimate curvature of 0.0028/inch was reached. A maximum ratio between transverse and longitudinal strain of 0.35 was obtained on the compressive side.

The average concrete strength, which is taken as average strength of the cry-cured and the moist-cured cylinders, is about 6000 psi. An ultimate moment of 207 in.-kip. was reached experimentally and failure was indicated by a rapidly dropping load. A maximum deflection of 0.874 inches was reached. Theoretical analysis was performed with an f''_c of 0.85 times 6000 psi which is equal to 5100 psi. A moment of 223 in.-kip. was obtained for the corresponding experimental ultimate curvature which can be seen in Fig. 13. A difference of 55% was observed between experimental and theoretical curvatures for a moment of 152 in.-kip.

Theoretical and experimental moment-strain relationships for a mid-height section are compared in Fig. 14. Good agreement can be seen for both compressive and tensile strains. The initial offset at zero moment indicates the compressive strain induced by the axial load.

Moment-deflection relationship for a mid-height section was compared. The maximum difference of 28%, which can be seen in Fig. 15, was observed between experimental and theoretical values at ultimate load. This can be attributed to imperfections of the column and lack of concentricity of axial load. Fig. 16 shows the variation with moment of the longitudinal and transverse strains, obtained experimentally on the compressive side.

After the experiment, the column was cut open with a grinder without much disturbance to the concrete inside and a picture showing cracks of concrete on the tensile side is shown in Fig. 17.

5.3 Prestressed Columns

5.3.1 Column NS2

NS2 was prestressed with two tendons symmetrically placed with respect to the center of the cross-section and in the bending plane. This column was tested under an axial load of 105 kips and increased bending moment. The column had an initial deflection of 0.200 inches at mid-height after the application of the axial load. The tendons were each stressed to approximately 160 ksi. This amounts to a prestress of 755 psi in the concrete which is equal to 0.127 f_c''. The average concrete strength was found to be approximately 7000 psi at the time of testing. Analysis was performed with an f_c'' of 5950 psi.

A maximum longitudinal compressive strain of 7784$\mu\varepsilon$ was reached experimentally with a curvature of 0.0024/in. Ratio between transverse and longitudinal strain of 0.304 was observed at the time of failure. Failure was evident when no increase in the bending moments was accompanied by an increase in deflection. A maximum moment of 191 in.kip was reached experimentally at which the maximum deflection was found to be 0.788 inch.

A theoretical analysis shows 195 in.-kip. moment for a curvature of 0.0024/in. A difference of 28% was observed between theoretical and experimental curvatures for a moment of 141 in.-kip. (Fig. 18).

The applied axial load represents 45 percent of the ultimate axial load of the column assuming there is no confinement of concrete by the steel. No increase in strength due to confinement seemed to have occurred in this column. This can be observed from graphs. No further increase of axial load was considered because all the pre-stress would be lost by the application of only axial load.

Experimental moment-deflection, moment-strain curves are in good agreement with theoretical ones as shown in Figs. 19 and 20. Fig. 21 shows the relationship between transverse and longitudinal strains with moment. Fig. 22 shows the end crippling of steel tube due to local stresses. Fig. 23 shows the cracks on the tension side of concrete which are smaller in number than the nonprestressed column NS1, shown in Fig. 17.

5.3.2 Column NS3

NS3 is a column similar to NS2 except that the applied axial load was only 20 kips. This is to create a situation very close to pure bending. At the same time as is well known for reinforced concrete, maximum bending moment occurs under certain axial load. The axial load represents only about 8.5% of the crushing load.

After the application of the axial load, a deflection of 0.200 inches was measured experimentally. This could be due to imperfections of the column. The prestressing was done with two tendons, which gives an amount of prestress equal to 0.120 f_c''. The average concrete strength was found to be 6000 psi. The experiment was not continued to collapse because of equipment problems and total rotation of the knife edges.

Experimental and theoretical moment-deflection curves are plotted in Fig. 24. A maximum difference of approximately 150% was found between the theory and experiment. The main reason for this discrepancy is the end sleeves. The end sleeves were loose so that the column could move freely up to about a half inch. As the moment was applied the end sleeves rotate and moved the column laterally until it touches one of the edges of the sleeve. So the measured deflection is not the true deflection but movement of the column plus the normal deflection. After reaching a certain stage in the loading, the movement of the column is stopped and from there onwards the true deflection is measured. It is not possible to separate these two quantities because the column moved laterally gradually as the bending moment was applied.

Moment-curvature graphs, shown in Fig. 25, indicate good agreement between theory and experiment. The experimental maximum moment obtained was 216 in.-kip at a curvature of 0.0024/in. while the theoretical moment was 233 in.-kip for the corresponding curvature. Moment-strain curves in Fig. 26 also shows good agreement. A maximum ratio of transverse to longitudinal strain of 0.39 was observed in the experiment. Fig. 27 shows the variation of longitudinal and transverse strains on the compressive side throughout its loading range.

As compared to its counterpart, the nonprestressed column, there is theoretically an increase of 10 in.-kip. in moment capacity. The concrete contribution in the non-prestressed column is about 28 in.-kip. and so by prestressing the same contribution has been increased to 38 in.-kip., which is an increase of approximately 36%. But as the contribution of steel tube is so high, the overall increase of moment is only about 4.5% over nonprestressed section. Fig. 28 shows the column during testing.

5.3.3 Column NS4

NS4 is prestressed with three tendons symmetrically placed, one in the centre and the other two at equal distance from the centre of the cross-section as shown in Fig. 29. An axial load of 20 kip was applied to determine if any strength increase occurs over NS3, because of the increased area of prestressing wires. The tendons were stressed initially to an average of 160 ksi which created a prestress in the concrete of 0.222 f_c'. The average concrete strength was about 6000 psi. The initial deflection was about 0.061 inches after the application of the axial load. NS4, like NS3, could not be tested up to failure because of equipment problems.

Experimental and theoretical moment-deflection values are shown in Fig. 30 and a discrepancy similar to that of NS3 was found. The reasons for the discrepancy again are same. Moment-curvature and moment-strain values are compared in Figs. 31 and 32 and show a reasonable agreement. A maximum ratio of transverse to longitudinal strain of 0.38 was found which can be observed from the graph for longitudinal and lateral strains in Fig. 33.

Experimentally, a maximum moment 218 in kip was reached with a curvature of 0.0031/in. Theoretically, a moment of 240 in.-kip. was obtained for the same curvature. There is no significant advantage obtained by increasing the prestress here either theoretically or experimentally because the additional tendon was placed in the centre of the cross-section which does not contribute to any increase in bending moment. So it can be concluded that there is no real advantage when a tendon is placed centrally in a column.

5.3.4 Column NS5

NS5, prestressed symmetrically with four tendons, two tendons each on the compression and on the tension faces, is shown in Fig. 34. They are at equal distance from the centre of cross-section thus creating a uniform prestress. A constant axial load of 20 kip was applied and bending moment was applied gradually until collapse. The purpose of this column, to observe the effect of increased prestress, was again the same as for NS4.

An initial deflection of 0.050 inches was observed after application of axial load. The prestressing amounts to 0.296 f_c'' where f_c'' is the average concrete strength determined to be 0.85 times 6000 psi which is equal to 5100 psi. The experiment could not be continued to collapse because of equipment problems.

Moment-deflection curves, shown in Fig. 35, indicate the same discrepancy as shown in NS4. Moment-curvature and moment-strain graphs are in reasonable agreement with theoretical results as shown in Figs. 36 and 37. Fig. 38 shows the relationship between transverse strains and longitudinal strains with moment.

The experimental maximum moment reached was 195 in.-kip. at a curvature of 0.0020 /in. At this stage the knife edge had rotated fully. So the test could not be completed. The change in stress in the prestressing tendons is as shown in Fig. 39. There is good agreement between theoretical and experimental results showing that the theory for unbonded tendons is satisfactory.

Theoretically at 0.0040/in. curvature a moment of 265 in.-kip was obtained which is an increase of about 7.5% over NS4. The increase over nonprestressed section was about 16.2% which means concrete contribution due to prestressing was increased about 123% over nonprestressed.

5.3.5 <u>Column NS6</u>

NS6, prestressed with five tendons which are symmetrically placed like NS5 with one additional tendon in the centre as shown in Fig. 40. The applied axial load was 20 kips and there was no initial deflection after the application of axial load. All the tendons were prestressed to 160 ksi, on average, which amounts to a prestress in the concrete of 0.37 f_c''. The average concrete strength was about 6000 psi. This column, like NS5, also could not be tested up to failure.

Moment-curvature, moment-deflection, and moment-strain curves are shown in Figs. 41, 42 and 43. In the moment-deflection graph in Fig. 41, the initial offset could be due to the movement of the column in the sleeve. When this offset was uniformly subtracted, the experimentally corrected curve is shown as a dotted line. This reduced the discrepancy considerably between the theoretical and experimental results. The maximum ratio between transverse and longitudinal strains was determined to be 0.36 from the experimental information in Fig. 44 which shows the lateral and longitudinal strains. There is no increase in strength over NS5 which means there is no advantage in having a central tendon.

Experimentally a moment of 218 in.-kip was obtained at 0.0028/in. curvature as compared to a theoretical moment of 255 in.-kip. Fig. 45 and 46 show the column NS6 during the test.

5.4 Discussion

When the moment-curvature's graphs are superimposed for NS3, NS4, NS5 and NS6, it is observed that for NS6 the moments are lower than NS5 indicating the optimum amount of prestressing is about 0.296 f_c'' for this column. This can be seen in Fig. 47. The area of the prestressing is about 1.68% of concrete area. The amount of prestress was always calculated as total prestressing force divided by transformed area of the total concrete-filled tube. This was done because of the observed strain immediately after prestressing indicated that steel has also been prestressed simultaneously with the concrete. This is necessary also to maintain the bond between the concrete and the steel tube which is a basic assumption in the analysis. For NS3, NS4, NS5 and NS6, no cracks were observed in the concrete on the tension side when the columns were cut open. This might be due to the closing of cracks after unloading in the prestressed columns. Because the columns were not tested up to collapse, no permanent cracks were found. From the observation of strains on these columns it can be said they were only tested up to 70% of their ultimate strength. This also confirms the theory.

The theoretical ultimate moments for a curvature of 0.0056/in. and an axial load of 20.0 kips were compared in Table 3 for NS3, NS4, NS5 and NS6. It can be observed that with two prestressing tendons a 9.1% increase in strength was obtained over a nonprestressed section. With four tendons a 20.8% increase was obtained over a nonprestressed section. This increase was at a curvature of 0.0056/in. and this decreases in the service load range. The contribution of steel, however, was constant for all the cases. The concrete contribution in the nonprestressed section was only 31 in.-kip whereas for the case of four tendons it was about 79 in.-kip indicating a 155% increase for concrete contribution. This could be significant for a thin walled column where concrete carries a major portion of load.

Fig. 48 shows the interaction diagrams for nonprestressed NS3, NS4, NS5 and NS6. The advantages of prestressing can be clearly seen where there is significant bending. The maximum advantage is in the pure bending region. Obviously the axial load capacity will be decreased because of the prestressing force. For example, in NS6 the axial load capacity was reduced by about 30% because of prestressing.

From Fig. 49, where moment-deflection curves are superimposed, it can be observed that prestressed sections deflect less than a nonprestressed column. A similar behaviour can be observed with the moment-curvature graphs. This indicates the higher ductility of the prestressed columns. Additional details of the column can be seen in Figs. 50 to 52.

5.5 Sources of Error

Although the reasons for the discrepancies are pointed out above, the following additional reasons might have also contributed.

i) Initial imperfections of the column

ii) The assumed perfect bond between the steel and the concrete might have not been present during the entire loading period

iii) Effect of confinement which are significant when L/D $<$ 15 are not considered in the analysis

iv) Residual stresses due to ~~welding~~ of shear connectors and properties of the materials

v) Approximations in the analysis of unbonded prestressed concrete-filled tubular column.

vi) Measurement of deflections due to movement of the column in the gap provided by the end-sleeves.

CHAPTER 6

CONCLUSIONS AND RECOMMENDATIONS

6.1 General

Six concrete-filled tubular columns, five prestressed and one nonprestressed were tested under a constant axial load and an increasing bending moment. All columns were uniformly prestressed. The area of prestressing steel was varied in four columns and axial load was varied for only one column. The following conclusions can be drawn from this investigation.

6.2 Conclusions

1. Prestressing a concrete-filled tubular column can increase the load carrying capacity when it is subjected to a large amount of bending moment. In this investigation a 20% increase was achieved theoretically for a particular column.

2. As the axial load increases, the increase in strength reduces and no triaxial effects seemed to be apparent.

3. An exact theory was developed for an unbonded prestressed concrete-filled tubular column.

4. As the area of prestressing steel increases, the increase in strength reaches an optimum value. In this investigation, however, that was found to be equal to 1.68% of the concrete area.

6.3 Recommendations

1. By changing parameters like the thickness of steel tube and diameter of the steel tube, the effects of prestressing could be studied.

2. The effect of bond strength between the steel tube and the concrete core should be studied particularly when they are prestressed.

3. More experimentation should be done to check the validity of the theory presented in this investigation.

4. Any movement of the column in the sleeve should be completely prevented in the experiment.

FIGURES

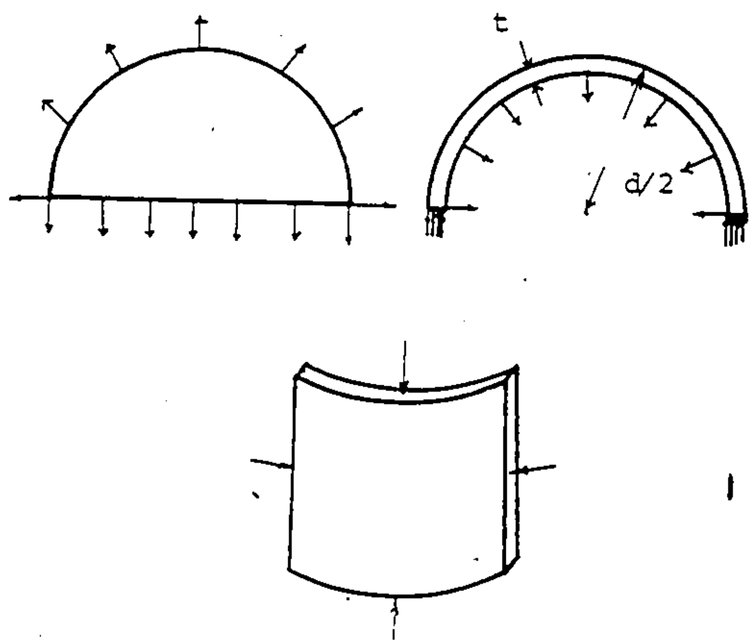

FIG. 1 INITIAL STAGE WHEN $\mu_{CONC} < \mu_{STEEL}$.

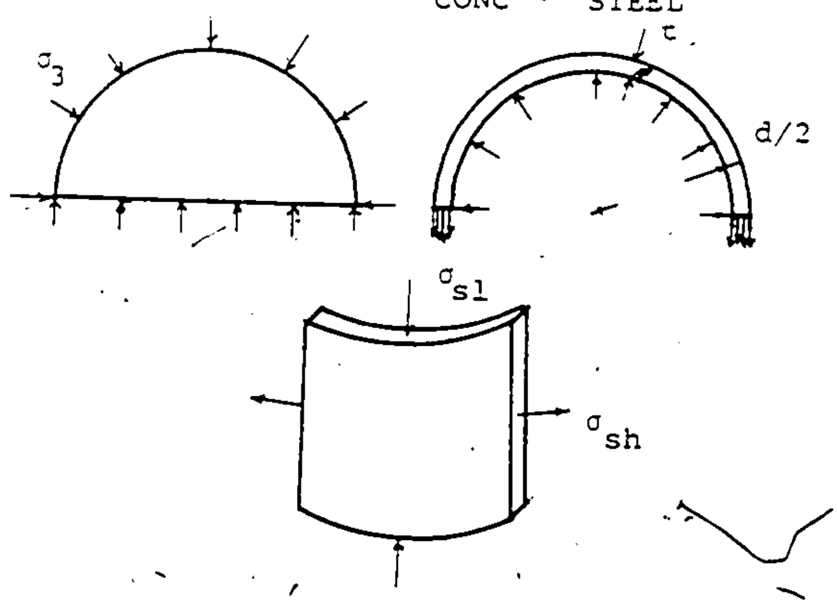

FIG. 2 FINAL STAGE WHEN $\mu_{CONC} > \mu_{STEEL}$.

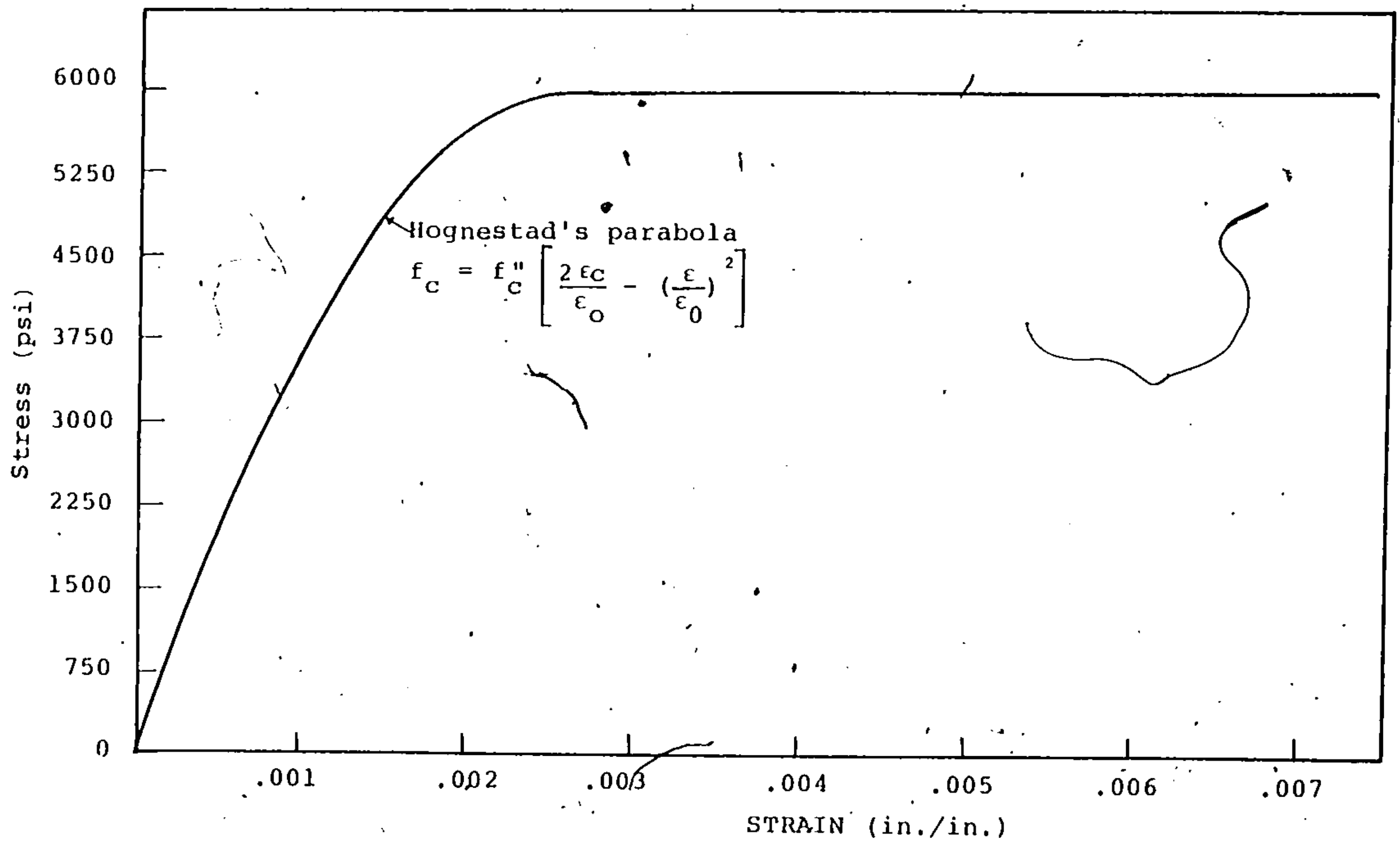

FIG. 3 STRESS-STRAIN CURVE FOR CONFINED CONCRETE.

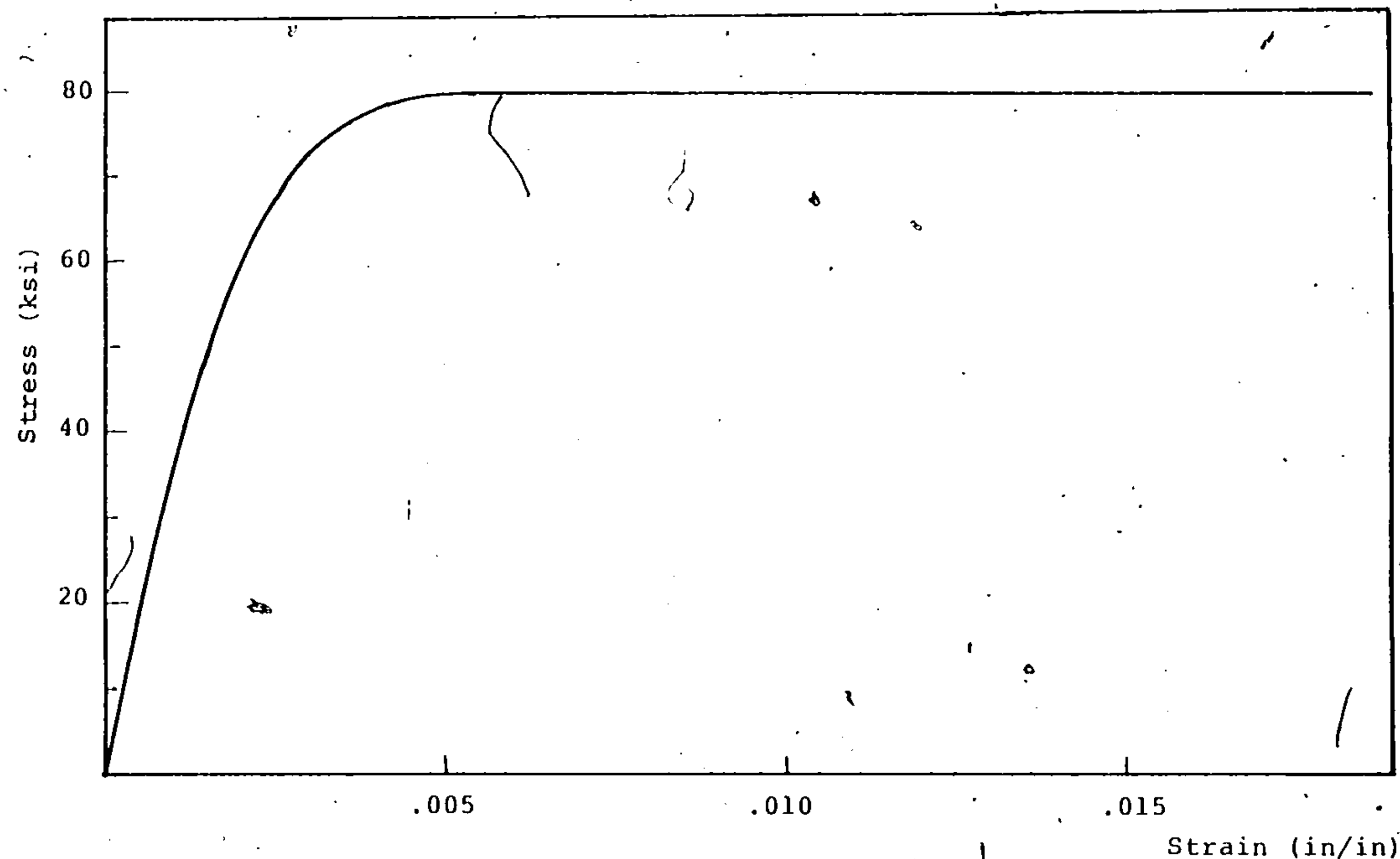

FIG. 4 STRESS-STRAIN CURVE FOR HOLLOW STEEL TUBE.

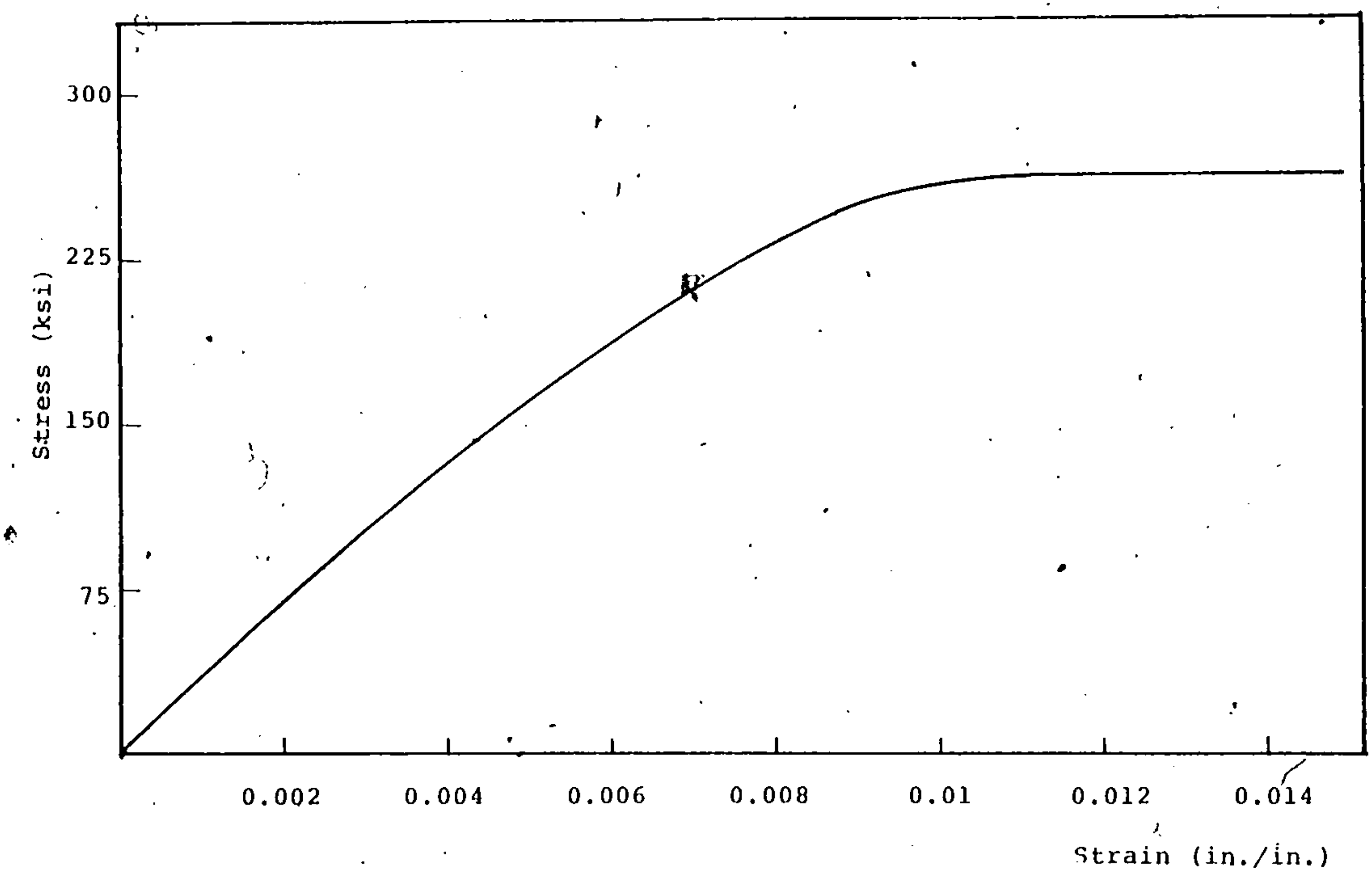

FIG. 5 STRESS-STRAIN CURVE FOR PRESTRESSING WIRE.

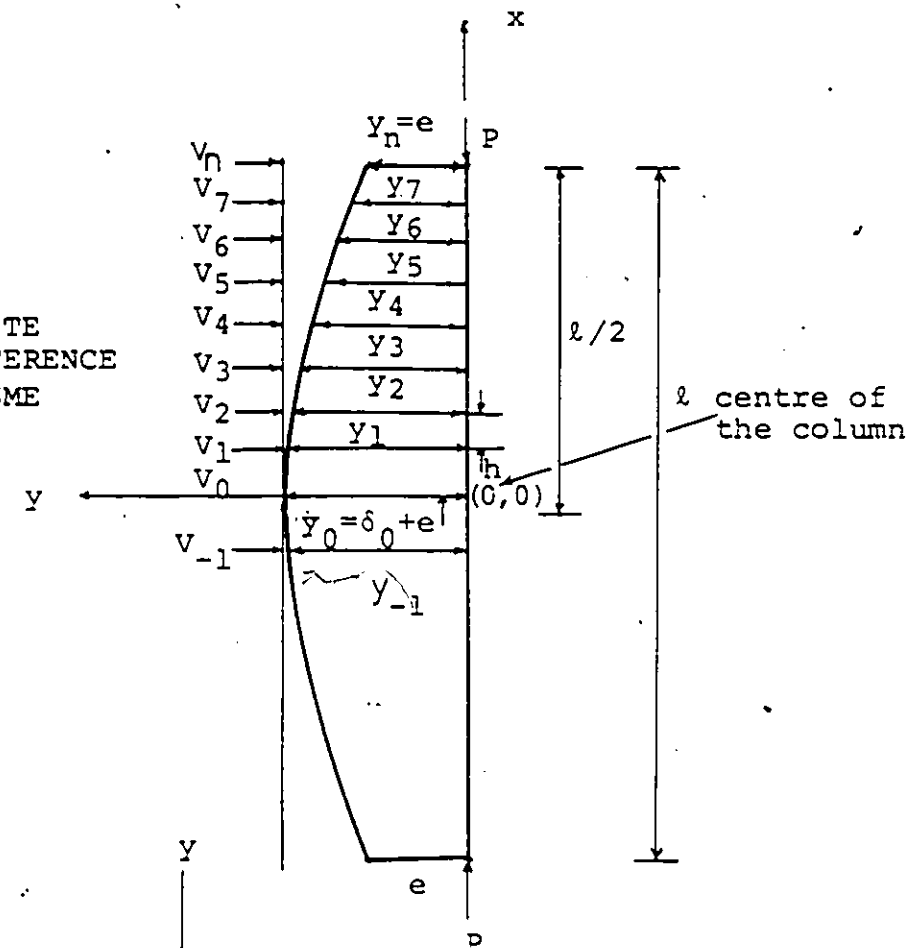

FIG. 6 FINITE DIFFERENCE SCHEME

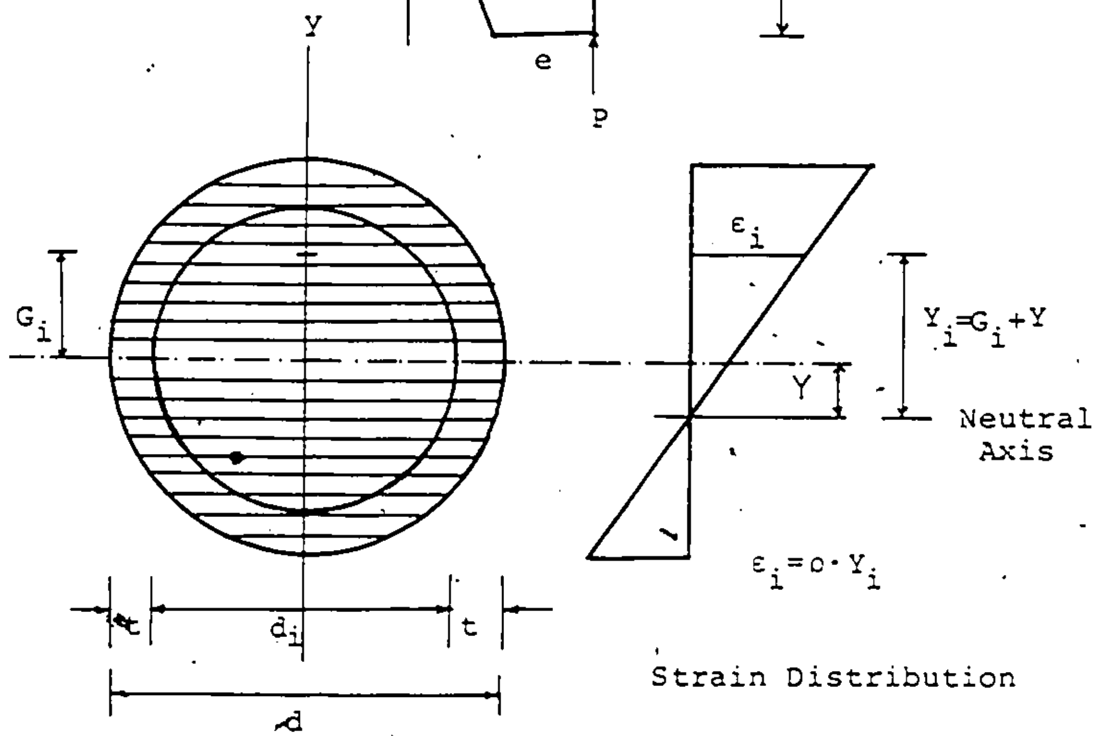

FIG. 7 STRIP METHOD

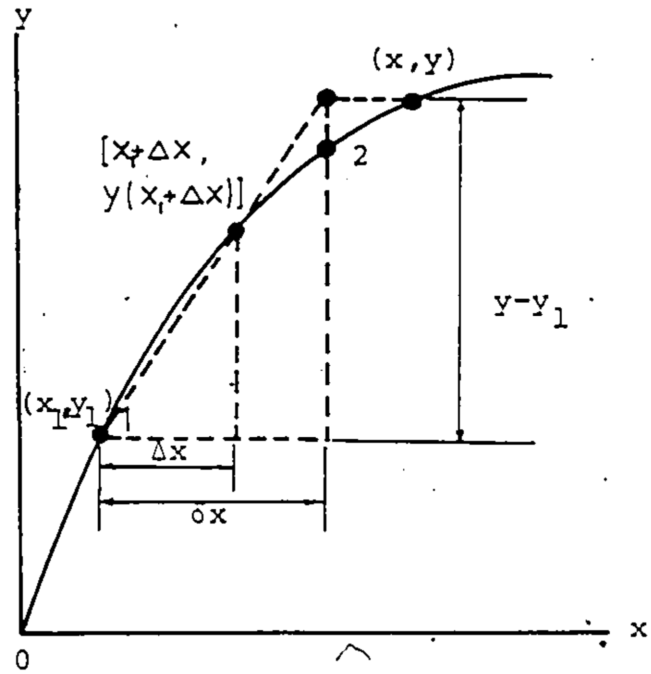

FIG. 8 GRAPHICAL INTERPRETATION OF NUMERICAL PROCESS.

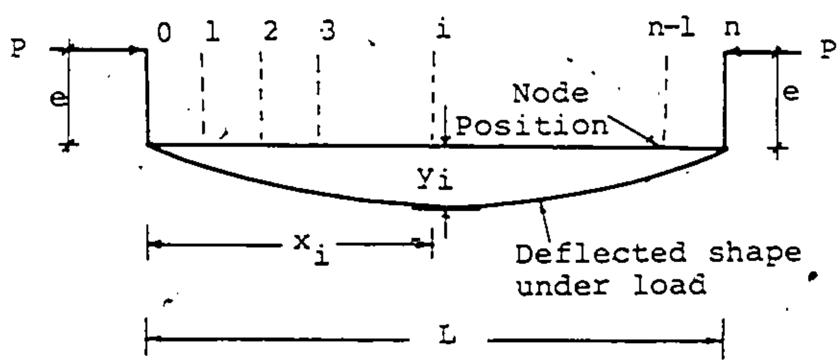

FIG. 9 NEWMARK'S NUMERICAL INTEGRATION SCHEME.

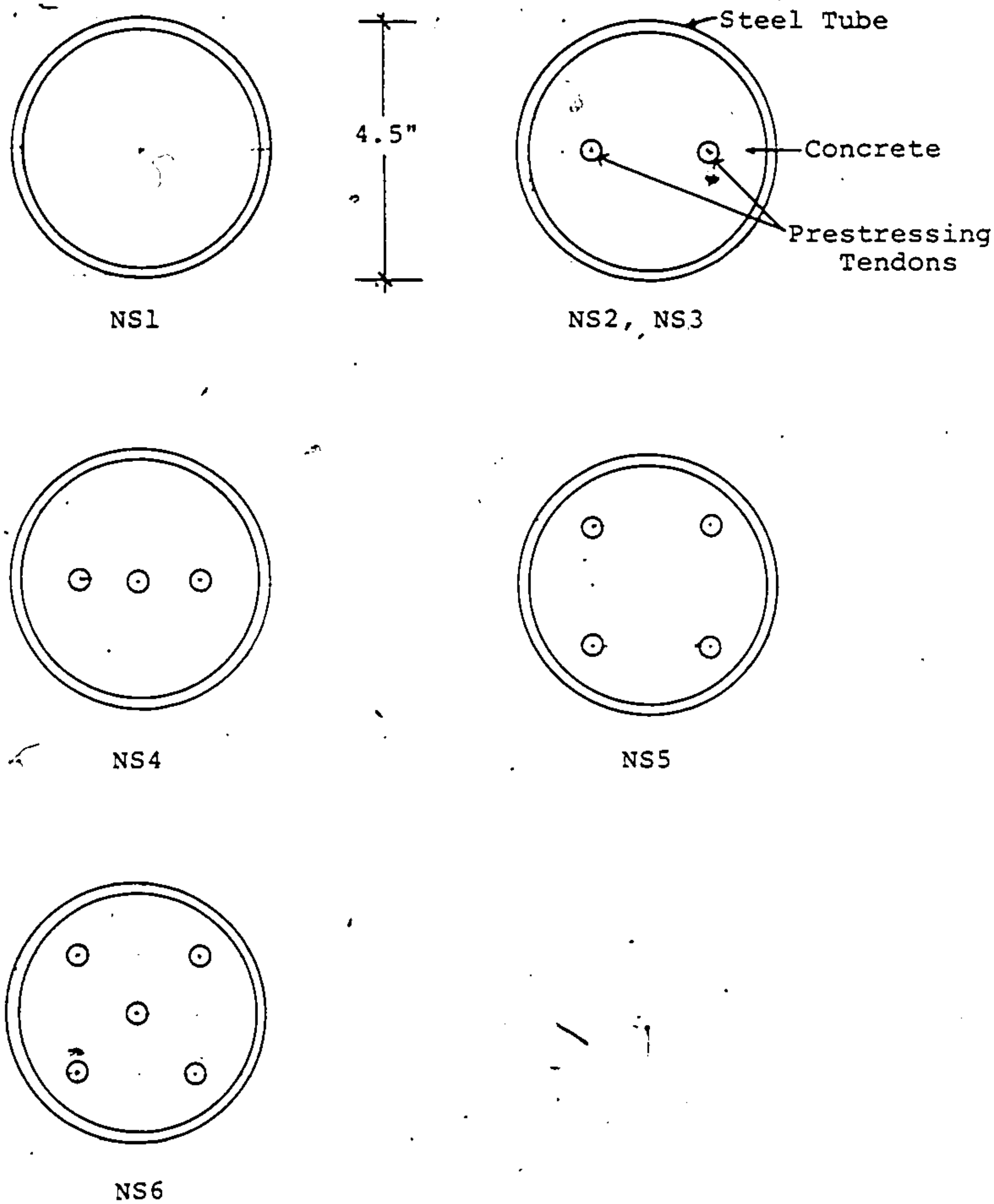

FIG. 10 CLASSIFICATION OF COLUMNS

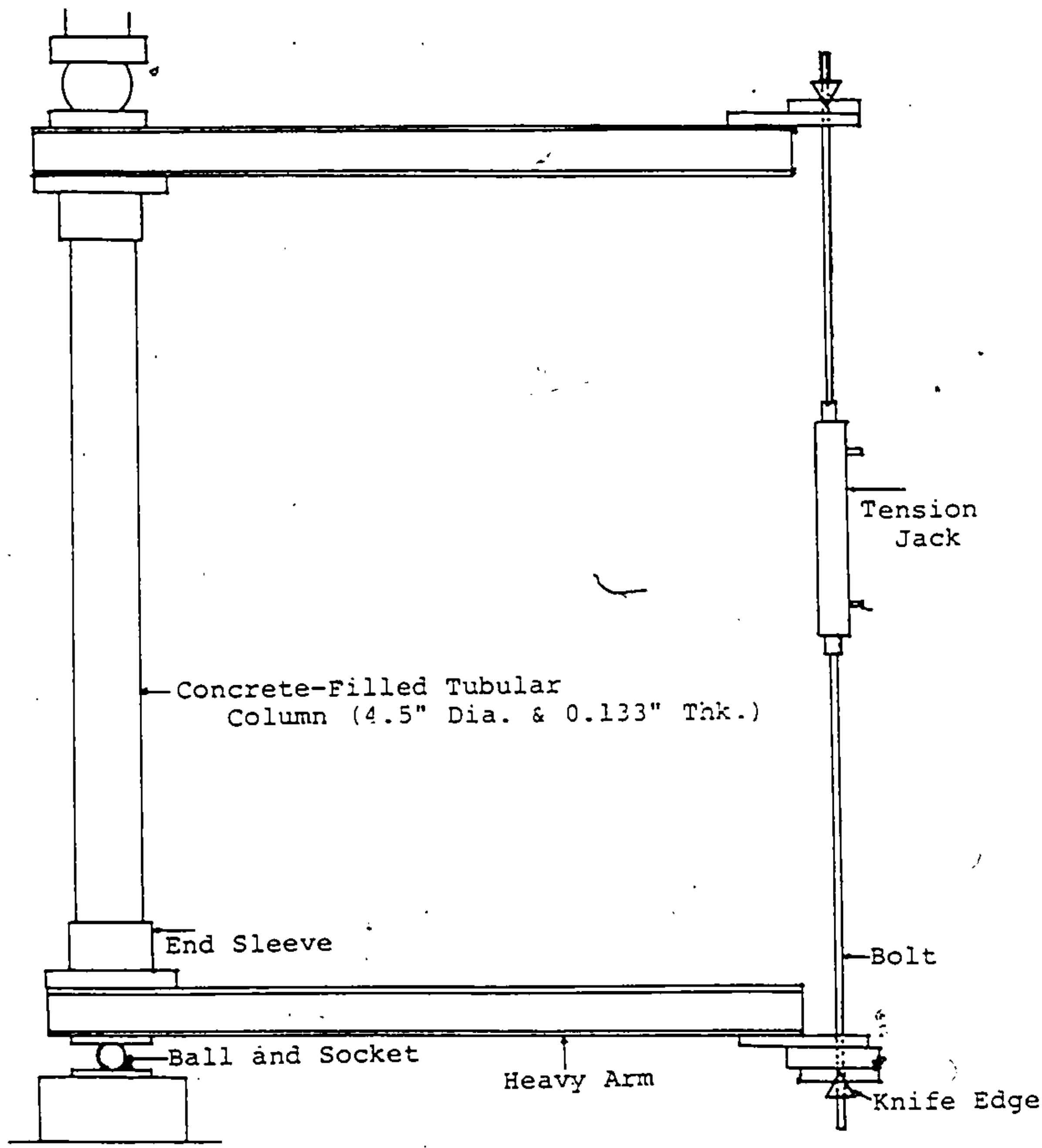

Fig. 11 LOADING APPARATUS

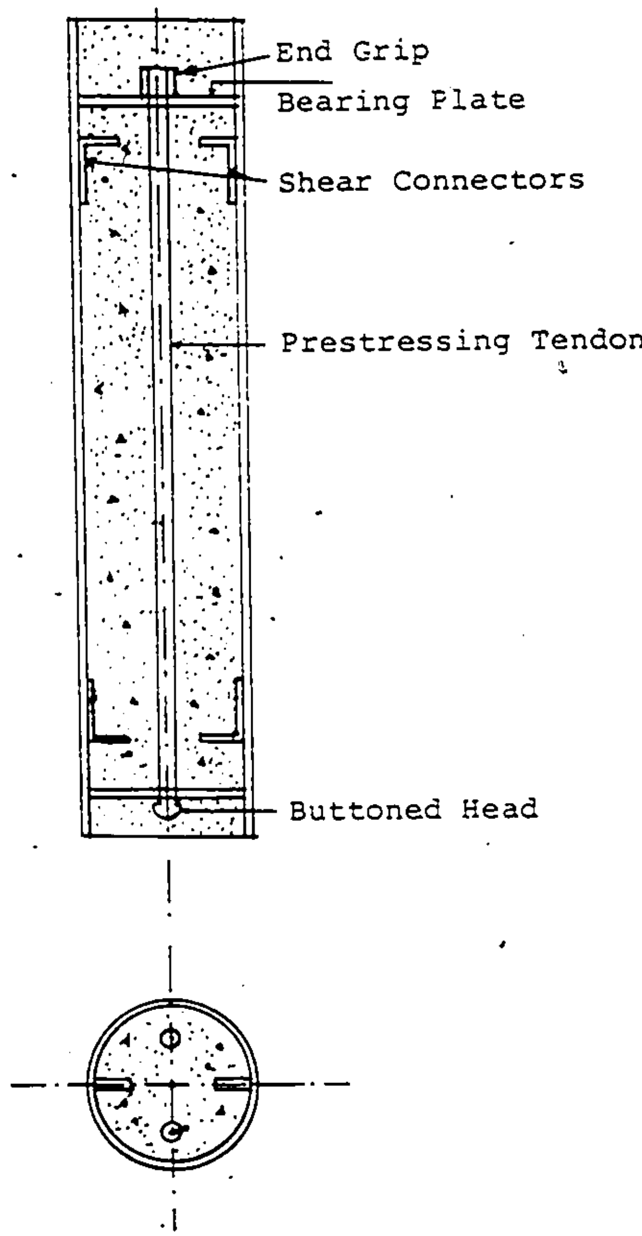

FIG. 12 TYPICAL CROSS-SECTION THROUGH A PRESTRESSED CONCRETE-FILLED TUBULAR COLUMN.

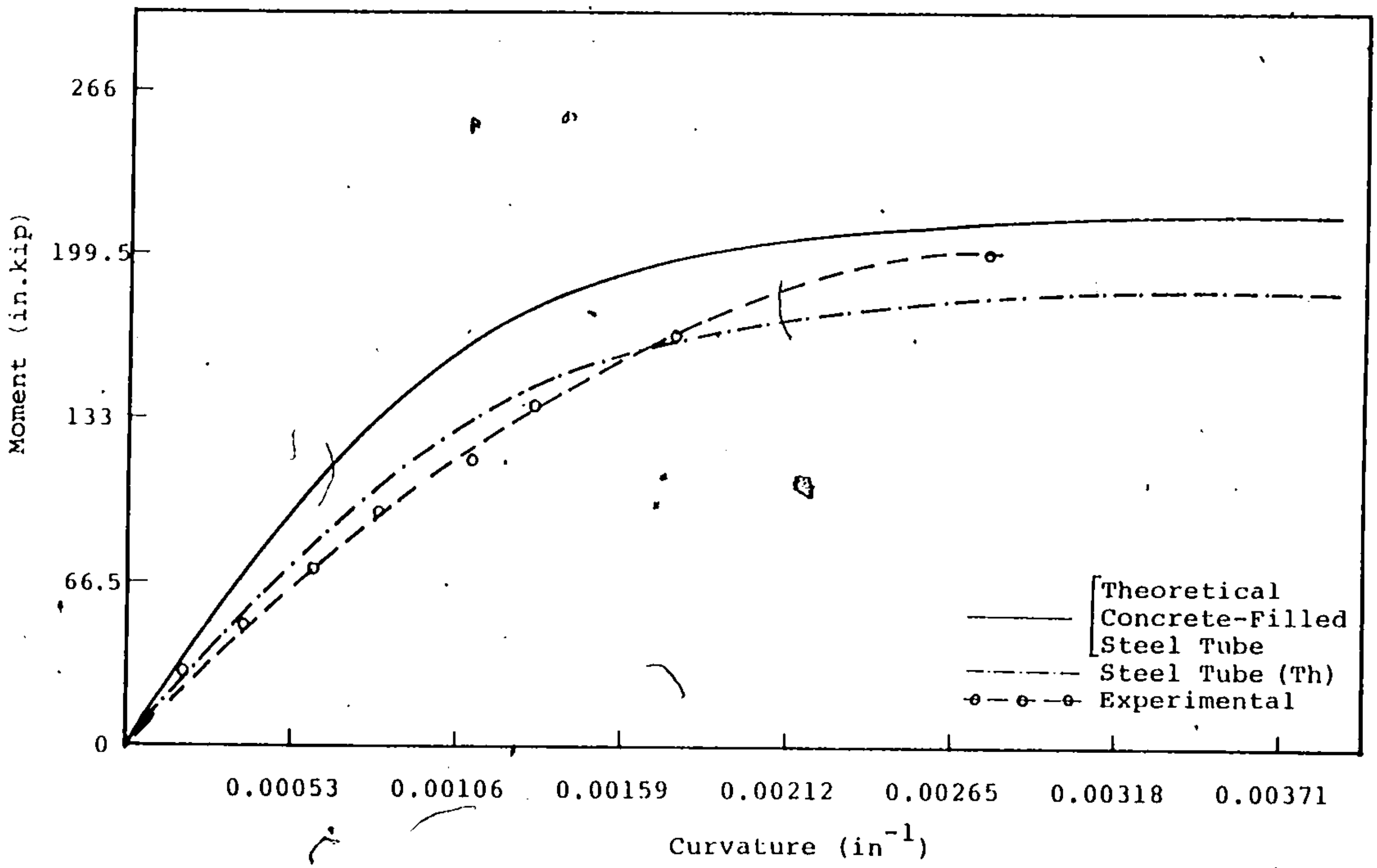

FIG. 13 MOMENT-CURVATURE RELATIONSHIP FOR NS1.

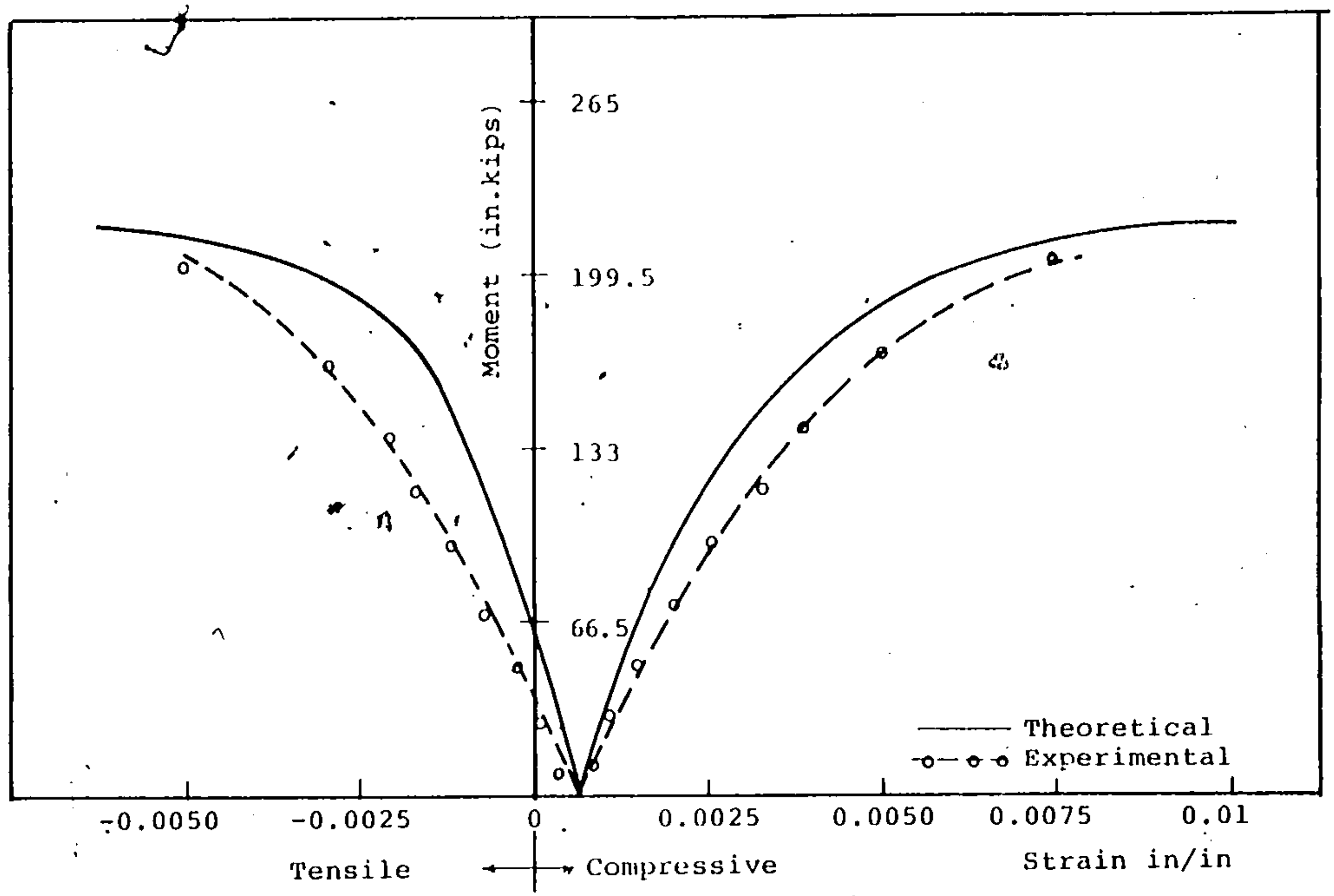

FIG. 14 MOMENT-STRAIN RELATIONSHIP FOR NS1.

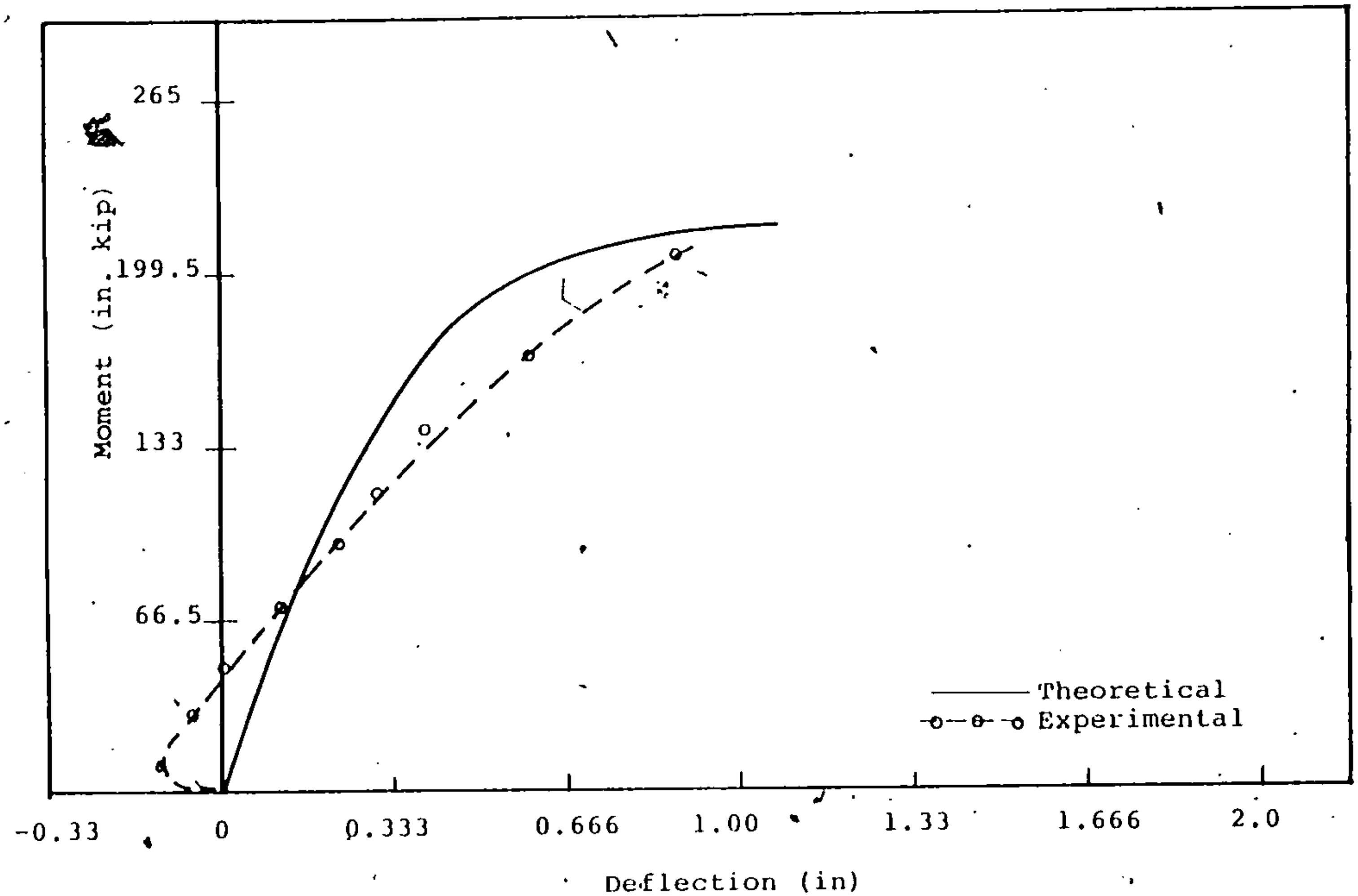

FIG. 15 MOMENT-DEFLECTION RELATIONSHIP FOR NS1.

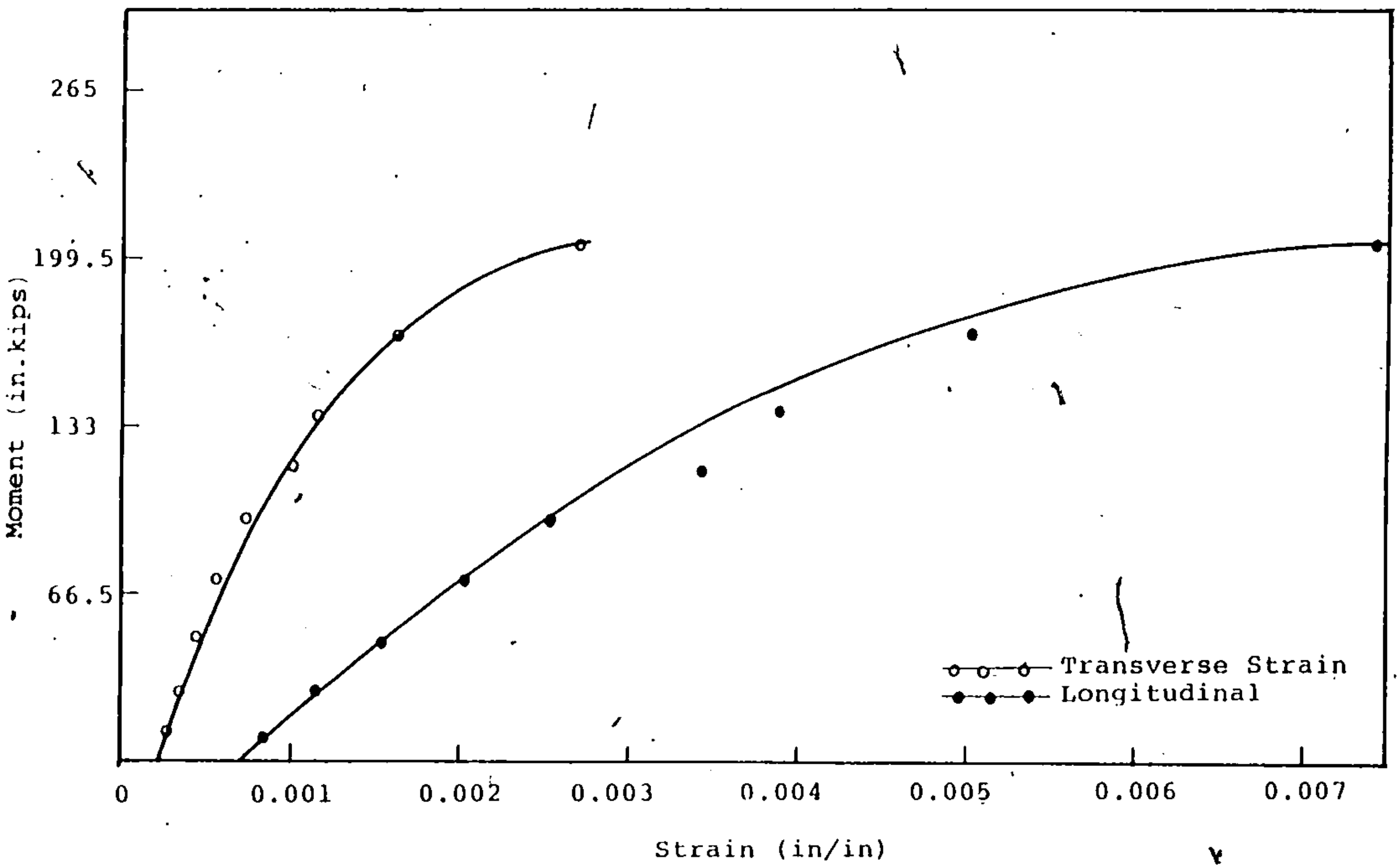

FIG. 16 LONGITUDINAL AND TRANSVERSE STRAIN VS. MOMENT FOR NS1. (COMPRESSIVE SIDE).

FIG. 17 CRACKING OF CONCRETE FOR NS1.

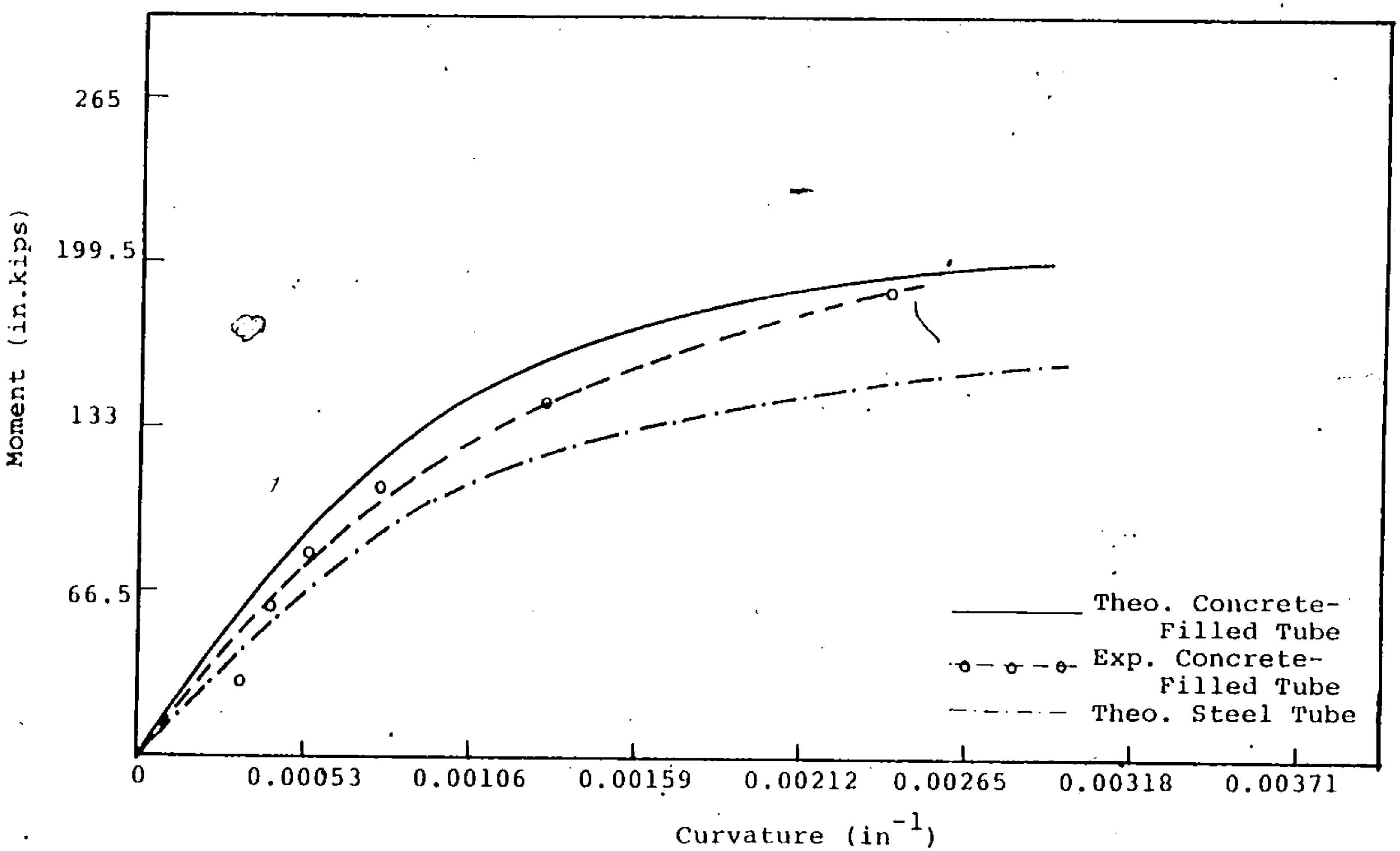

FIG. 18 MOMENT-CURVATURE RELATIONSHIP FOR NS2.

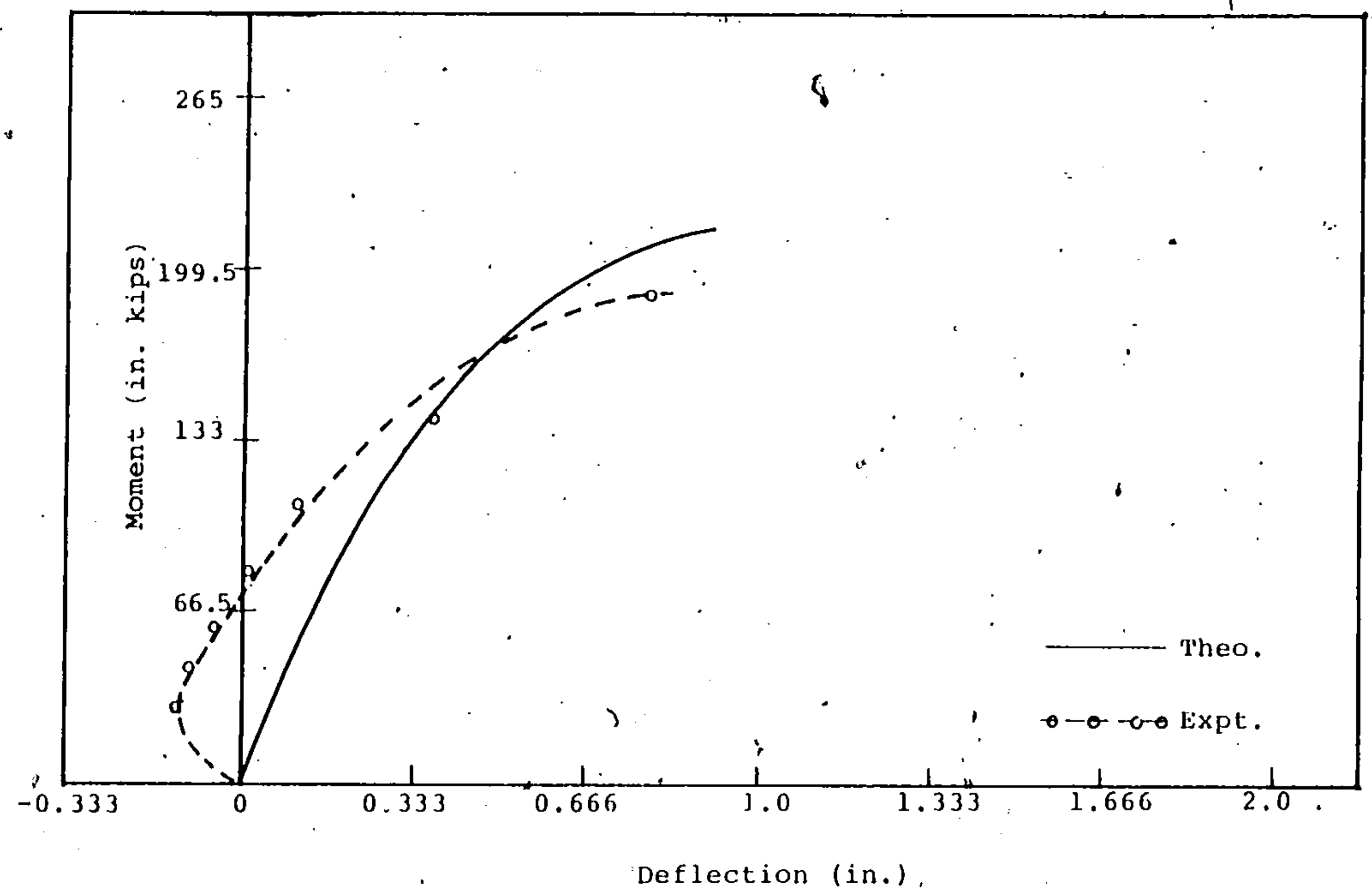

FIG. 19 MOMENT-DEFLECTION RELATIONSHIP FOR NS2.

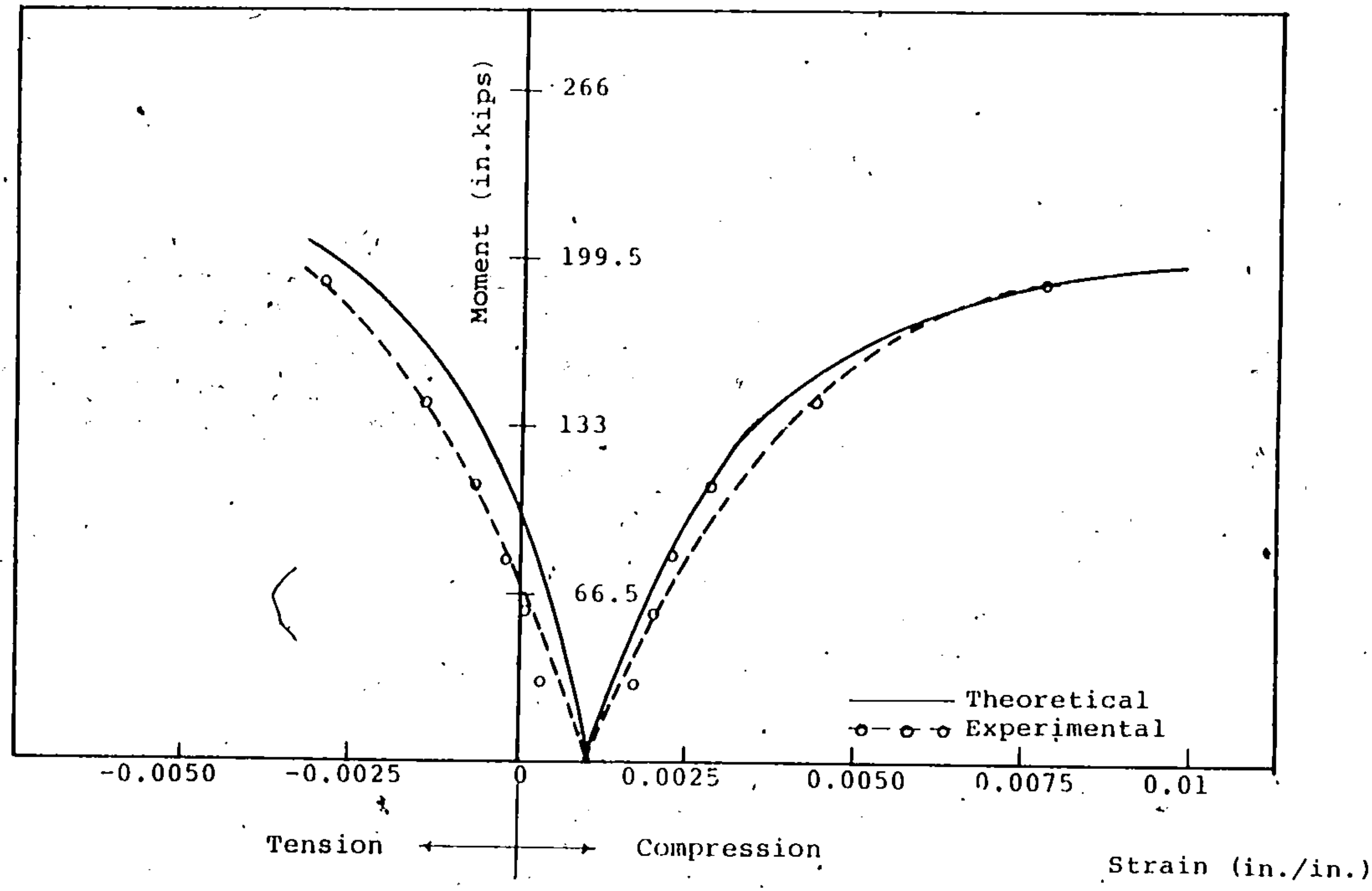

FIG. 20 MOMENT-STRAIN RELATIONSHIP FOR NS2

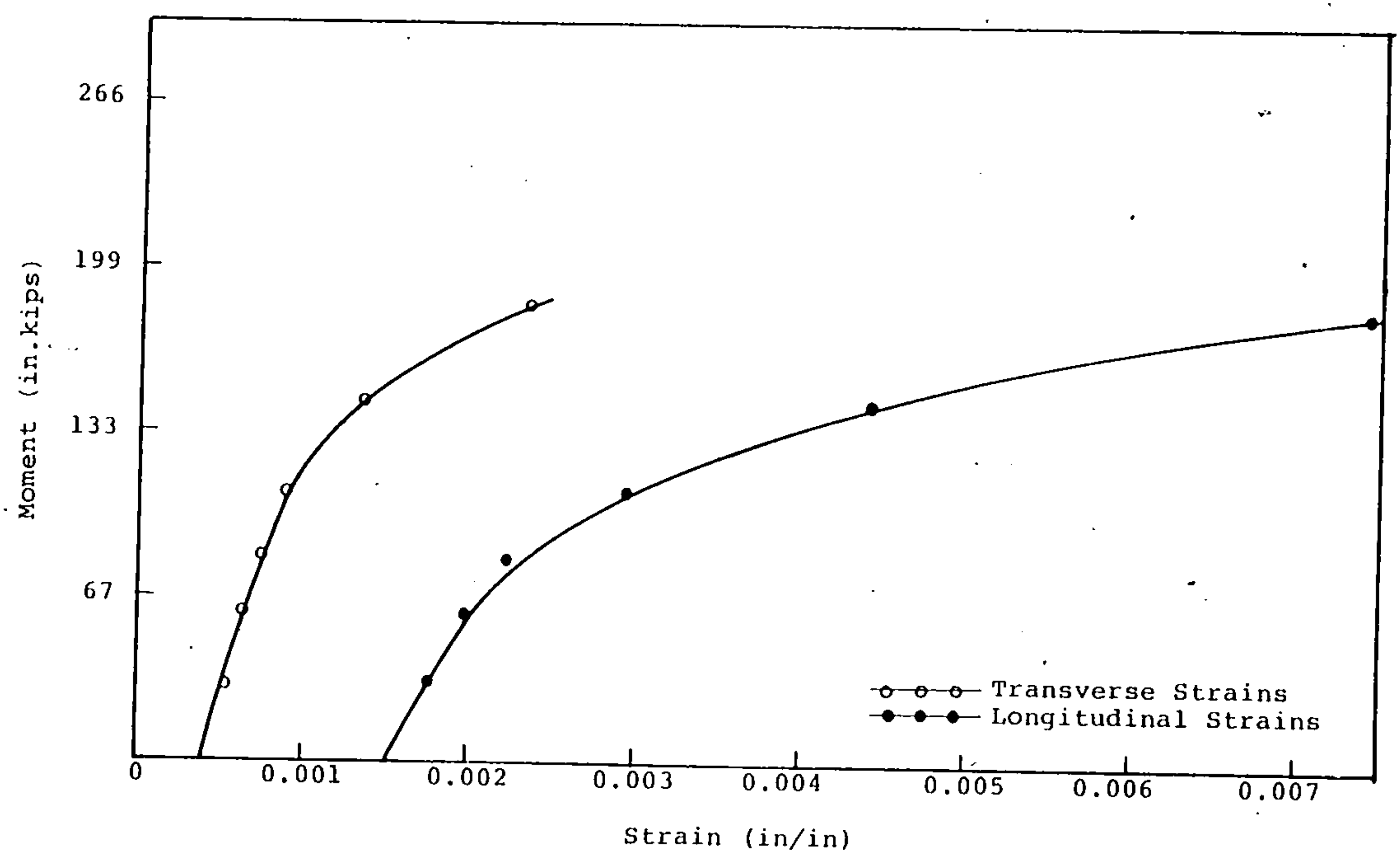

FIG. 21 LONGITUDINAL AND TRANSVERSE STRAIN VS. MOMENT FOR NS2 (COMPRESSIVE SIDE).

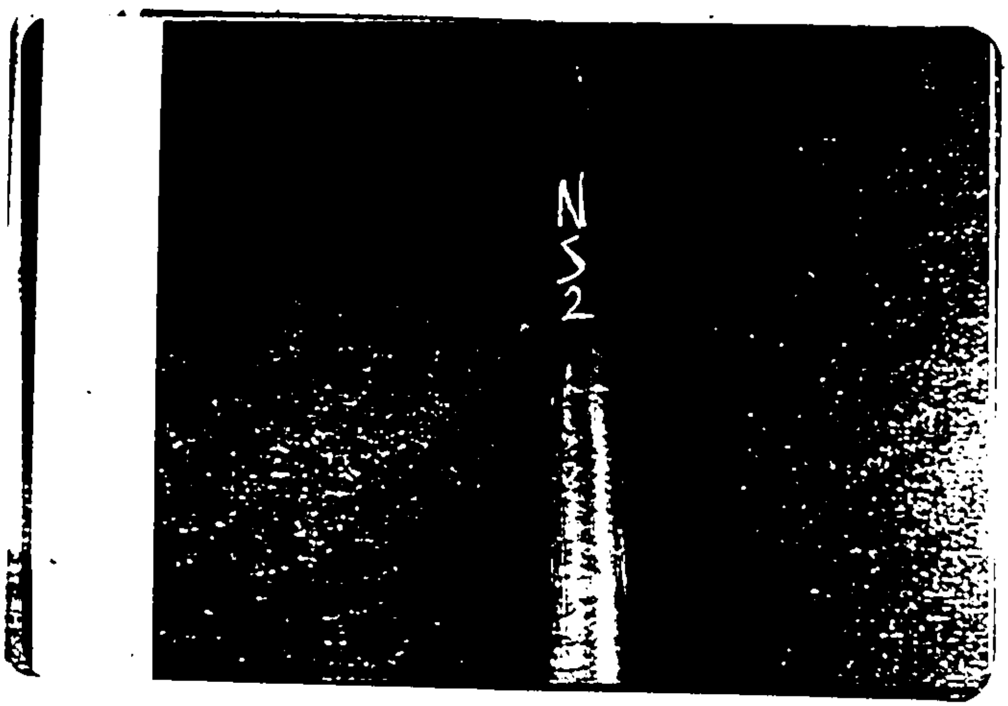

FIG. 22 CLOSE-UP VIEW OF NS2 AFTER THE TEST.

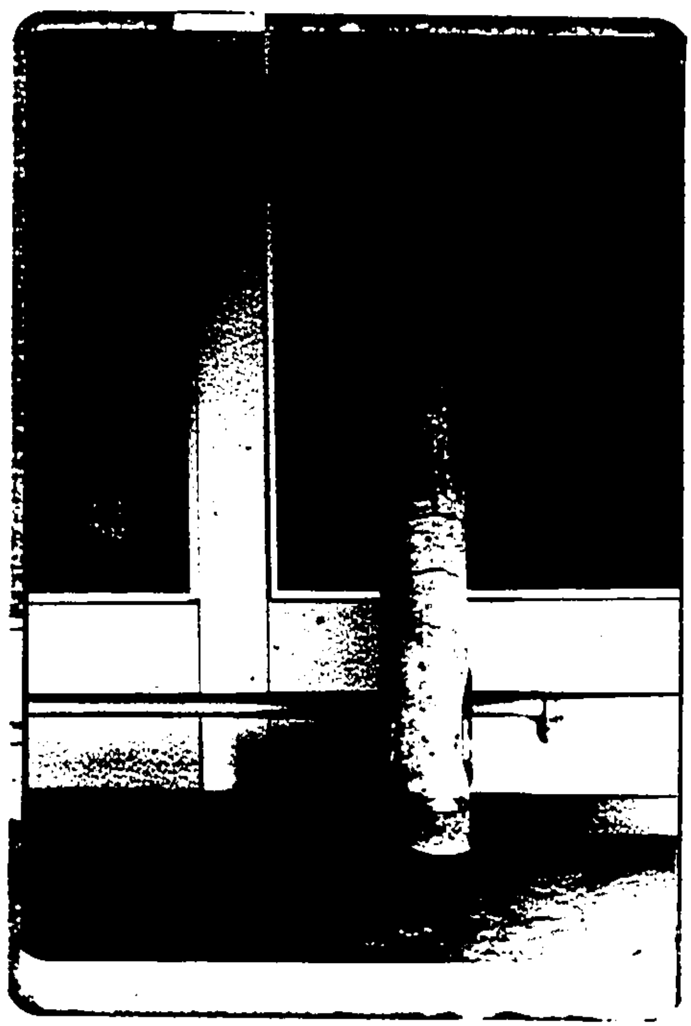

FIG. 23 CRACKS ON CONCRETE FOR NS2.

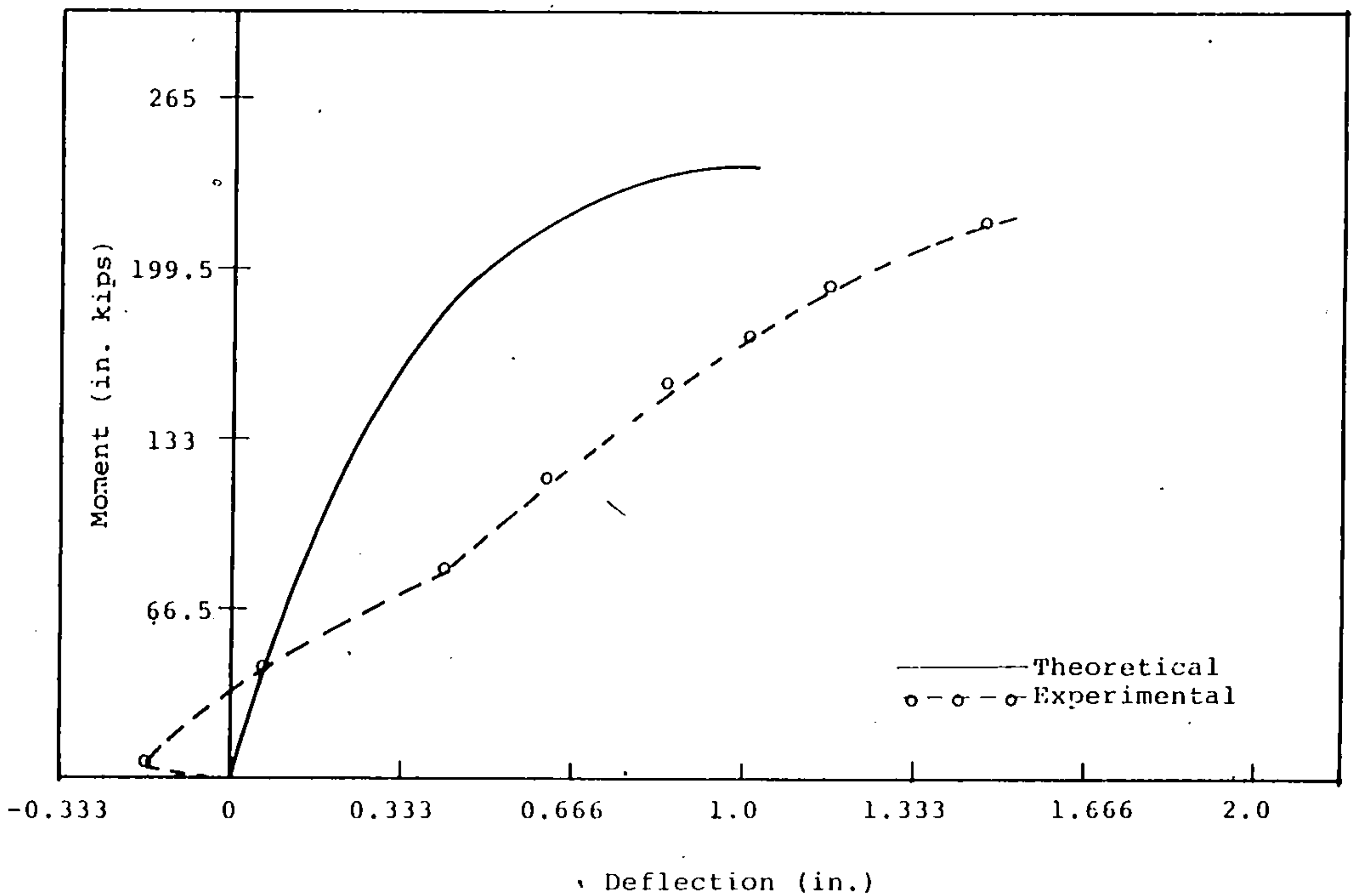

FIG. 24 MOMENT-DEFLECTION RELATIONSHIP FOR NS3.

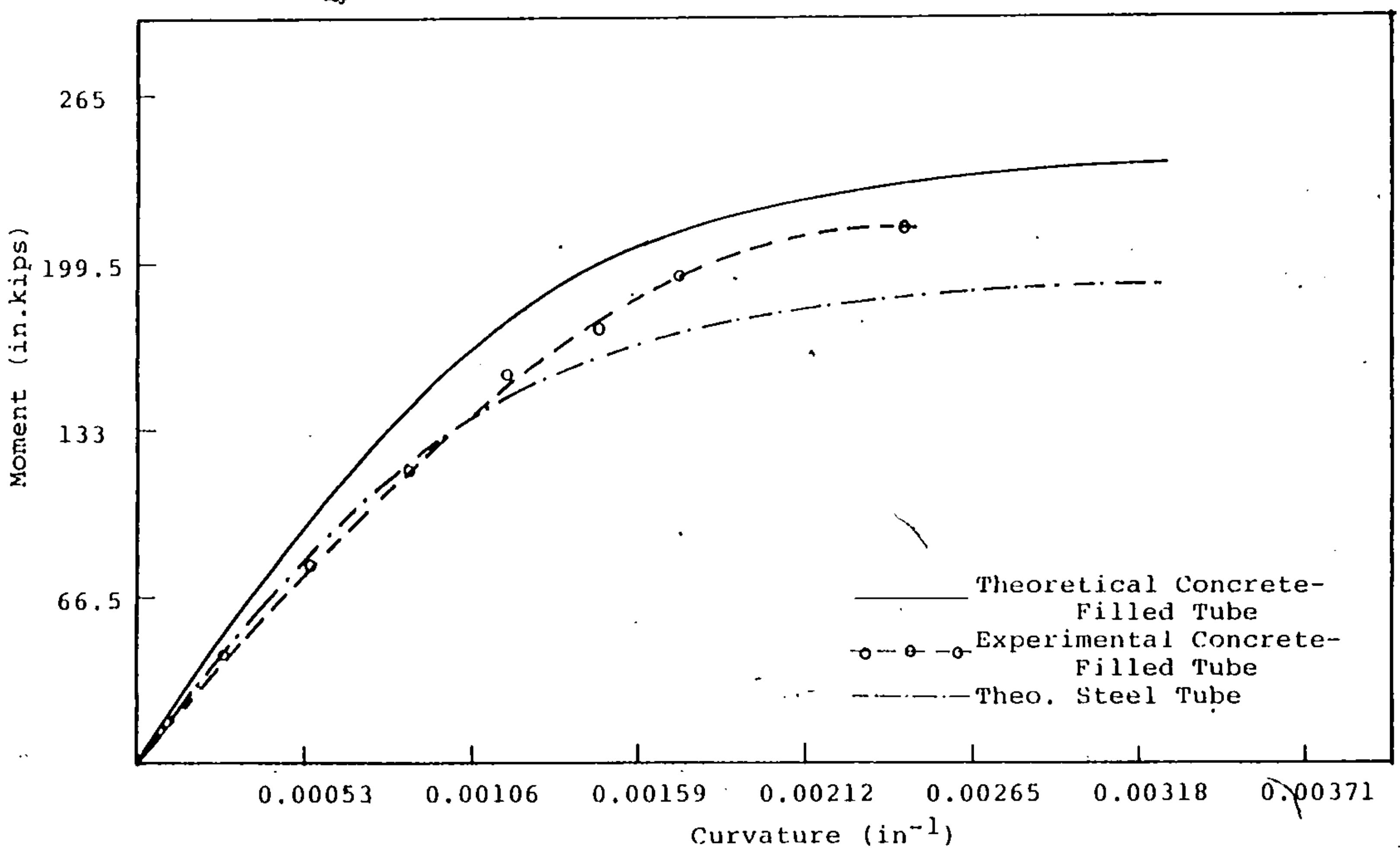

FIG. 25 MOMENT-CURVATURE RELATIONSHIP FOR NS3.

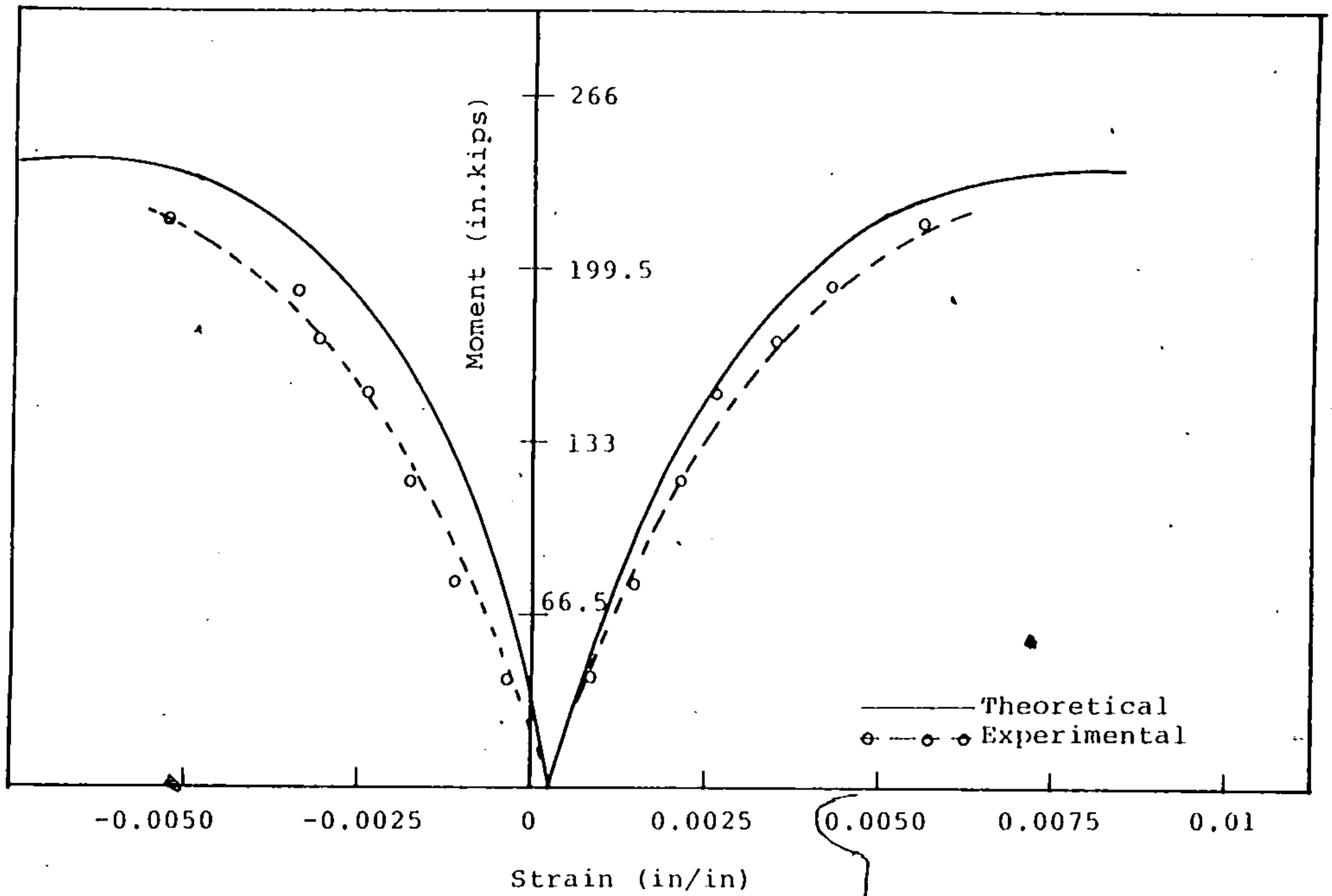

FIG. 26 MOMENT-STRAIN RELATIONSHIP FOR NS3.

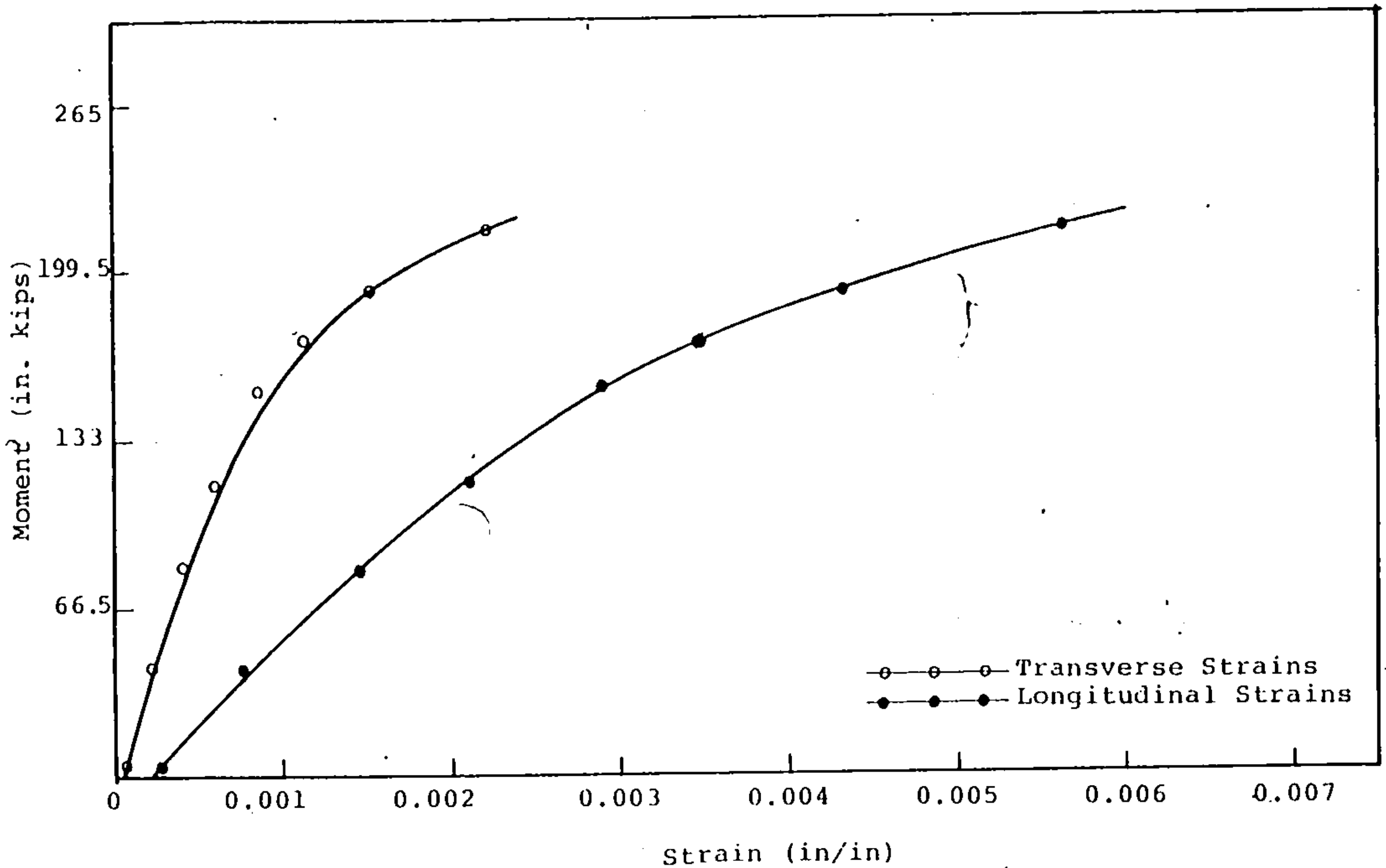

FIG. 27 LONGITUDINAL AND TRANSVERSE STRAIN VS. MOMENT FOR NS3 (COMPRESSIVE SIDE)

FIG. 28 COLUMN NS3 DURING THE TESTING.

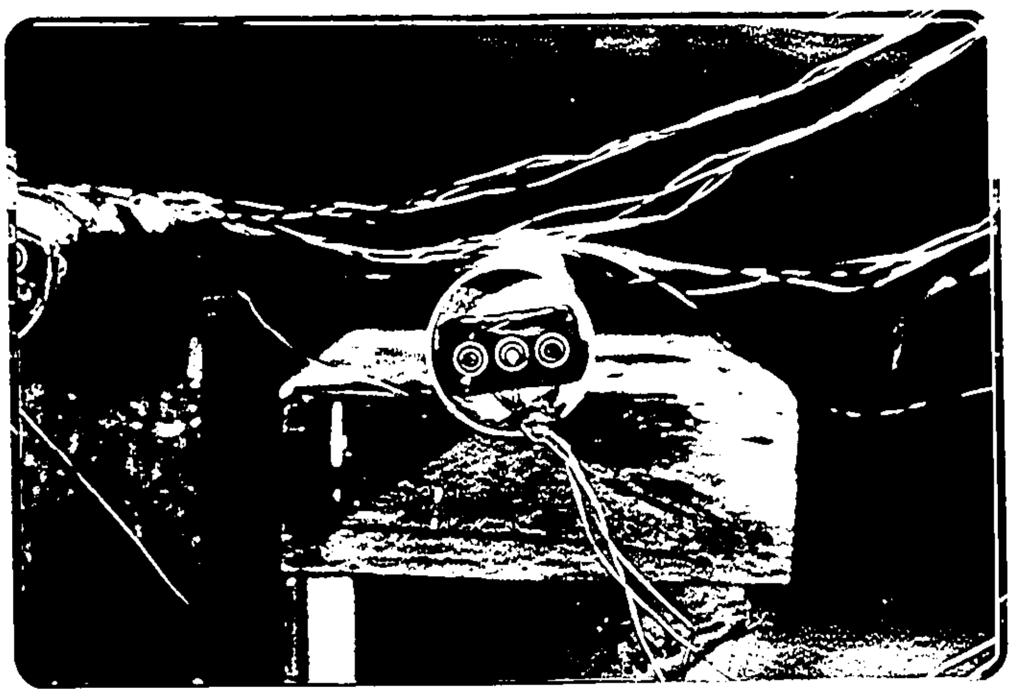

FIG. 29 COLUMN NS4 AFTER PRESTRESSING.

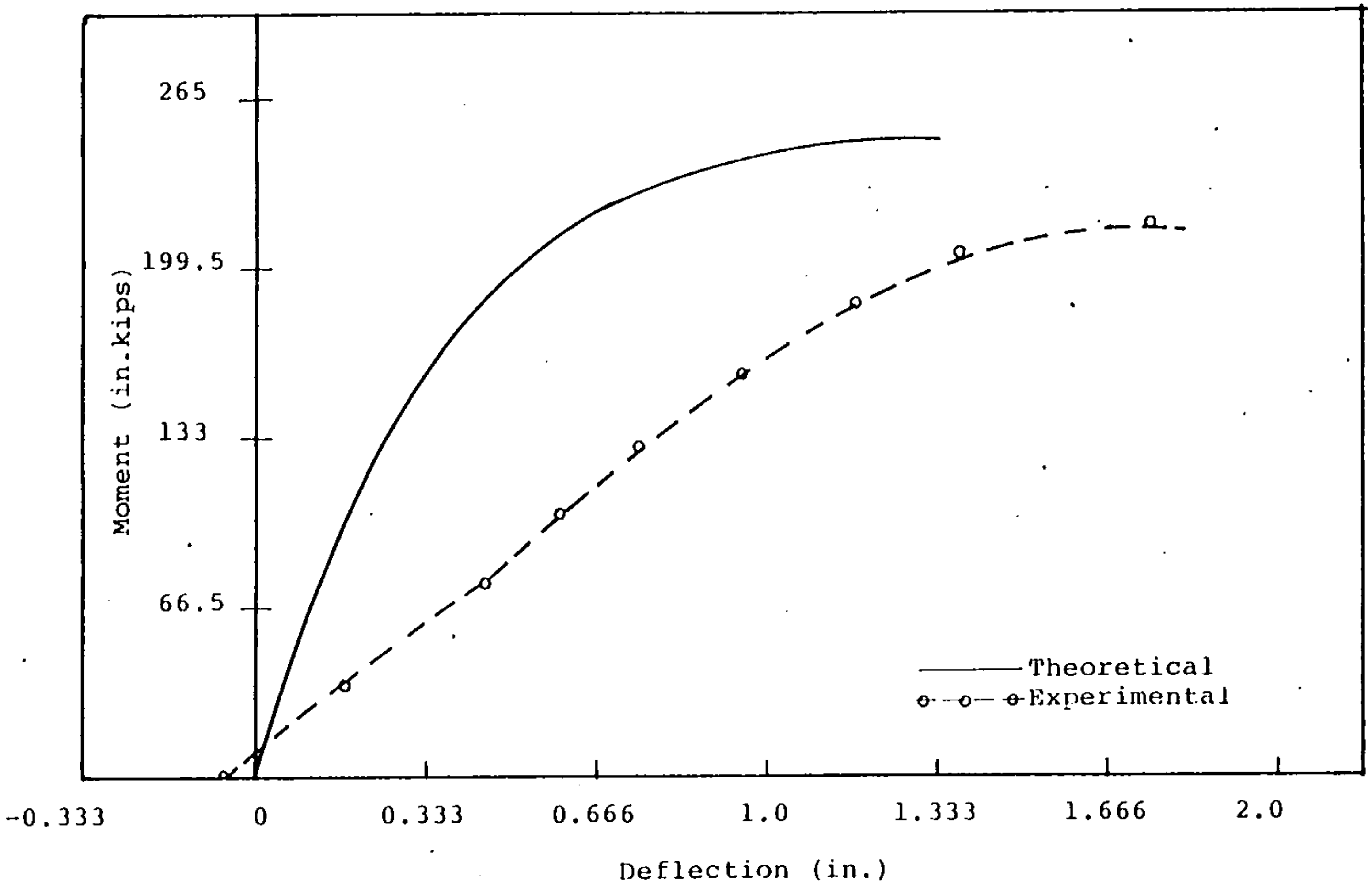

FIG. 30 MOMENT-DEFLECTION RELATIONSHIP FOR NS4.

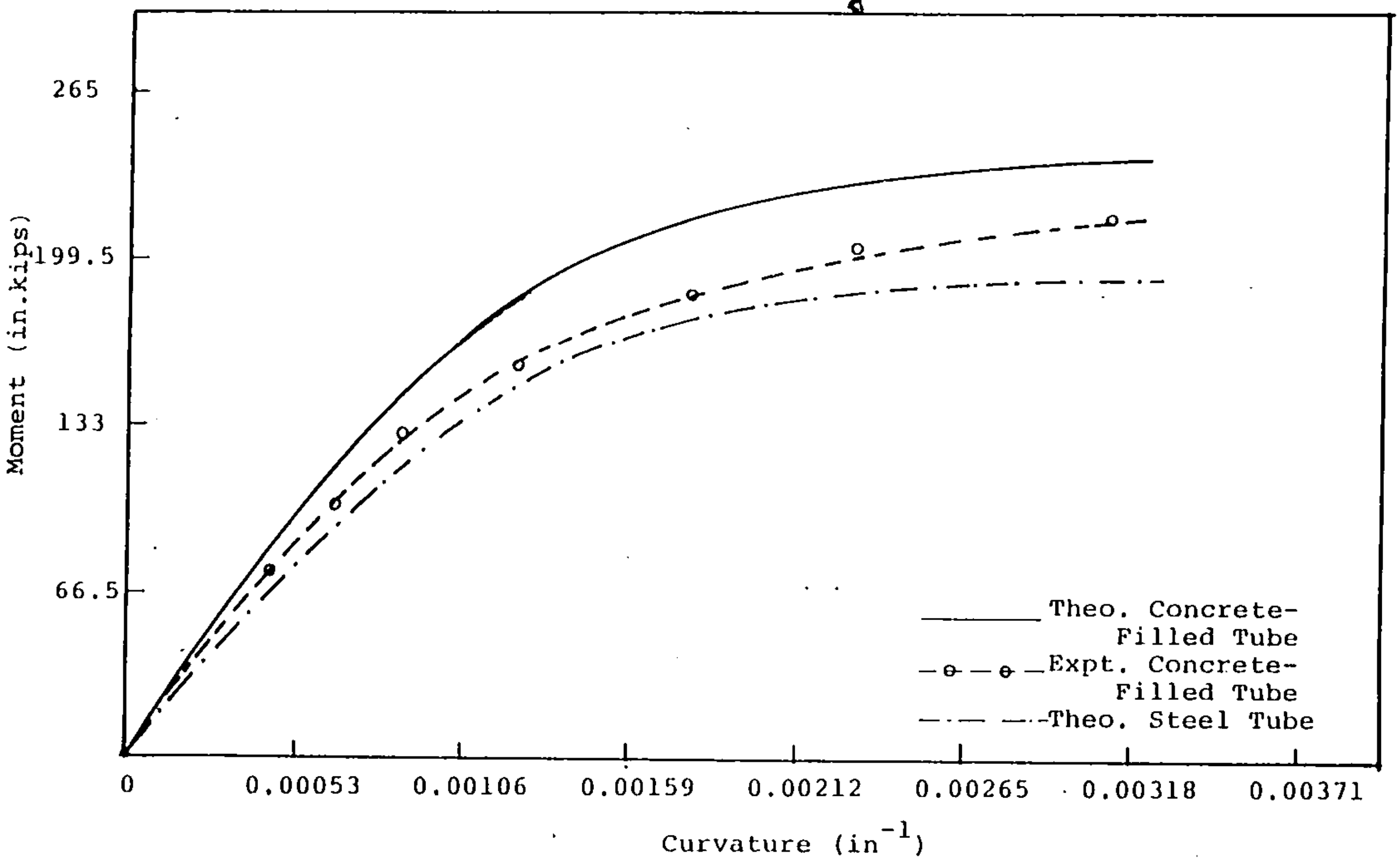

FIG. 31 MOMENT-CURVATURE RELATIONSHIP FOR NS4.

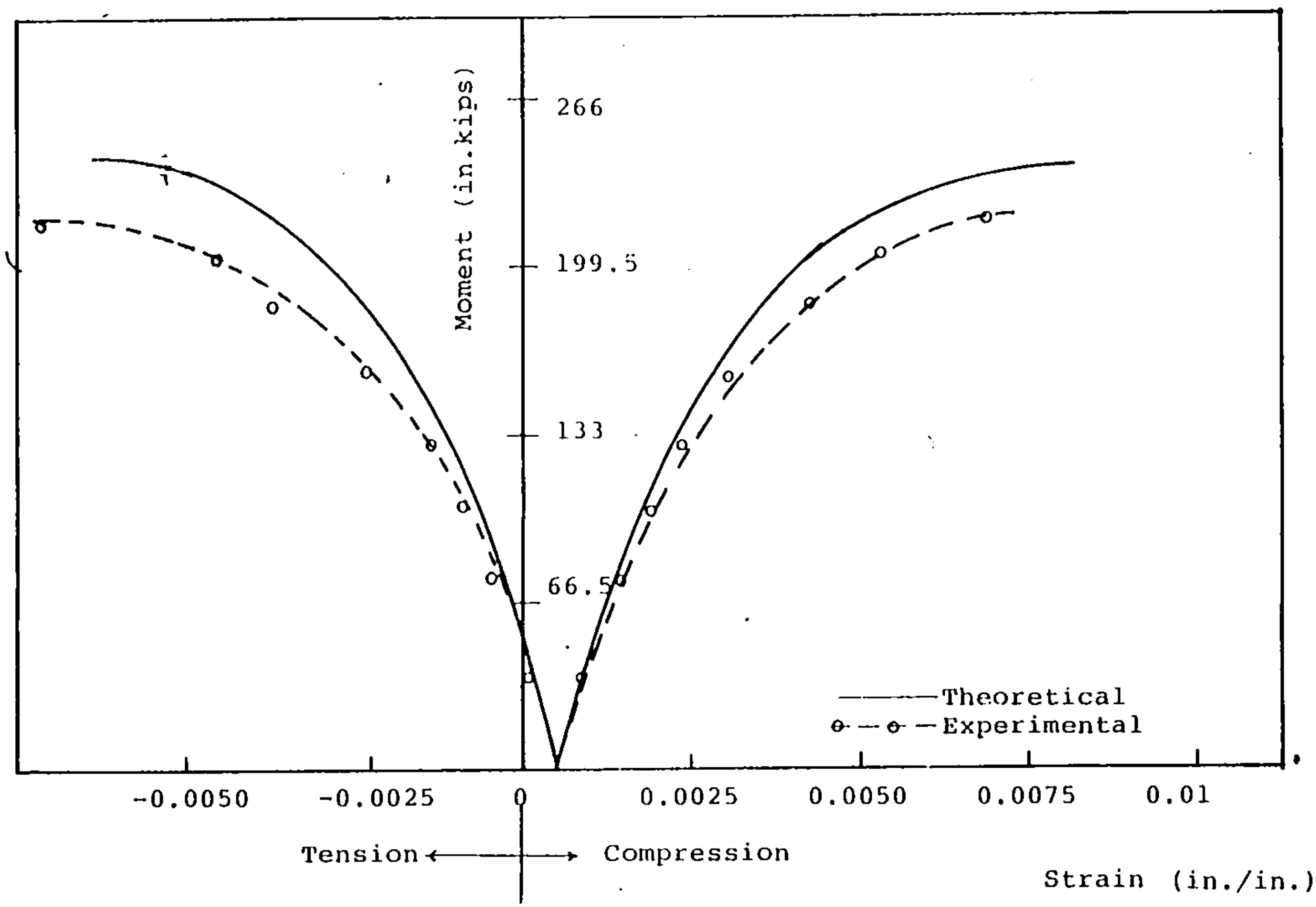

FIG. 32 MOMENT-STRAIN RELATIONSHIP FOR NS4.

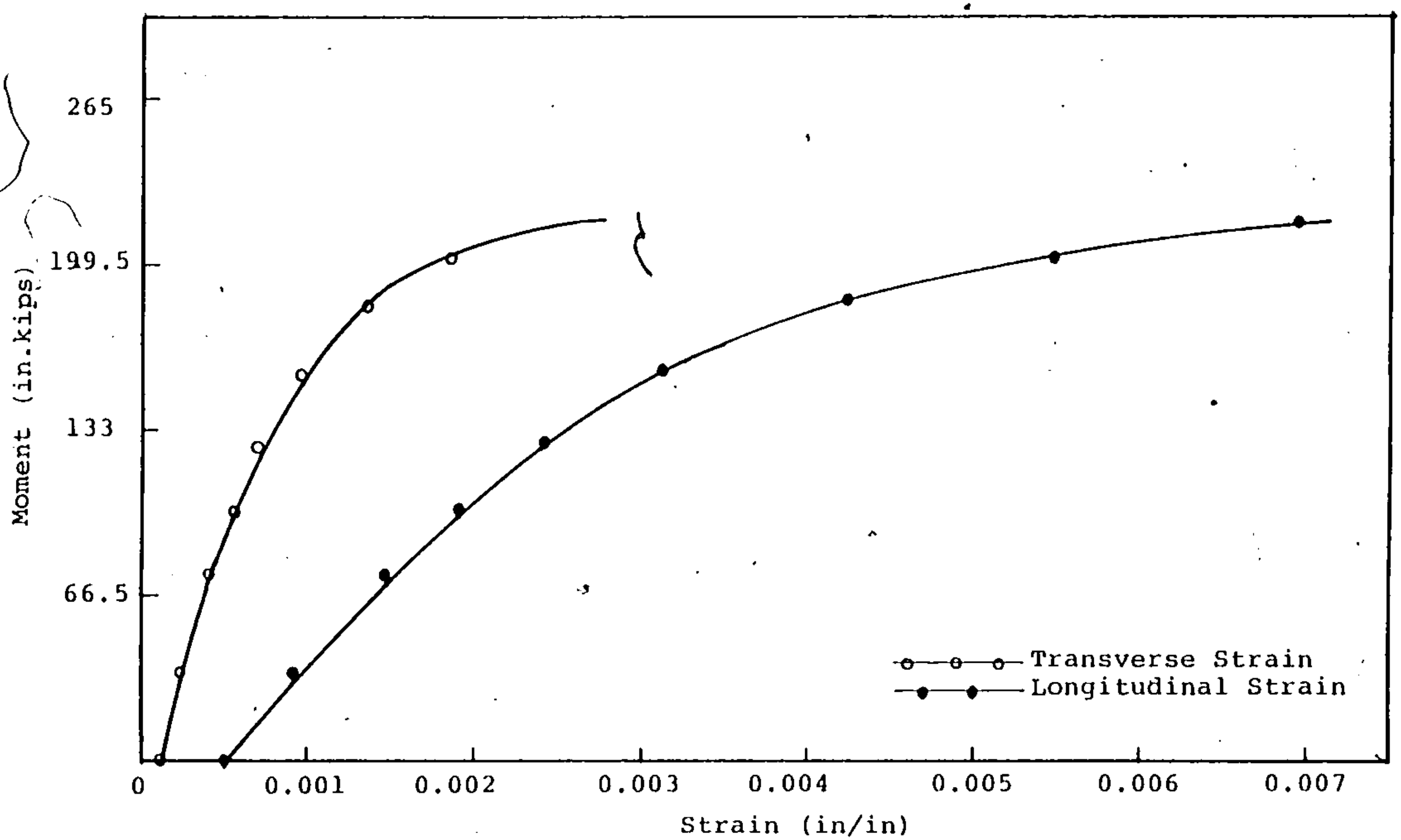

FIG. 33 LONGITUDINAL STRAIN AND TRANSVERSE STRAIN VS. MOMENT FOR NS4 (COMPRESSIVE SIDE).

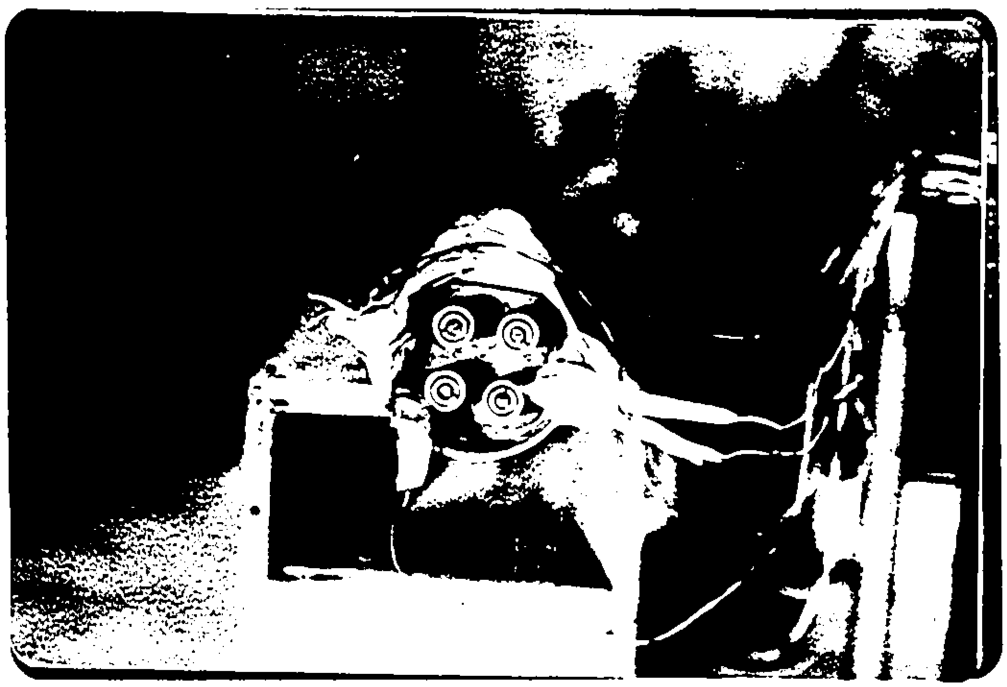

FIG. 34 COLUMN NS5 AFTER PRESTRESSING.

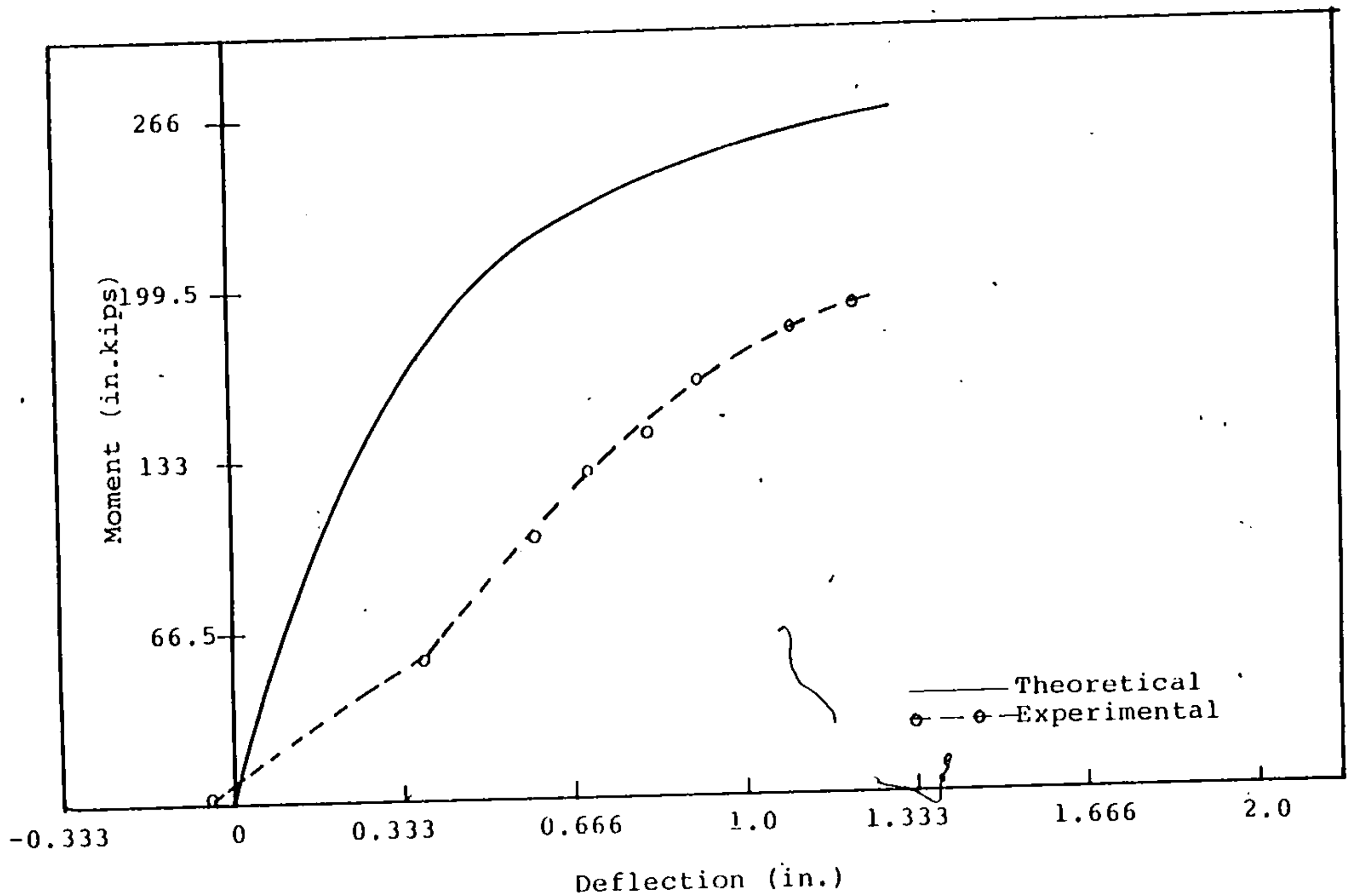

FIG. 35 MOMENT-DEFLECTION RELATIONSHIP FOR NS5.

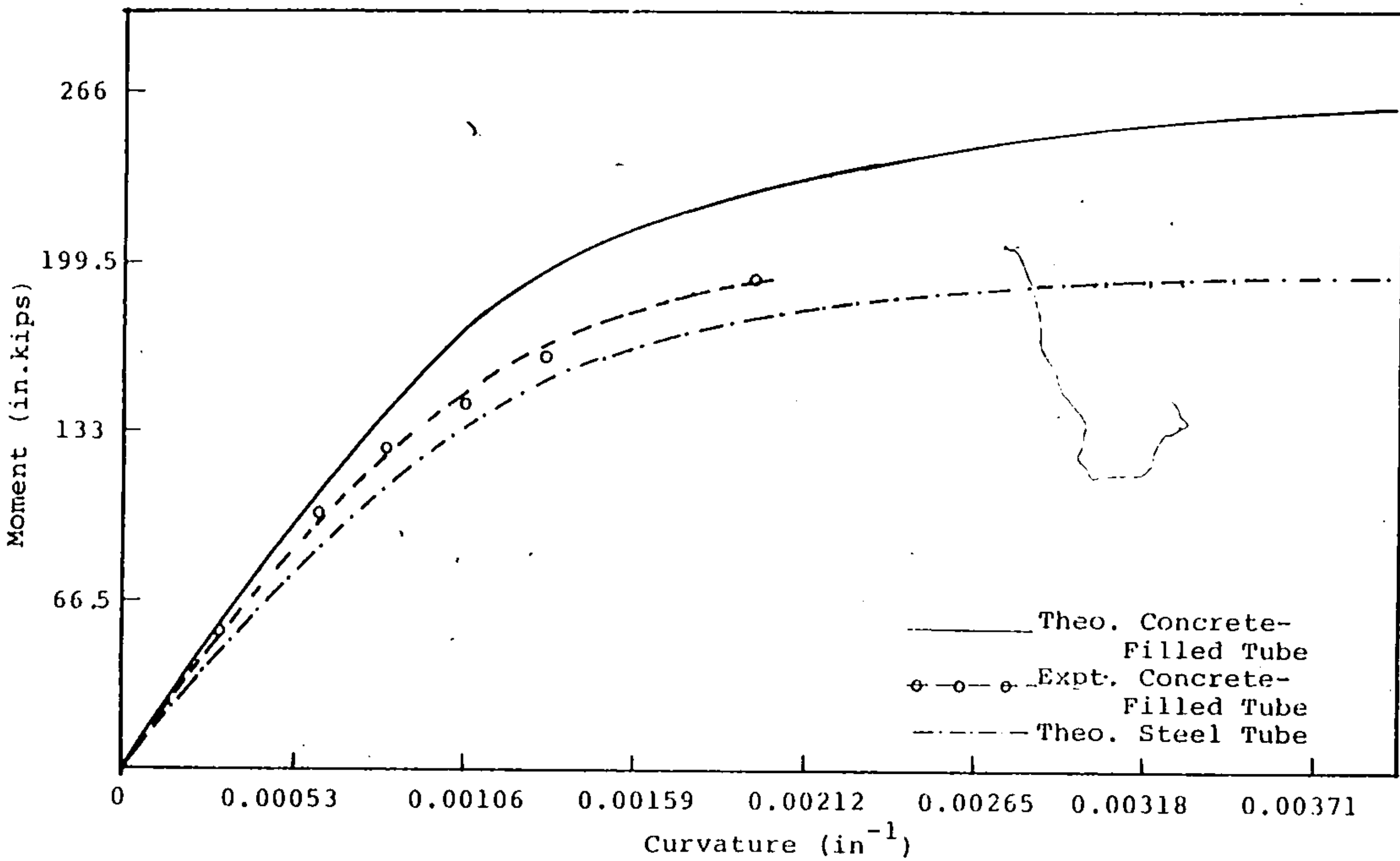

FIG. 36 MOMENT-CURVATURE RELATIONSHIP FOR NS5.

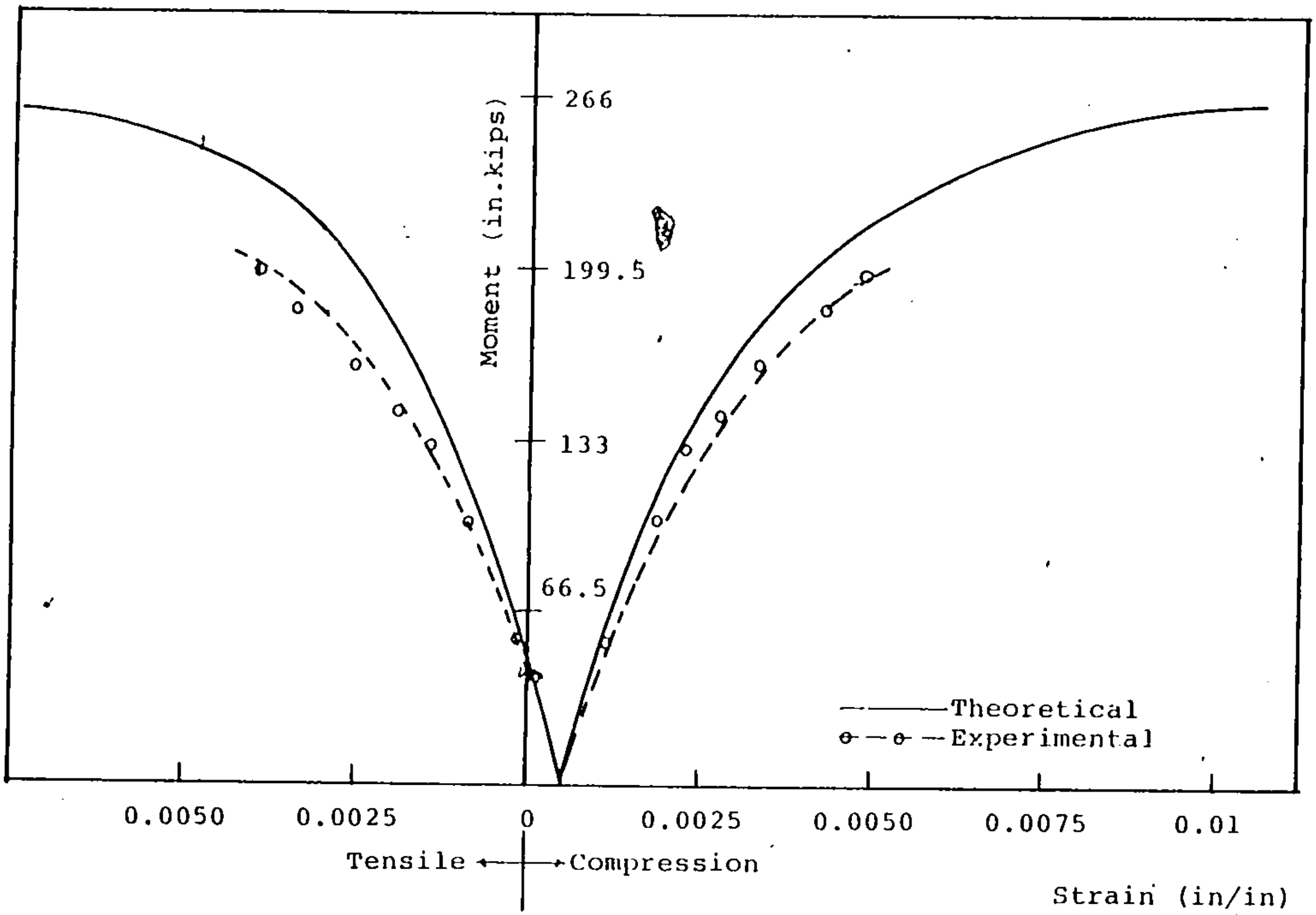

FIG. 37 MOMENT-STRAIN RELATIONSHIP FOR NS5.

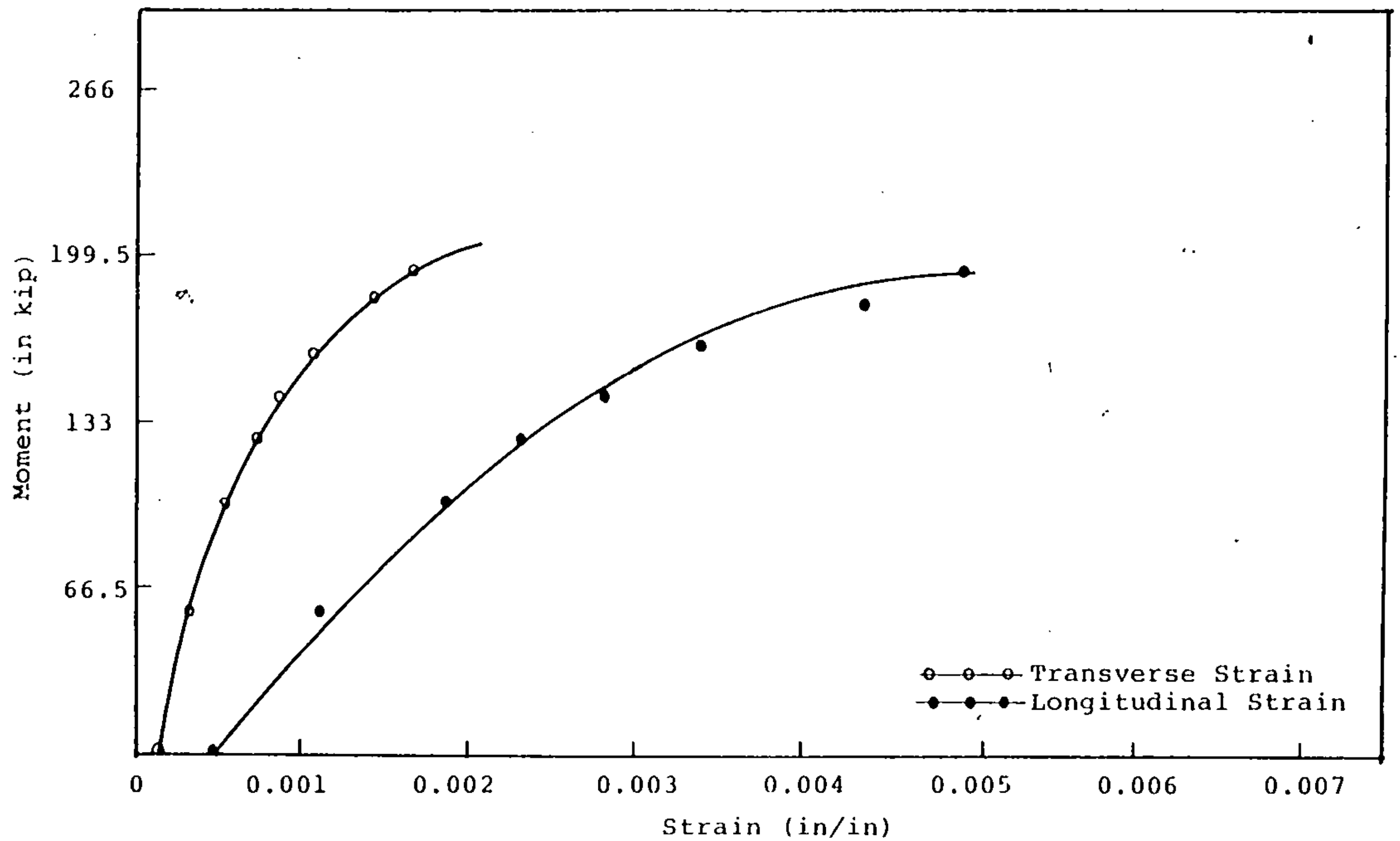

FIG. 38 LONGITUDINAL STRAIN AND TRANSVERSE STRAIN VS. MOMENT FOR NS5 (COMPRESSIVE SIDE).

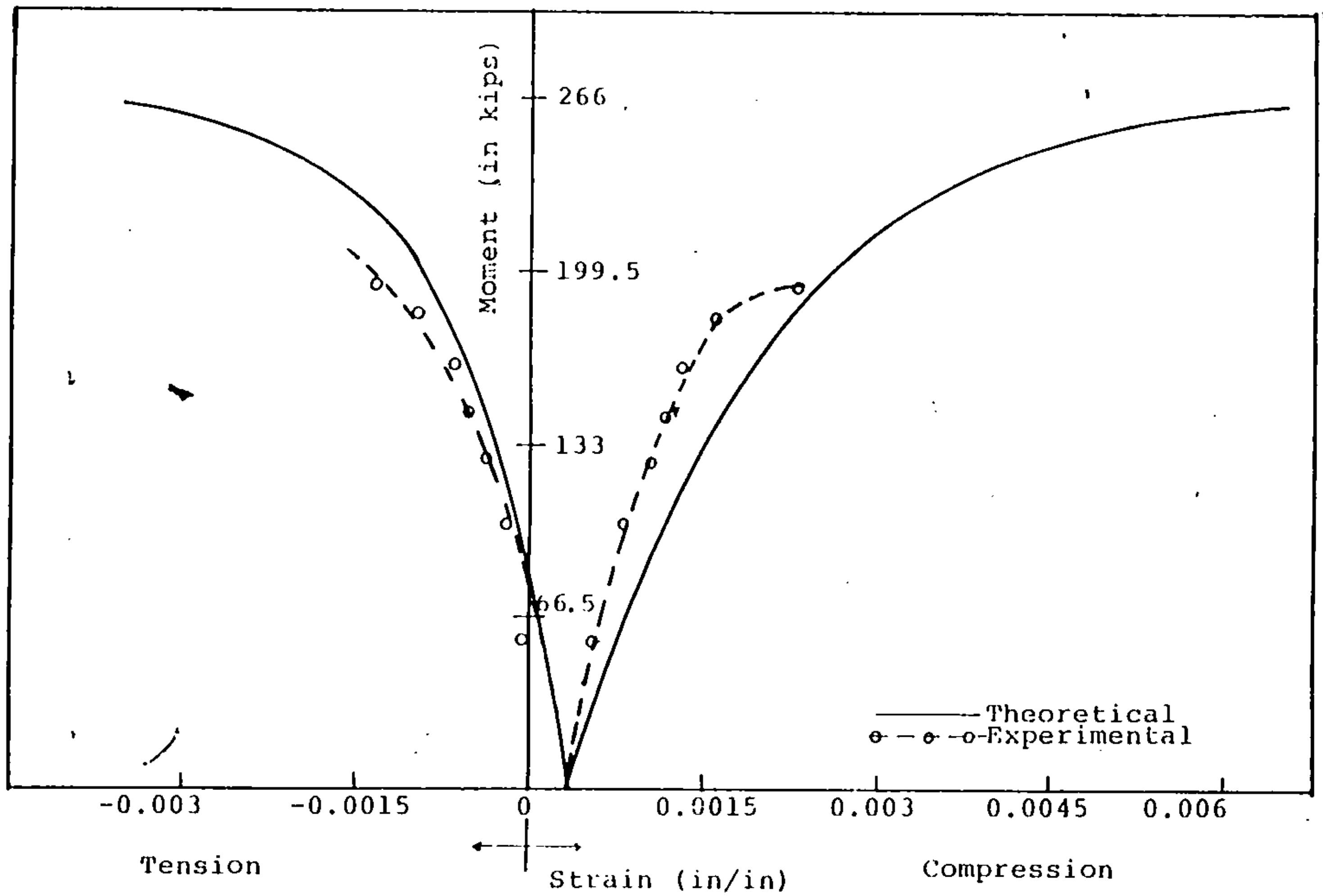

FIG. 39 STRAIN IN PRESTRESSING TENDONS VS. MOMENT FOR NS5.

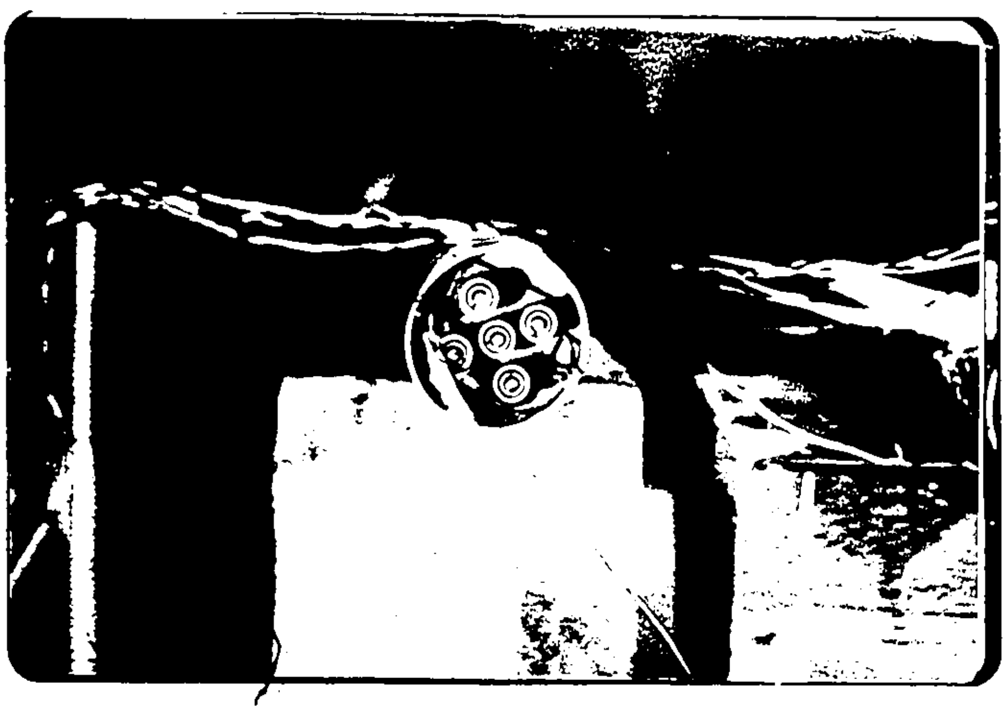

FIG. 40. COLUMN NS6 AFTER PRESTRESSING.

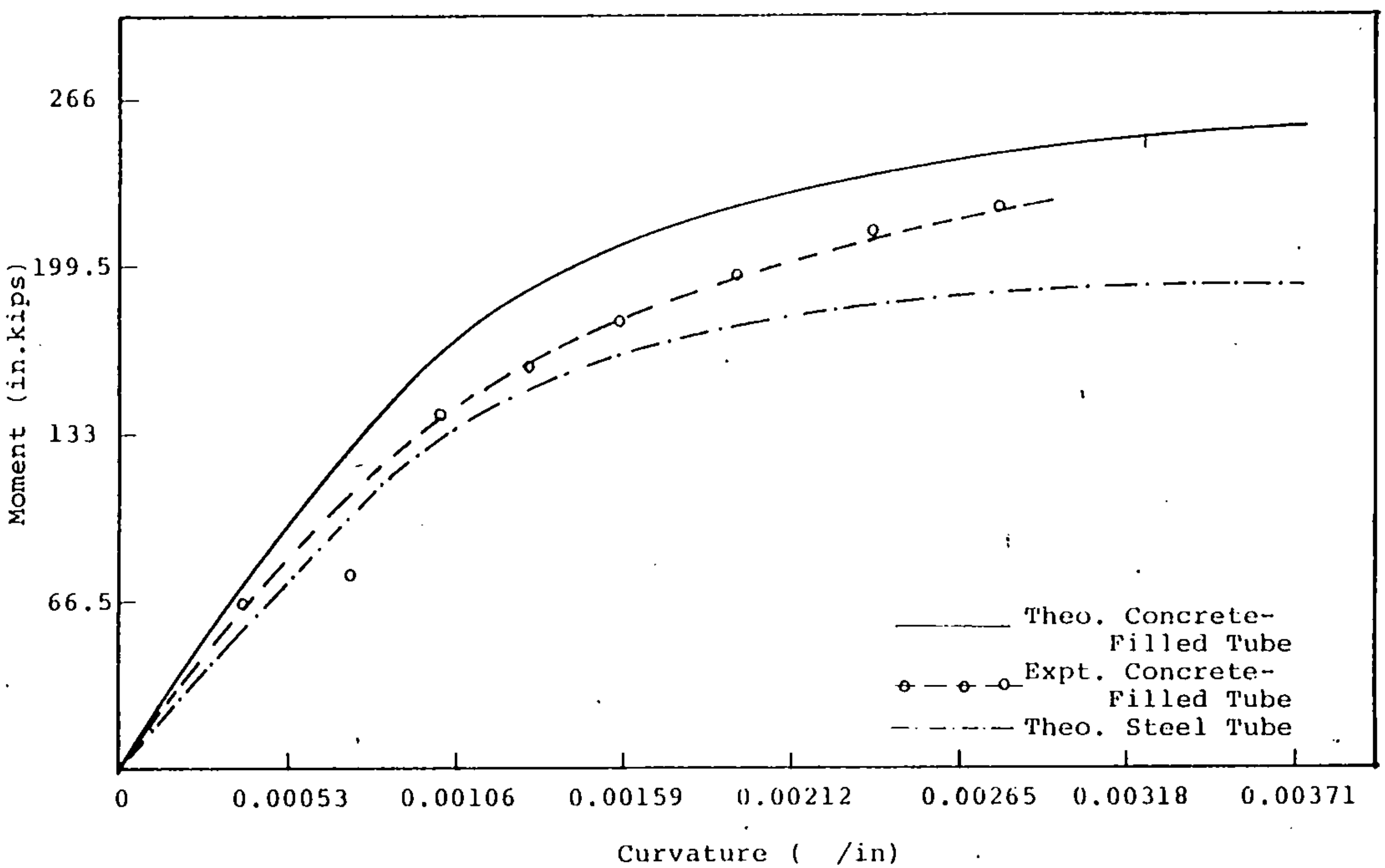

FIG. 41 MOMENT-CURVATURE RELATIONSHIP FOR NS6.

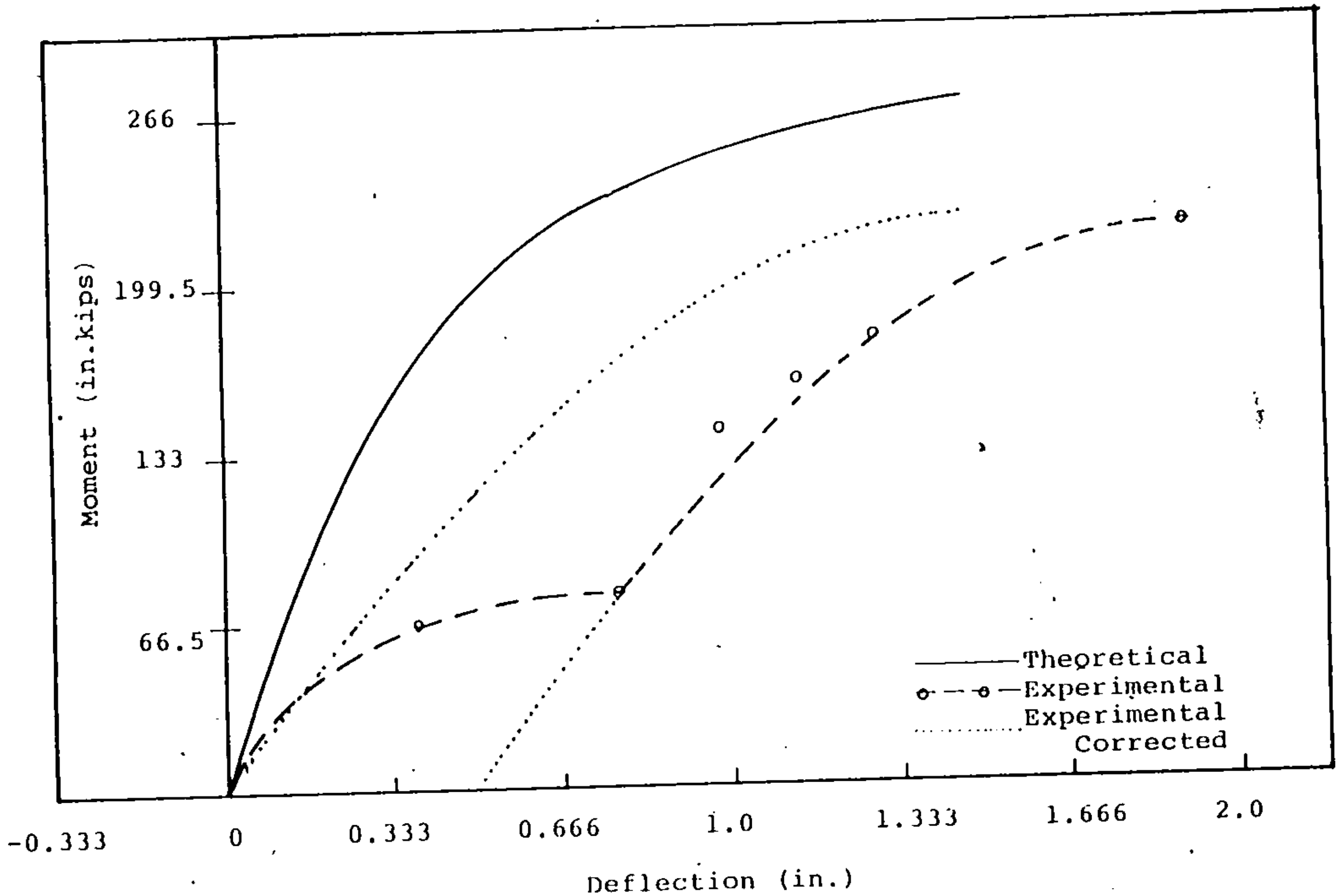

FIG. 42 MOMENT-DEFLECTION RELATIONSHIP FOR NS6.

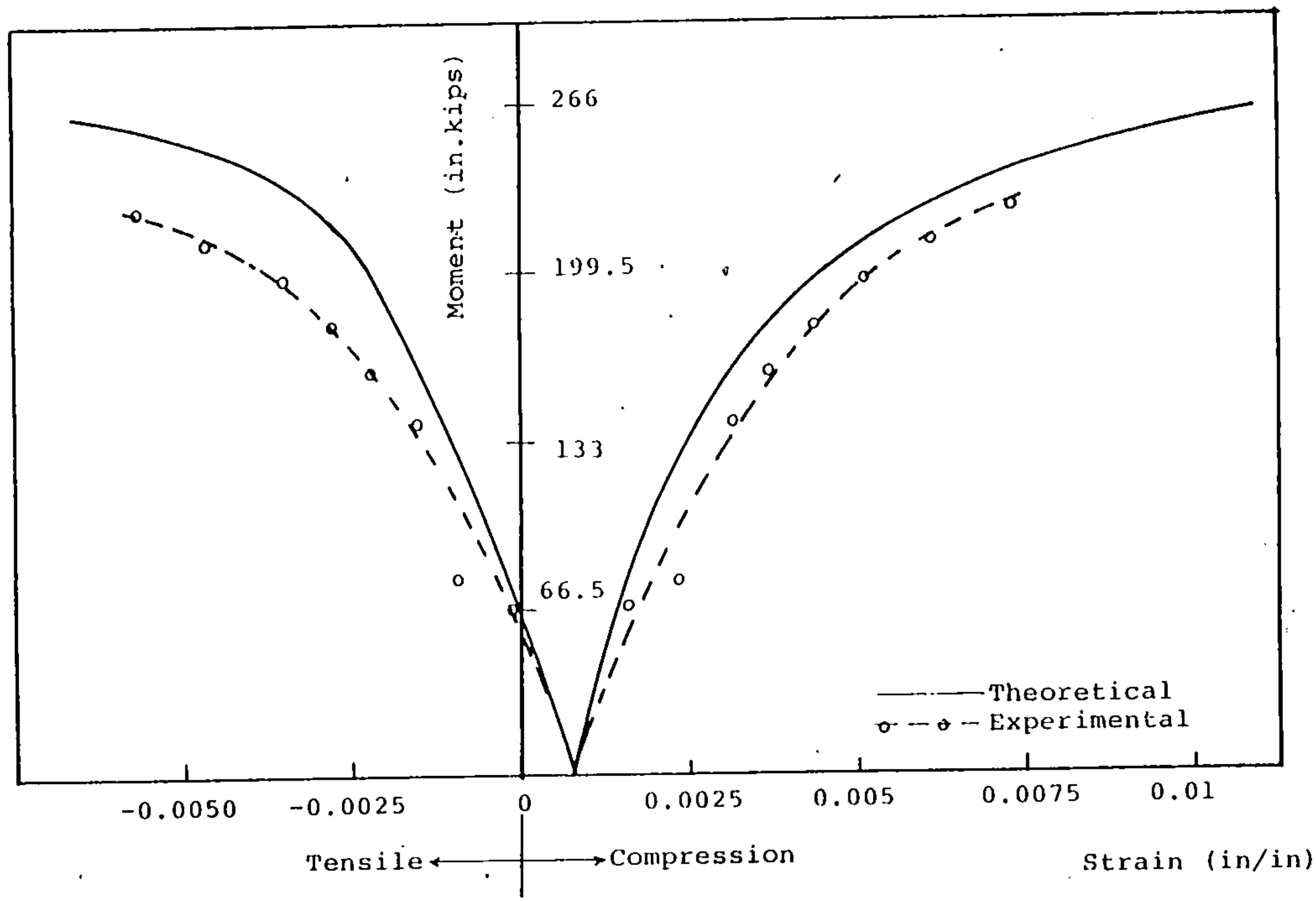

FIG. 43 MOMENT-STRAIN RELATIONSHIP FOR NS6.

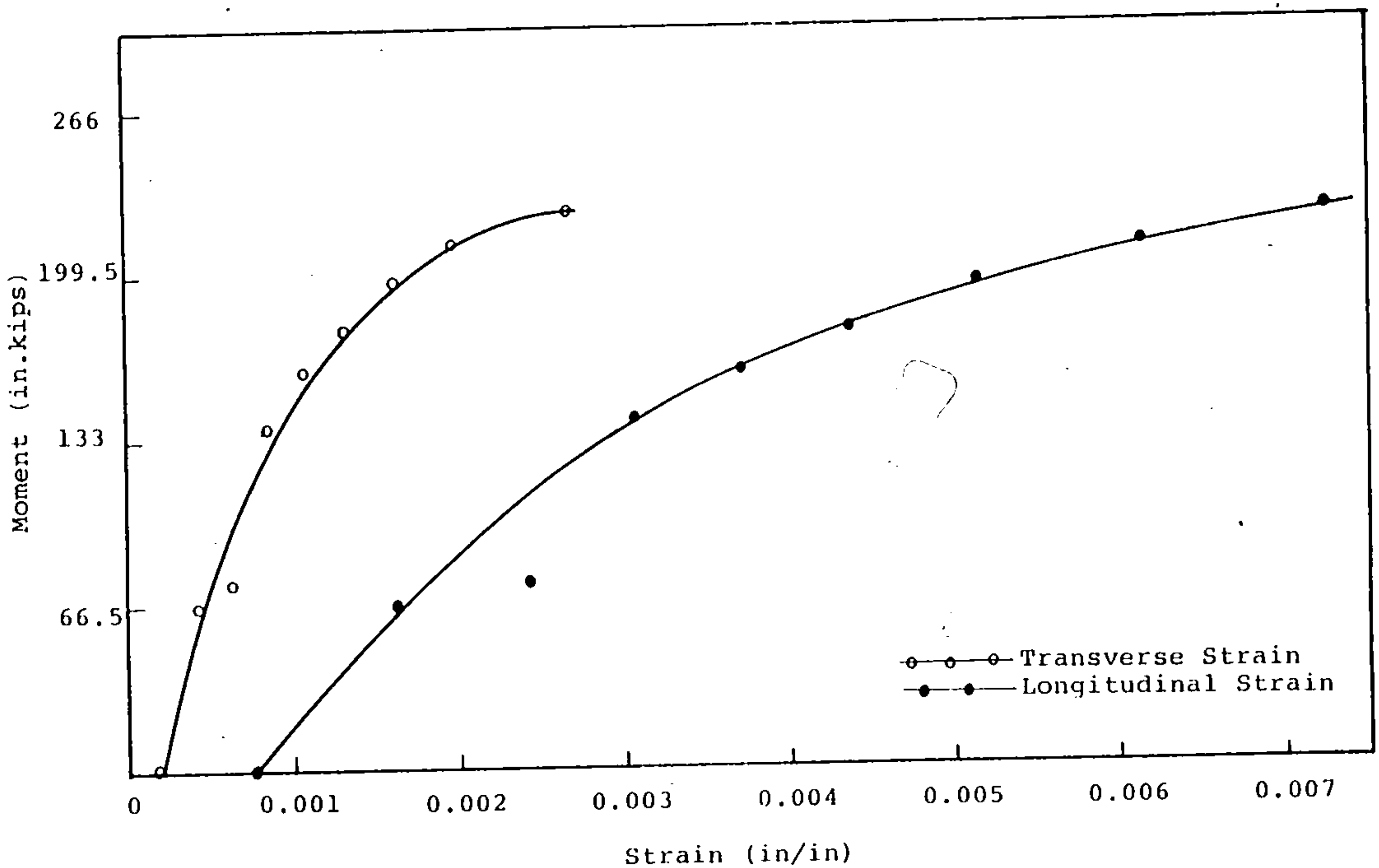

FIG. 44 LONGITUDINAL STRAIN AND TRANSVERSE STRAIN VS. MOMENT FOR NS6 (COMPRESSION SIDE).

FIG. 45 COLUMN NS6 DURING THE TESTING.

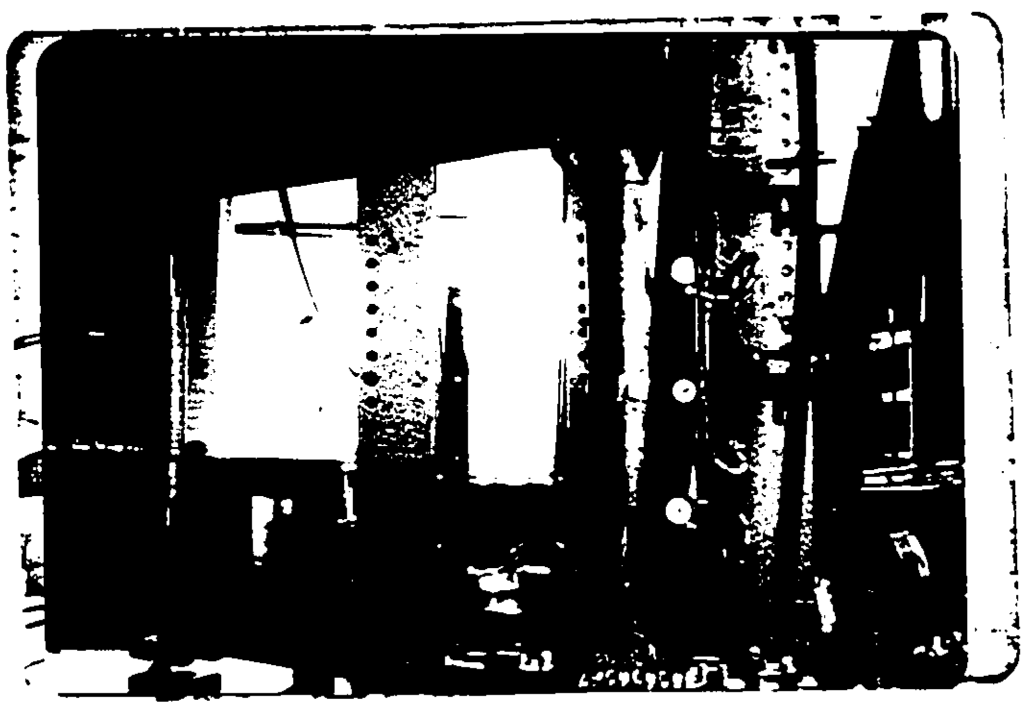

FIG. 46 COLUMN NS6 DURING THE TESTING SHOWING THE DEFLECTION GAUGES.

S. No	DESIGNATION	TYPE	DIMENSIONS OF STEEL TUBE	CONCRETE STRENGTH AT THE TIME OF TESTING	CONSTANT AXIAL LOAD APPLIED
1	NS1	Nonprestressed	Outer Diameter Equals 4.5" Thickness Equals 0.133"	6000 psi	70.0 kips
2	NS2	Prestressed with two tendons.		7000 psi	105.0 kips
3	NS3	Prestressed with two tendons.		6000 psi	20.0 kips
4	NS4	Prestressed with three tendons.		6000 psi	20.0 kips
5	NS5	Prestressed with four tendons.		6000 psi	20.0 kips
6	NS6	Prestressed with five tendons.		6000 psi	20.0 kips

TABLE 1 CLASSIFICATION OF COLUMNS

Column	Experimental Maximum Moment (in kips)	Experimental Maximum Curvature (in^{-1})	Theoretical Moments Correspond to Curvatures in Col.3	$\frac{M_{exp.}}{M_{th.}}$
NS1	207	0.0028	223	0.93
NS2	191	0.0024	195	0.98
NS3	216	0.0024	233	0.93
NS4	218	0.0031	240	0.91
NS5	195	0.0020	219	0.89
NS6	218	0.0028	255	0.85

TABLE 2 COMPARISON BETWEEN THEORETICAL AND EXPERIMENTAL MOMENTS

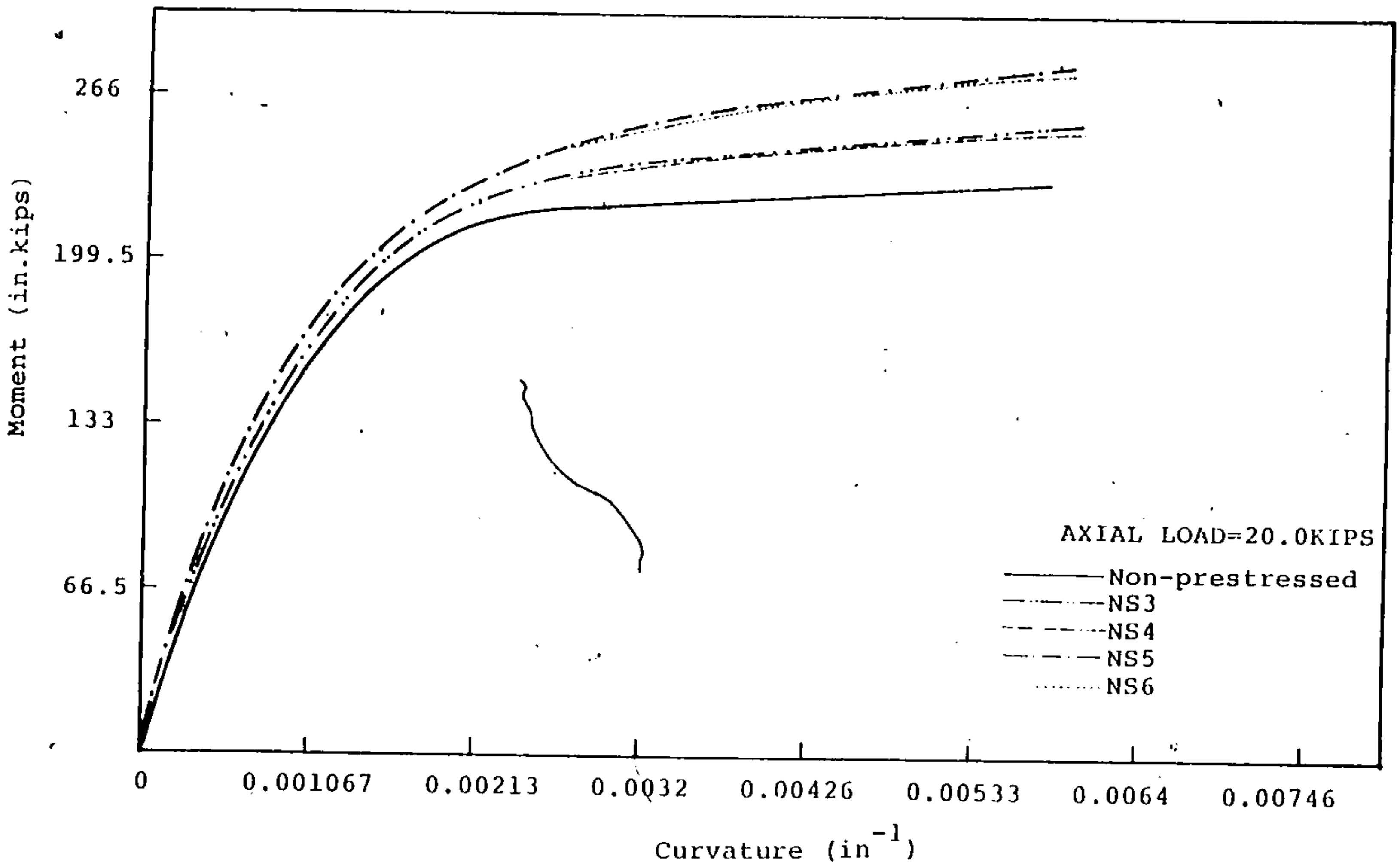

FIG. 47 MOMENT-CURVATURE RELATIONSHIPS.

Column	Theoretical Moment at a Curvature of $0.0056 in^{-1}$ (in kip)	Theoretical Moment of a Nonprestressed Section (in kip)	Increase in Moment (in kip)	% Increase Over Non-Prestressed	Contribution of Steel (in kip)	Contribution of Concrete (in kip)	% Increase in Concrete Contribution Over Nonpre-stressed
NS3	254	231	21	9.1	200	54	74
NS4	255	231	24	10.3	200	55	77
NS5	279	231	48	20.8	200	79	155
NS6	280	231	49	21.2	200	80	158

TABLE 3 COMPARISON OF STRENGTHS BETWEEN NONPRESTRESSED AND PRESTRESSED COLUMNS AT A CURVATURE OF $0.0056\ in^{-1}$.

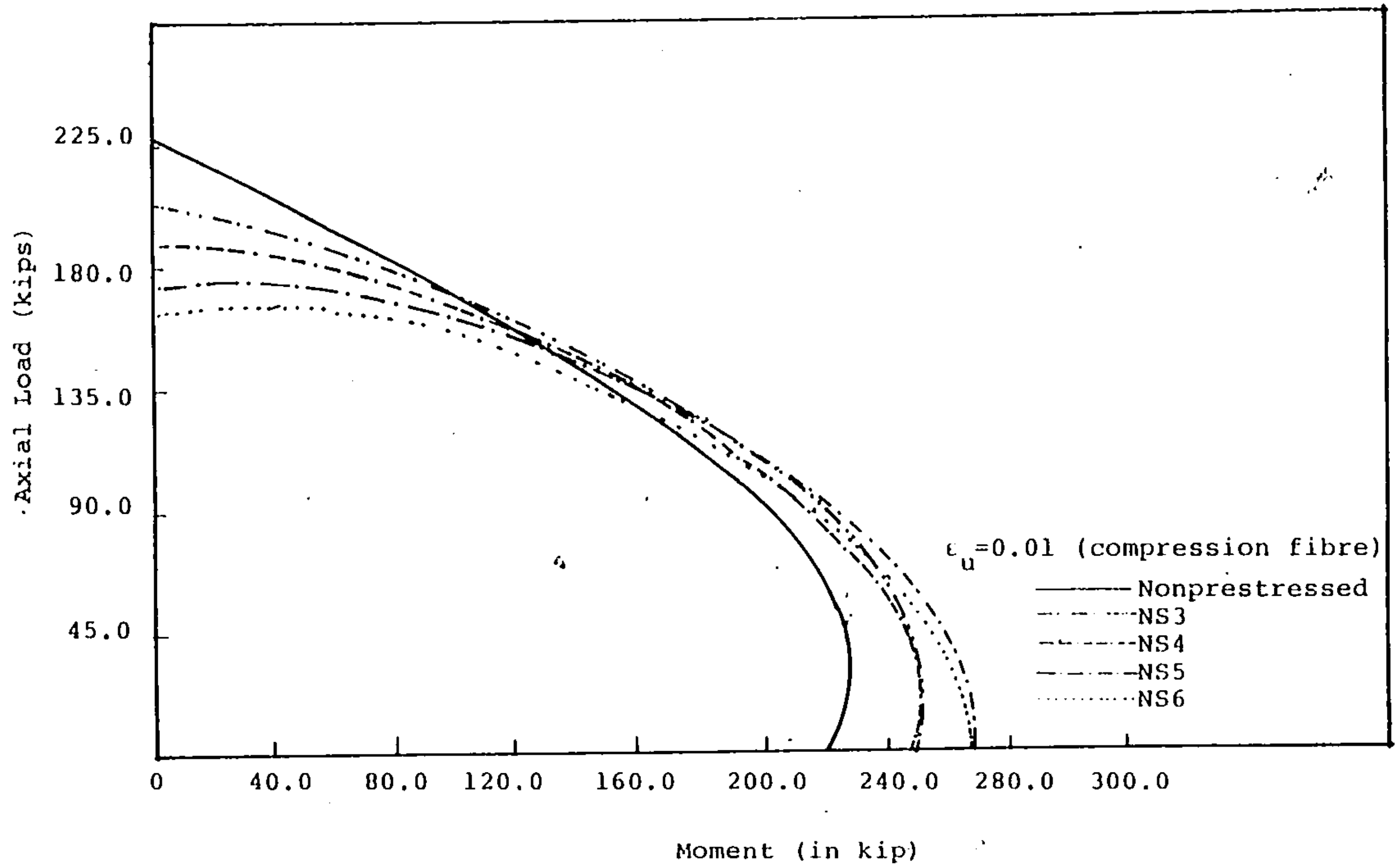

FIG. 48 INTERACTION DIAGRAM.

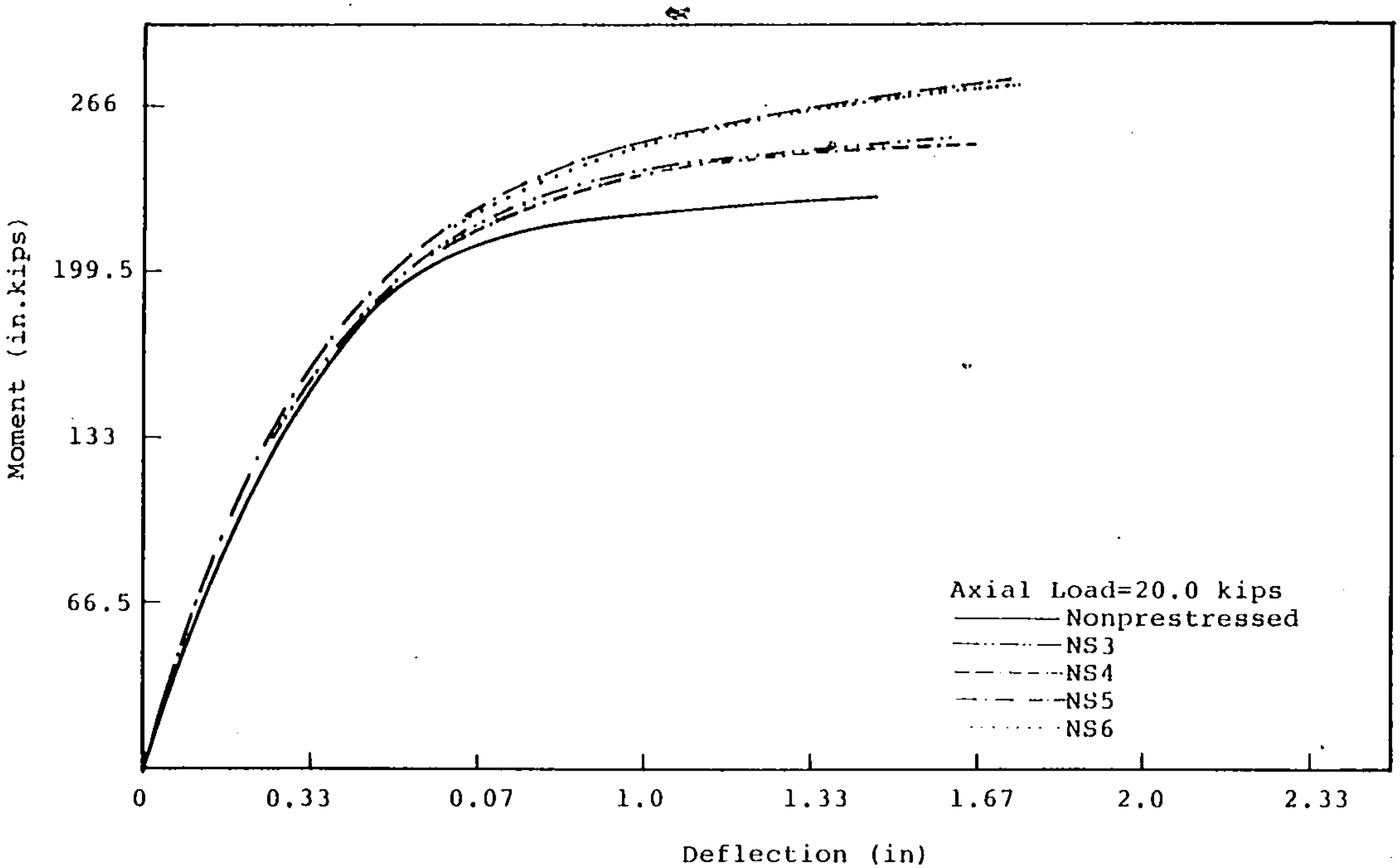

FIG. 49 MOMENT-DEFLECTION RELATIONSHIPS.

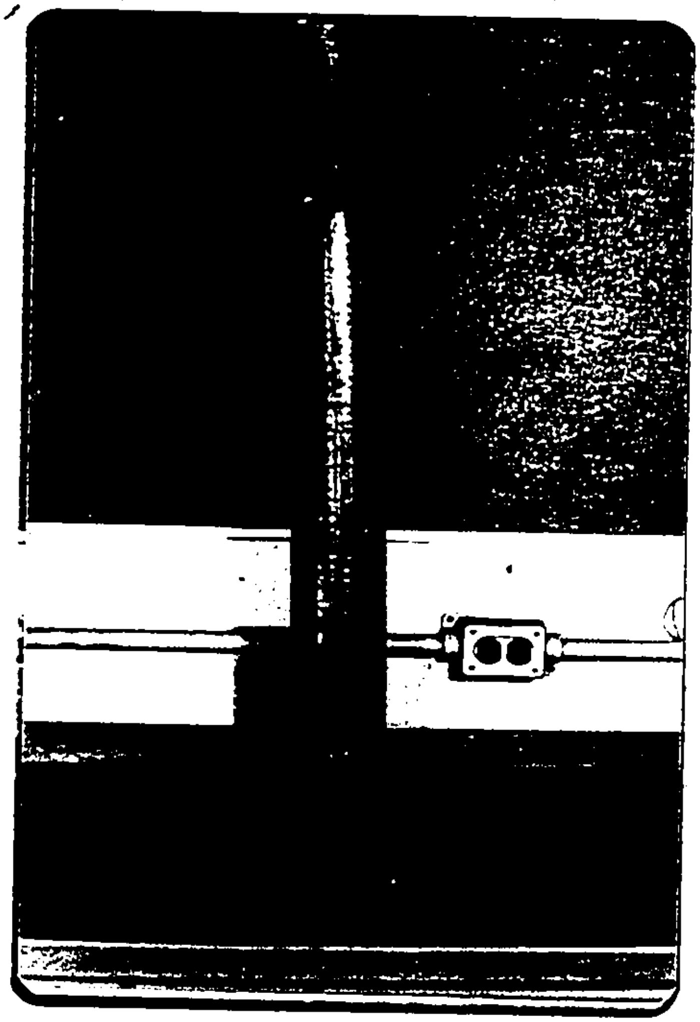

FIG. 50 TYPICAL COLUMN AFTER TEST (NOTE THE LOCAL BUCKLING OF STEEL TUBE AT TOP).

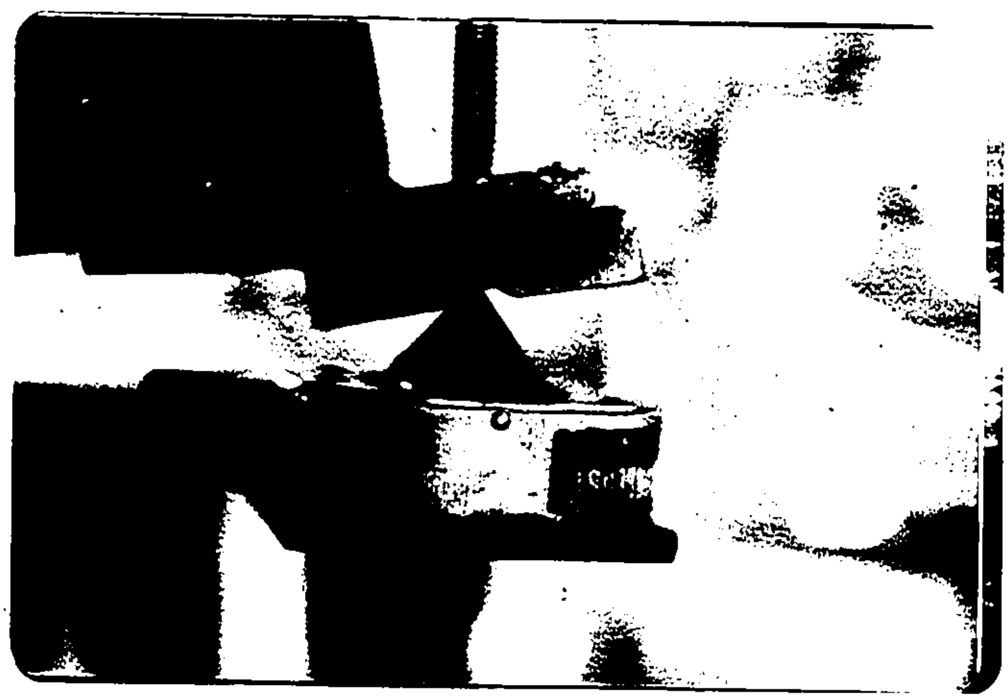

FIG. 51 BOTTOM KNIFE EDGE.

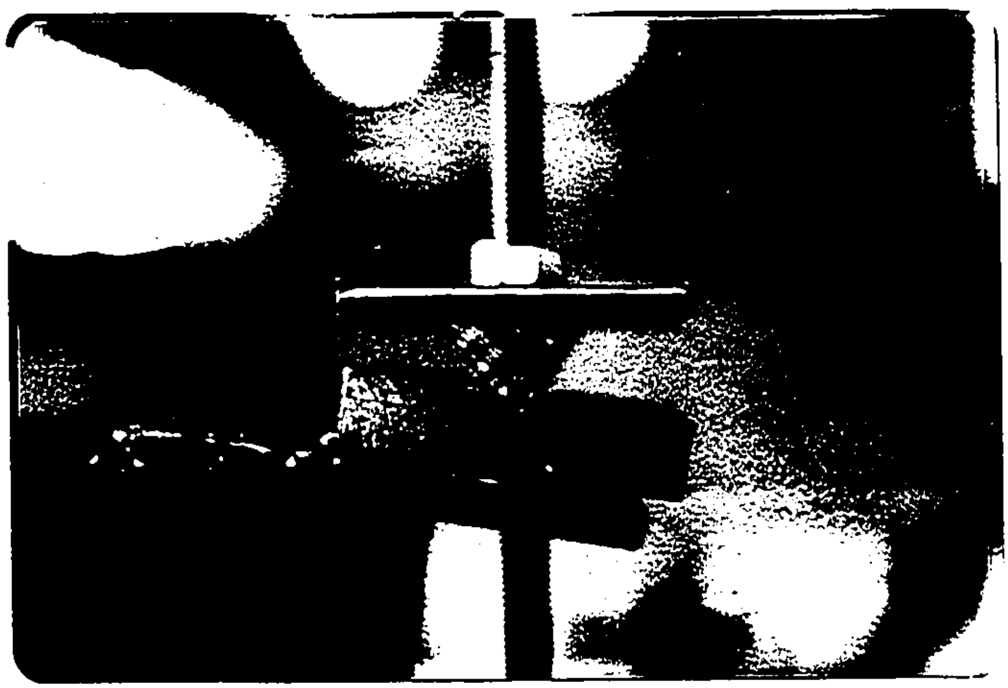

FIG. 52 TOP KNIFE EDGE.

APPENDICES

APPENDIX A

Concrete Mix Design

Three trial mixes were made to get good workable concrete with 2 to 3 in. slump and w/c ratio of 0.4. The object was to achieve a concrete strength of at least 7000 psi. The 'mass' method based upon an estimated mass of the cement per cubic meter, was used. An Engineering bulletin issued by CPCA "Design and Control of Concrete Mixtures" (42) was referred for standard quantities. The steps in the proportioning procedures are shown as follows:

Properties of the Materials:

Cement:	Type 30, High Early Strength Cement
Coarse Aggregate:	Maximum size 3/8"
	Relative density 2.68
	Absorption 0.5%
	Total moisture content 2%
	Dry rodded mass 1600 kg/m^3
Fine Aggregate:	Relative density 2.64
	Absorption 0.7%
	Total moisture content 6%
	FM 2.60
Concrete Desired:	Non-air entrained $f_c' = 7000$ psi
Slump:	2 to 3 inches

Estimated mass of a cubic meter of Non-Air entrained concrete made with 3/8" (10 mm)	=	2285 kg/m^3
Approximate mixing water requirements For 2 in (50 mm) slump and 3/8" (10 mm) aggregate	=	205 kg/m^3
Water/Cement ratio = 0.4, therefore cement	=	512.5 kg/m^3
Volume of coarse aggregate per unit volume of concrete (0.48 x 1600)	=	768 kg/m^3
Estimated mass of sand is the difference between the mass of fresh concrete and the total mass of the other ingredients: 2285 - 1485.5	=	799.5 kg/m^3

<u>Concrete Quantities for Mix are</u>:

Cement	512 kg/m^3
Water	205 kg/m^3
Coarse aggregate	768 kg/m^3
Sand	800 kg/m^3

All the above calculations were based on dry aggregates. Actually, aggregates contained some moisture. The dry masses were increased to compensate for the moisture that is absorbed in and contained on the surface of each particle. The mixing water was reduced by an amount equal to the free moisture contributed by the aggregates.

Tests indicate an average moisture content in fine aggregate of 6%.

So corrected quantity for fine aggregate:

800 x 1.06 = 848 kg/m^3

Absorbed water does not become part of the mixing water and must be excluded from the adjustment in added water. Thus, surface moisture contributed by the fine aggregate 6% - 0.7% = 5.3%. The estimated requirement for added water becomes:

$$205 - 800(0.053) = 162.6 \text{ kg/m}^3$$

Final quantities for concrete of 1m^3 are:

Cement	512 kg/m^3
Water	163 kg/m^3
Coarse aggregate	768 kg/m^3
Fine aggregate	848 kg/m^3

APPENDIX B

Description of the Computer Program

The computer program to find moments, deflections and curvatures of a prestressed concrete-filled tubular column for a particular axial load can be described in the following steps:

1) Input Data:

Generally three cards are sufficient to input the data for idealised elastic-perfectly plastic materials. The data to be read on first card are:

a) outer diameter of steel tube (DD1)

b) thickness of steel tube (THK)

c) 28 day concrete cylinder strength (FCU)

d) yield strength of steel tube (SS)

e) modulus of elasticity of steel tube (EA)

f) number of divisions the half column length was divided (KK)

g) yield stress of the prestressing wire (FYP)

h) yield strain of steel tube (EPL)

i) applied axial load (P)

j) true length of column (TL)

k) number of stress-strain values for prestressed tendon to be read (N1); N1 = 0 if idealised elastic-perfectly plastic material properties are used.

l) number of stress-strain values for hollow steel tube in tension to be read (N2); N2 = 0 if idealised elastic-perfectly plastic material properties to be used

m) number of stress-strain values for hollow steel tube in compression (N3); N3 = 0 if the material properties are equal in tension and compression

n) diameter of the prestressing wire (DPR)

The data to be read on the second card are:

a) location of the prestressing tendon from the extreme compression fibre. For the,

   i) 1st layer of bars (PR1)

   ii) 2nd layer of bars (PR2)

   iii) 3rd layer of bars (PR3)

b) the maximum strain under which maximum stress occurs for concrete (EO)

c) type of stress-strain curve to be used (TYPE); TYPE=1 if elastic-perfectly plastic material to be used, otherwise TYPE=any number except 1

d) starting case of prestressing to be analysed (NSTA); NSTA can be 1 to 5 indicating one to five tendons in the column

e) finishing case of prestressing to be analysed (INC); (INC) can be 1 to 5 indicating one to five tendons in the column

f) area of the prestressing wire (APR)

g) modulus of elasticity of the prestressing wire (YMPR)

h) type of stress-strain curve being used for hollow steel tube in tension (ITYP); ITYP = 1 if elastic-perfectly plastic material to be used, otherwise ITYP = any number except 1

i) type of stress-strain curve being used for hollow steel tube in compression (TYPC); TYPC = 1 if the material properties are equal in tension and compression, otherwise TYPC = any number except 1

j) yield strain of the prestressing wire (EYS)

The data to be read on third card are:

a) initial stresses in the prestressing tendon after creep and shrinkage losses. For

   i) the tendons in first layer (FPSC)

   ii) the tendons in second layer (FPSM)

   iii) the tendons in third layer (FPST)

b) initial strains in the prestressing tendon for the corresponding stresses in a) above. For

   i) the tendons in first layer (ESEC)

   ii) the tendons in second layer (ESEM)

   iii) the tendons in third layer (ESET)

c) actual length of the column (ACL)

2) Write the input data.

3) Select a value for the curvature (R) and the neutral axis depth (C).

4) Find the internal axial force and the bending moment for the strain distribution in step (3) through subroutines COMPIL, FCI, FSTL3, PRST, COSINE, CALI, NUE and ECOMP.

5) If the internal axial force satisfies the external applied axial load within acceptable tolerance (1% in this case), find the deflection through subroutines

DFLECT and GURFI. If not repeat step 4 with a new value of C.

6) Once the convergence in step 5 is achieved, repeat steps 3 to 5 with a different value of curvature.

7) Write the out which consists of,

a) bending moments, curvatures and deflections

b) strain at compressive and tensile extreme fibres

c) final stresses in the prestressing tendons

d) plot graphs for moment-curvature and moment-deflection for the applied axial load (CALCO3)

A flowchart describing above features is shown on next page. A listing of computer program is given in Appendix C.

<u>The Advantages and Limitations of the Computer Program</u>

This computer program can calculate the bending moments, curvatures and deflections for a particular axial load for prestressed and nonprestressed concrete-filled tubular columns. The program is simplified so that only three input data cards are sufficient to describe any particular column to be analysed. This program can be modified very easily. to accommodate different material properties and effects of confinement.

This program can only calculate the bending moments and deformations for circular concrete-filled tubular columns. This can be modified to accommodate other non-circular shapes. This program is written for the five cases of prestressing with tendons in three layers. For any other configuration, the program has to be modified.

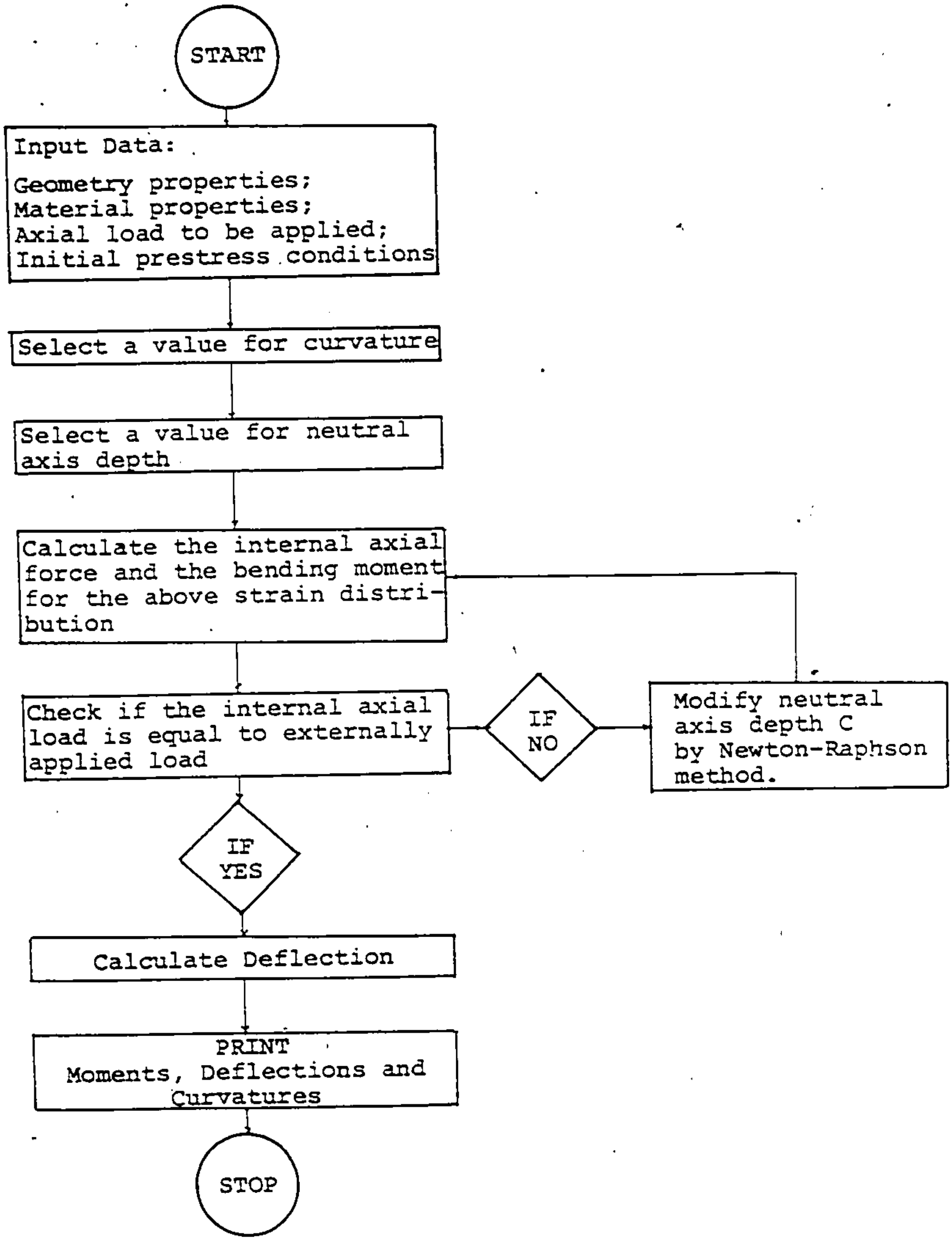
START
Input Data:
Geometry properties;
Material properties;
Axial load to be applied;
Initial prestress conditions
Select a value for curvature
Select a value for neutral axis depth
Calculate the internal axial force and the bending moment for the above strain distribution
Check if the internal axial load is equal to externally applied load
IF NO
Modify neutral axis depth C by Newton-Raphson method.
IF YES
Calculate Deflection
PRINT
Moments, Deflections and Curvatures
STOP

APPENDIX C

LISTING OF THE COMPUTER PROGRAM

```
LEVEL  21                 MAIN                DATE = 81333          19/09/11

C      *****************************************************************
C      *      THE ANALYSIS OF PRESTRESSED CONCRETE FILLED STEEL TUBULAR COLUMNS  *
C      *****************************************************************
C
C
C      *****************************************************************
C      *      THIS COMPUTER PROGRAM CALCULATES  MOMENT-CURVATURE AND MOMENT-DE-  *
C      *      -FLECTION RELATIONSHIP FOR A PARTICULAR AXIAL LOAD BY FINITE DIFF-  *
C      *      -ERENCE APPROACH.THIS PROGRAM ALSO COMPARES THE RESULTS OF          *
C      *      THE PRESTRESSED SECTION WITH  THE NONPRESTRSSSED SECTION .          *
C      *****************************************************************
C
C
C
C      *****************************************************************
C      *                   NOTATION                                        *
C      *        DDI   =OUTER DIAMETER OF STEEL TUBE                        *
C      *        THK   =THICKNESS OF STEEL TUBE                             *
C      *        SE    =YIELD STRESS OF STEEL TUBE                          *
C      *        EA    =YOUNG'S MODULUS OF ELASTICITY                       *
C      *        FCU   =28 DAY COMPRESSIVE STRENGTH OF STANDARD 6 INCH DIA CYLINDERS*
C      *        KK    =NUMBER OF STATIONS OF A HALF COLUMN LENGTH IN THE FINITE-  *
C      *               -DIFFERENCE SUBROUTINE                              *
C      *        P     =APPLIED AXIAL LOAD                                  *
C      *        FYP   =YIELD STRESS OF PRESTRESSING WIRE                   *
C      *        EPL   =YIELD STRAIN OF STEEL TUBE                          *
C      *        TL    =EFFECTIVE LENGTH OF THE COLUMN                      *
C      *        ACL   =ACTUAL LENGTH OF THE COLUMN                         *
C      *        FPR  |                                                     *
C      *        EPPR |=STRESS-STRAIN VALUES OF THE PRESTRESSING TENDON FROM *
C      *               TENSILE TEST                                        *
C      *        FST  |                                                     *
C      *        EPS  |=STRESS-STRAIN VALUES OF HOLLOW STEEL TUBE FROM TENSILE TEST *
C      *        FSC  |                                                     *
C      *        ESC  |=STRESS-STRAIN VALUES OF HOLLOW STEEL TUBE FROM COMPRESSION *
C      *               TEST                                                *
C      *        N1    =NO. OF STRESS-STRAIN VALUES OF FPR.EPPR             *
C      *        N2    =NO. OF STRESS-STRAIN VALUES OF FST.EPS              *
C      *        N3    =NO. OF STRESS-STRAIN VALUES OF FSC.ESC              *
C      *        DPR   =DIAMETER OF PRESTRESSING WIRE                       *
C      *        PR1  |=LOCATION OF PRESTRESSING TENDON FROM EXTREME FIBRE  *
C      *        PR2  |                                                     *
C      *        PR3  |                                                     *
C      *        E0    =MAXIMUM STRAIN AT WHICH MAXIMUM STRESS OCCURS FOR CONCRETE *
C      *        TYPE  =1. IF IDEALISED PRESTRESS STRESS-STRAIN CURVE IS USED *
C      *              =ANY NUMBER OTHER THAN 1. IF EXACT STRESS-STRAIN VALUES *
C      *               ARE USED                                            *
C      *        ITYP  =1. IF IDEALISED STEEL TUBE STRESS-STRAIN CURVE IS USED *
C      *              =ANY NUMBER OTHER THAN 1.IF EXACT VALUES ARE TO BE USED *
C      *        TYPC  =1.IF STRESS-STRAIN CURVE IS IDENTICAL IN TENSION&COMPRESSION*
C      *              =ANY NUMBER OTHER THAN 1.IF EXACT VALUES ARE TO BE USED *
C      *        NSTA  =STARTING CASE(SELECT 1/2/3/4/5 ) INDICATES NO.OF TENDONS *
C      *        INC   =FINISHING CASE(SELECT 1/2/3/4/5 )                   *
C      *        APR   =AREA OF PRESTRESSING WIRE                           *
C      *        YMPR  =YOUNG"S MODULUS OF PRESTRESSING WIRE IF TYPE=1.OTHRWISE 0 *
C      *        EYS   =YIELD STRAIN OF PRESTRESSING WIRE                   *
C      *        FPSC  =INITIAL STRESS IN THE PRESTRESSING TENDON(COMPRESSION) *
C      *        FPST  =INITIAL STRESS IN THE PRESTRESSING TENDON (TENSION) *
C      *        FPSM  =INITIAL STRESS IN THE PRESTRESSING TENDON (MIDDLE)  *
C      *        ESEC  =INITIAL STRAIN IN THE PRESTRESSING TENDON(COMPRESSION) *
C      *        ESET  =INITIAL STRAIN IN THE PRESTRESSING TENDON (TENSION) *
C      *        ESEM  =INITIAL STRAIN IN THE PRESTRESSING TENDON (MIDDLE)  *
C      *        XP    =INTERNAL AXIAL LOAD                                 *
C      *        XM    =INTERNAL RESISTING BENDING MOMENT(PRIMARY BENDING MOMENT+ *
C      *               SECONDARY BENDING MOMENT)                           *
C      *        R     =CURVATURE CORRSPONDS TO XP.XM                       *
C      *        DTA   =DEFLECTION FROM FINITE DIFFERENCE APPROACH          *
C      *        ESE   =INITIAL STRAIN IN THE PRESTRESSING TENDON           *
C      *        ECE   =UNIFORM STRAIN IN THE CONCRETE CAUSED BY PRESTRSSING FORCE *
C      *        ECC   =CHANGE OF STRAIN CAUSED IN THE PRESTRESSING TENDON (COMP.) *
C      *        ECT   =CHANGE OF STRAIN CAUSED IN THE PRESTRSSING TENDON (TENS.) *
C      *        EPRC |=TOTAL CHANGE IN TENDON STRAINS(EXT.LOAD+LOSS/GAIN IN *
C      *        EPRT | THE PRESTRSSING TENDON-INITIAL COMP.STRAIN IN CONCRETE) *
C      *        EPRM |                                                     *
C      *                                                                   *
C      *        STRC |=STRESSES IN PRESTRSSING TENDONS CORRESPOND TO EPRC.EPRT *
C      *        STRT |                                                     *
C      *        STRM |                                                     *
```

```
C      *                                                                    *
C      *        XP1 |*AXIAL LOAD.BENDING MOMENT FOR THE PRESTRESSED SECTION *
C      *        XM1 |                                                       *
C      *        C    *NEUTRAL AXIS DEPTH FROM EXTREME COMPRESSION FIBRE     *
C      **********************************************************************
C
C
C
C      **********************************************************************
C      *          NAMES OF SUBROUTINES & FUNCTIONS USED AND THEIR PURPOSE   *
C      *                                                                    *
C      *                                                                    *
C      *         SUBROUTINE/FUNCTION                 PURPOSE                *
C      *                                                                    *
C      *         PRST                 STRESS-STRAIN CURVE FOR PRESTRESSING TENDON *
C      *         FSTL3                STRESS-STRAIN CURVE FOR MILD STEEL TUBING   *
C      *         FCI                  STRESS-STRAIN CURVE FOR CONCRETE            *
C      *         COMPIL               CALCULATION OF INTERNAL BENDING MOMENT      *
C      *                              AND AXIAL LOAD FOR A GIVEN STRAIN DISTRIBUT-*
C      *                              -ION                                        *
C      *         DFLECT               CALCULATION OF DEFLECTED SHAPE BY FINITE    *
C      *                              DIFFERENCE APPROACH                         *
C      *         GURFI                TO FIND THE STRAIN DISTRIBUTION FOR A       *
C      *                              PARTICULAR AXIAL LOAD, BENDING MOMENT BY    *
C      *                              GURFINKEL'S METHOD                          *
C      *         CALI.NUE             TO FIND LOSS/GAIN OF STRAIN IN UNBONDED     *
C      *                              POST TENSIONED TENDONS BY NUMERICAL         *
C      *                              INTEGRATION                                 *
C      *         COSINE               TO FIND APPROXIMATE DEFLECTIONS BY          *
C      *                              ASSUMING PART COSINE WAVE AS DEFLECTION     *
C      *                              CURVE                                       *
C      *         ECOMP                TO FIND THE INITIAL CONCRETE STRAIN         *
C      *                              CAUSED BY PRESTRESSING                      *
C      **********************************************************************
C
C
C
       IMPLICIT REAL*8(A-H,O-Y)
       INTEGER TYPE,TYPC
       DIMENSION ZP1(18).ZM1(18).ZP2(18).ZM2(18).ZP3(18).
      *ZM3(18).ZP4(18).ZM4(18).ZP5(18).ZM5(18).ZP6(18).ZM6(18).
      *ZD1(18).ZD2(18).ZD3(18).ZD4(18).ZD5(18).ZD6(18).
      *ZS1(18).ZS2(18).ZS3(18).ZS4(18).ZS5(18).ZS6(18).
      *OTT(30).FORC(5.25).FORT(5.25).FORM(5.25).STR(25).STD(25
      *).STC(5.25).STT(5.25).Z(30).V(20).EM(20).DKN(20).RHO(20)
       COMMON/AREA1/DD1.DD2.THK.KK
       COMMON/AREA2/SE.EA.FCU.PU.PL.FPR(20).EPPR(20).FST(25).EPS(25).EPL
      *.N1.N2.N3
       COMMON/AREA3/STRC.STRT.STRM.FSC(25).ESC(25).ECE
       COMMON/AREA4/PR1.PR2.PR3.ACL
       COMMON/AREA5/APR.FPS.ESE.EO
       COMMON/AREA6/TYPE.TYPC
       COMMON/AREA7/FPSC.FPST.FPSM.ESEC.ESET.ESEM
       COMMON/AREA8/YMPR.EYS.ITYP
       COMMON/AREA9/ECC.ECM.ECT
       COMMON/AREA10/FYP
       DATA ZD1(1)/0.0/.ZM1(1)/0.0/.ZP1(1)/0.0/.ZD2(1)/0.0/.ZM2(1)/0.0/.
      *ZP2(1)/0.0/.ZD3(1)/0.0/.ZM3(1)/0.0/.ZP3(1)/0.0/.ZD4(1)/0.0/.
      *ZM4(1)/0.0/.ZP4(1)/0.0/.ZD5(1)/0.0/.ZM5(1)/0.0/.ZP5(1)/0.0/.ZD6(1)
      */0.0/.ZM6(1)/0.0/.ZP6(1)/0.0/.ZS1(1)/0.0/.ZS2(1)/0.0/.ZS3(1)/0.0/.
      *ZS4(1)/0.0/.ZS5(1)/0.0/.ZS6(1)/0.0/
       CALL PLOTID('PRAKASH          '.'912300X190')
       CALL XLIMIT(160.0)
C*****INPUT DATA*********************************************************
       READ(5.1) DD1.THK.FCU.SE.EA.KK.FYP.EPL.P.TL.N1.N2.DPR
     1 FORMAT(F5.2.F6.4.F4.2.F6.3.E8.6.I5.F6.2.F7.5.F6.2.F6.2.I3.I3.F6.4)
       READ(5.2)PR1.PR2.PR3.EO.TYPE.NSTA.INC.APR.YMPR.ITYP.TYPC.EYS
     2 FORMAT(3(F5.2).F6.4.I3.I3.I3.F5.2.F7.1.2I2.F5.3)
       READ(5.3) FPSC.FPST.FPSM.ESEC.ESET.ESEM.ACL
     3 FORMAT(6(F10.5).F5.2)
       IF(ITYP.EQ.1) GO TO 4
       READ(5.5) (FPR(I).EPPR(I).I=1.N1)
     5 FORMAT(F10.5.F10.5)
     4 IF(TYPE.EQ.1) GO TO 6
       READ(5.7)(FST(I).EPS(I).I=1.N2)
     7 FORMAT(F10.5.F12.8)
       IF(TYPC.EQ.1) GO TO 6
       READ(5.7)(FSC(I).ESC(I).I=1.N2)
```

```
FORTRAN IV G LEVEL  21                MAIN               DATE = 81333          19/09/11

0031          8    CONTINUE
              C********************PRINT THE INPUT DATA*******************************************
0032               PRINT8
0033          8    FORMAT(////.10X.'UNITS ARE INCHES AND KIPS'./////)
0034               PRINT9
0035          9    FORMAT(10X.'PROPERTIES OF CIRCULAR PRESTRSSED CONCRETE')
0036               PRINT10
0037          10   FORMAT(10X.'FILLED TUBULAR COLUMNS SUBJECTED TO AXIAL LOAD')
0038               PRINT11
0039          11   FORMAT(10X.'AND UNIAXIAL BENDING'.////)
0040               PRINT12.OD1
0041          12   FORMAT(10X.'OUTER DIAMETER OF STEEL TUBE'.24X.F5.2.///)
0042               PRINT13.THK
0043          13   FORMAT(10X.'THICKNESS OF STEEL TUBE'.30X.F6.4.///)
0044               PRINT14.SE
0045          14   FORMAT(10X.'YIELD STRESS OF STEEL TUBE'.26X.F6.3.///)
0046               PRINT15.EPL
0047          15   FORMAT(10X.'YIELD STRAIN OF STEEL TUBE'.27X.F6.4.///)
0048               PRINT16.EA
0049          16   FORMAT(10X.'YOUNG"S MODULUS OF ELASTICITY'.20X.F10.4.///)
0050               PRINT17.FYP
0051          17   FORMAT(10X.'YIELD STRESS OF PRESTRESSING WIRE'.15X.F6.2.///)
0052               PRINT18.DPR
0053          18   FORMAT(10X.'DIAMETER OF PRESTRESSING WIRE'.24X.F6.4.///)
0054               PRINT19.FCU
0055          19   FORMAT(10X.'28 DAY CONCRETE CYLINDER STRNGTH'.20X.F5.3.///)
0056               PRINT20.TL
0057          20   FORMAT(10X.'TOTAL LENGTH OF COLUMN (C/C OF HINGE)'.15X.F6.3.///)
0058               PRINT21.KK
0059          21   FORMAT(10X.'NO.OF STATIONS ALONG THE HALF COLUMN LENGTH'.8X.I3.//)
0060               PRINT22.N1
0061          22   FORMAT(/.10X.'NO.OF STRESS-STRAIN VALUES OF PRESTRESSED WIRE'.5X.
                  1I3.///)
0062               PRINT23.N2
0063          23   FORMAT(10X.'NO. OF STRESS-STRAIN VALUES OF STEEL TUBE'.10X.I3.///)
0064               PRINT24.P
0065          24   FORMAT(10X.'EXTERNAL APPLIED AXIAL LOAD'.24X.F7.3.///)
0066               PRINT25.ACL
0067          25   FORMAT(10X.'ACTUAL LENGTH OF THE COLUMN'.25X.F5.2.///)
0068               PRINT26.PP1
0069          26   FORMAT(10X.'LOCATION OF 1ST LAYER OF TENDONS FROM EXTREME FIBRE'.
                  11X.F5.2.///)
0070               PRINT27.PP2
0071          27   FORMAT(10X.'LOCATION OF 2ND LAYER OF TENDONS FROM EXTREME FIBRE'.
                  11X.F5.2.///)
0072               PRINT28.PP3
0073          28   FORMAT(10X.'LOCATION OF 3RD LAYER OF TENDONS FROM EXTREME FIBRE'.
                  11X.F5.2.///)
0074               PRINT29.EO
0075          29   FORMAT(10X.'STRAIN OF CONCRETE UNDER WHICH MAX. STRESS OCCURS'.4X
                  1.F6.4.///)
0076               PRINT30
0077          30   FORMAT(10X.'INDICATES THE MODE OF INPUT FOR STRESS-STRAIN FOR')
0078               PRINT31.TYPE
0079          31   FORMAT(10X.'HOLLOW STEEL TUBE'.34X.I3.///)
0080               PRINT32
0081          32   FORMAT(10X.'INDICATES WHETHER THE PROPERTIES OF HOLLOW STEEL ')
0082               PRINT33.TYPC
0083          33   FORMAT(10X.'TUBE ARE EQUAL IN TENSION AND COMPRESSION'.10X.I3.///)
0084               PRINT34
0085          34   FORMAT(10X.'INDICATES THE MODE OF INPUT FOR STRESS-STRAIN FOR')
0086               PRINT35.ITYP
0087          35   FORMAT(10X.'PRESTRESSING WIRE'.34X.I3.///)
0088               PRINT36.EYS
0089          36   FORMAT(10X.'YIELD STRIN FOR PRESTRESSING WIRE'.20X.F6.4.///)
0090               PRINT37.YMPR
0091          37   FORMAT(10X.'YOUNG"S MODULUS FOR PRESTRESSING WIRE'.12X.F8.2.///)
0092               PRINT38.APR
0093          38   FORMAT(10X.'AREA OF PRESTRESSING WIRE'.28X.F5.3.///)
0094               PRINT39.NSTA
0095          39   FORMAT(10X.'STARTING CASE OF IM(NO.OF TENDONS)'.17X.I3.///)
0096               PRINT40.INC
0097          40   FORMAT(10X.'FINISHING CASE OF IM(NO.OF TENDONS)'.16X.I3.///)
0098               PRINT41.FPSC
0099          41   FORMAT(10X.'INITIAL STRESS IN 1ST LAYER OF TENDONS'.13X.F6.2.///)
0100               PRINT42.FPSN
0101          42   FORMAT(10X.'INITIAL STRESS IN 2ND LAYER OF TENDONS'.13X.F6.2.///)
0102               PRINT43.FPST
```

```
 43   FORMAT(10X.'INITIAL STRESS IN 3RD LAYER OF TENDONS'.13X.F6.2.///)
      PRINT44.ESEC
 44   FORMAT(10X.'INITIAL STRAIN IN 1ST LAYER OF TENDONS'.15X.F6.4.///)
      PRINT45.ESEM
 45   FORMAT(10X.'INITIAL STRAIN IN 2ND LAYER OF TENDONS'.15X.F6.4.///)
      PRINT46.ESET
 46   FORMAT(10X.'INITIAL STRAIN IN 3RD LAYER OF TENDONS'.15X.F6.4.///)
      IF(ITYP.EQ.1) GO TO 47
      PRINT48
 48   FORMAT(10X.'STRESS-STRAIN VALUES FOR PRESTRESSING WIRE'.///)
      PRINT49
 49   FORMAT(13X.'STRESS'.23X.'STRAIN'.///)
      PRINT50.(FPR(I).EPPR(I).I=1.N1)
 50   FORMAT(10X.F10.4.20X.F10.6)
 47   IF(TYPE.EQ.1) GO TO 51
      PRINT52
 52   FORMAT(///.10X.'STRESS-STRAIN VALUES FOR HOLLOW STEEL TUBE'.///)
      PRINT53
 53   FORMAT(10X.'IN COMPRESSION'.//)
      PRINT54
 54   FORMAT(13X.'STRESS'.23X.'STRAIN'.//)
      PRINT55.(FST(I).EPS(I).I=1.N2)
 55   FORMAT(10X.F10.5.20X.F10.6)
      PRINT56
 56   FORMAT(///.10X.'IN TENSION'.//)
      PRINT57
 57   FORMAT(13X.'STRESS'.23X.'STRAIN'.//)
      PRINT55.(FSC(I).ESC(I).I=1.N2)
 51   CONTINUE
      DD2=DD1-(2*THK)
C*********************OUTPUT*****************************************************
      PRINT58
 58   FORMAT(////.10X.'THE FOLLOWING ARE THE RESULTS './/////)
      DO 59 LL =1.2
      C=.001
      IF(LL.EQ.2) GO TO 60
      PRINT61
 61   FORMAT(10X.'NON PRESTRESSED COLUMN'.//.10X.'BENDING MOMENT'.8X.
     1'CURVATURE'.11X.'DEFLECTION'.10X.'STEEL MOMENT'.8X.'EXTREME FIBRE
     1'.5X.'EXTREME FIBRE')
      PRINT62
 62   FORMAT(92X.'STRAIN(COMP.)'.6X.'STRAIN(TENS.)'.///)
C*************ANALYSIS OF NONPRESTRESSED SECTION*********************************
      DO 63 IR=1.15
      IRR=IR+1
      R=IR*.0004
      DNCR=0.005
      DO 64 IC=1.15
      C=C+DNCR
      ULST=C*R
      IM=100
      CALL COMPIL(R.C.XP.XM.IM.IR.TL.XS2.E)
      IF(DABS(XP-P).LE.0.1) GO TO 65
      C1=C+((.01*C)+.001)
      CALL COMPIL(R.C1.XP5.XM5.IM.IR.TL.XS2.E)
      DEL=(XP5-XP)/(C1-C)
      DNCR=(P-XP)/DEL
 64   CONTINUE
 65   STR(IRR)=E(1)
      STQ(IRR)=E(30)
      CALL DFLECT(XP.XM.DTA.R.C.KK.ENOM.TL.IM.IR.V.EM.OKN.RHO)
      ZD1(IR+1)=DTA
      ZP1(IR+1)=P
      ZM1(IR+1)=XM
      ZS1(IR+1)=XS2
      PRINT67.ZM1(IRR).ZP1(IRR).ZD1(IRR).ZS1(IRR).STR(IRR).STQ(IRR)
 67   FORMAT(10X.F10.4.10X.F10.6.10X.F10.6.10X.F10.4.2(10X.F10.6))
 63   CONTINUE
      GO TO 68
C*********ANALYSIS OF PRESTRESSED SECTIONS****************************************
 60   DO 69 IM=NSTA.INC
      C=.001
      DO 70 IR=1.15
      R=IR*.0004
      DNCR=0.00
      DO 71 IC=1.15
      C=C+DNCR
      ULST=C*R
```

```
              CALL COMPIL(R,C,XP1,XM1,IM,IR,TL,XS2,E)
              IF(DABS(XP1-P).LE.0.5) GO TO 72
              C2=C+((0.01*C)+.001)
              CALL COMPIL(R,C2,XP4,XM4,IM,IR,TL,XS2,E)
              DELZ=(XP4-XP1)/(C2-C)
              DNCP=(P-XP1)/DELZ
         71   CONTINUE
         72   CONTINUE
              STC(IM,IR)=E(1)
              STT(IM,IR)=E(30)
              CALL DFLECT(XP1,XM1,DT1,R,C,KK,ENOM,TL,IM,IP,V,EM,DKN,RHO)
              DTT(IM)=DT1
              IF(IM.EQ.1) GO TO 73
              IF(IM.EQ.2) GO TO 74
              IF(IM.EQ.3) GO TO 75
              IF(IM.EQ.4) GO TO 76
C***********PRESTRESSED COLUMN WITH 5 TENDONS************************************
              FORC(IM,IR)=STRC
              FORT(IM,IR)=STRT
              FORM(IM,IR)=STRM
              ZM2(IR+1)=XM1
              ZP2(IR+1)=R
              ZS2(IR+1)=XS2
              ZD2(IR+1)=DTT(5)
              GO TO 77
C***********PRESTRESSED COLUMN WITH 4 TENDONS************************************
         76   ZM3(IR+1)=XM1
              ZP3(IR+1)=R
              ZS3(IR+1)=XS2
              ZD3(IR+1)=DTT(4)
              FORC(IM,IR)=STRC
              FORT(IM,IR)=STRT
              GO TO 77
C***********PRESTRESSED COLUMN WITH 3 TENDONS************************************
         75   ZM4(IR+1)=XM1
              ZP4(IR+1)=R
              ZS4(IR+1)=XS2
              ZD4(IR+1)=DTT(3)
              FORC(IM,IR)=STRC
              FORT(IM,IR)=STRT
              FORM(IM,IR)=STRM
              GO TO 77
C***********PRESTRESSED COLUMN WITH 2 TENDONS************************************
         74   ZM5(IR+1)=XM1
              ZP5(IR+1)=R
              ZS5(IR+1)=XS2
              ZD5(IR+1)=DTT(2)
              FORC(IM,IR)=STRC
              FORT(IM,IR)=STRT
              GO TO 77
C*************PRESTRESSED COLUMN WITH 1 TENDON************************************
         73   ZM6(IR+1)=XM1
              ZP6(IR+1)=R
              ZS6(IR+1)=XS2
              ZD6(IR+1)=DTT(1)
              FORM(IM,IR)=STRM
         77   CONTINUE
         70   CONTINUE
         69   CONTINUE
         68   CONTINUE
         59   CONTINUE
              I=IR+1
              DO 78  K=NSTA,INC
              IF(K.EQ.5) GO TO 79
              IF(K.EQ.4) GO TO 80
              IF(K.EQ.3) GO TO 81
              IF(K.EQ.2) GO TO 82
              PRINT83
         83   FORMAT(///,10X,'PRESTRESSED COL - 1 TENDON',//,10X,'BENDING MOMENT
             1',8X,'CURVATURE',11X,'DEFLECTION',10X,'STEEL MOMENT',///)
              PRINT84 ,(ZM6(IRR),ZP6(IRR),ZD6(IRR),ZS6(IRR),IRR=2,I)
         84   FORMAT(10X,F10.4,10X,F10.6,10X,F10.6,10X,F10.4)
              PRINT85
         85   FORMAT(///,10X,'STRESS IN',13X,'EXTREME FIBRE',6X,'EXTREME FIBRE'
             *)
              PRINT86
         86   FORMAT(10X,'CENTRAL TENDON',8X,'STRAIN(COMP.)',6X,'STRAIN(TENS.)
             *',///)
```

```
FORTRAN IV G LEVEL  21                    MAIN                 DATE = 91333          19/09/11
                PRINT87.(FORM(K.IRR).STC(K.IRR).STT(K.IRR).IRR=1.IR)
          87    FORMAT(10X.F10.4.10X.F10.6.10X.F10.6)
                GO TO 98
          92    PRINT89
          89    FORMAT(///.10X.'PRESTRESSED COL - 2 TENOONS'.//.10X.'BENDING MOMEN
               1T'.8X.'CURVATURE'.11X.'DEFLECTION'.10X.'STEEL MOMENT'.///)
                PRINT90.(ZM5(IRR).ZP5(IRR).ZD5(IRR).ZS5(IRR).IRR=2.I)
          90    FORMAT(10X.F10.4.10X.F10.6.10X.F10.6.10X.F10.4)
                PRINT91
          91    FORMAT(///.10X.'STRESS IN'.13X.'STRESS IN'.11X.'EXTREME FIBRE'.6X.
               #'EXTREME FIBRE')
                PRINT92
          92    FORMAT(10X.'COMP.TENOON'.11X.'TENS.TENOON'.9X.'STRAIN(COMP.)'.
               #6X.'STRAIN(TENS.)'.//)
                PRINT93.(FORC(K.IRR).FORT(K.IRR).STC(K.IRR).STT(K.IRR).IRR=1.IR)
          93    FORMAT(10X.F10.4.10X.F10.4.10X.F10.6.10X.F10.6)
                GO TO 98
          51    PRINT94
          94    FORMAT(///.10X.'PRESTRESSED COL - 3 TENOONS'.//.10X.'BENDING MOMEN
               1T'.8X.'CURVATURE'.11X.'DEFLECTION'.10X.'STEEL MOMENT'.///)
                PRINT95.(ZM4(IRR).ZP4(IRR).ZD4(IRR).ZS4(IRR).IRR=2.I)
          95    FORMAT(10X.F10.4.10X.F10.6.10X.F10.6.10X.F10.4)
                PRINT96
          96    FORMAT(///.10X.'STRESS IN'.13X.'STRESS IN'.11X.'STRESS IN'.11X.'EX
               #TREME FIBRE'.5X.'EXTREME FIBRE')
                PRINT97
          97    FORMAT(10X.'COMP.TENOON'.11X.'CENTRAL TENOON'.6X.'TENS.TENOON'.9X
               #.'STRAIN(COMP.)'.5X.'STRAIN(TENS.)'.//)
                PRINT98.(FORC(K.IRR).FORM(K.IRR).FORT(K.IRR).STC(K.IRR).STT(K.IRR
               1).IRR=1.IR)
          98    FORMAT(10X.F10.4.10X.F10.4.10X.F10.4.10X.F10.6.10X.F10.6)
                GO TO 98
          50    PRINT99
          99    FORMAT(///.10X.'PRESTRESSED COL - 4 TENOONS'.//.10X.'BENDING MOMEN
               1T'.8X.'CURVATURE'.11X.'DEFLECTION'.10X.'STEEL MOMENT'.///)
                PRINT100.(ZM3(IRR).ZP3(IRR).ZD3(IRR).ZS3(IRR).IRR=2.I)
         100    FORMAT(10X.F10.4.10X.F10.6.10X.F10.6.10X.F10.4)
                PRINT101
         101    FORMAT(///.10X.'STRESS IN'.10X.'STRESS IN'.10X.'EXTREME FIBRE'.10X
               #.'EXTREME FIBRE')
                PRINT102
         102    FORMAT(10X.'COMP.TENOON'.8X.'TENS.TENOON'.8X.'STRAIN(COMP.)'.
               #10X.'STRAIN(TENS.)'.//)
                PRINT103.(FORC(K.IRR).FORT(K.IRR).STC(K.IRR).STT(K.IRR).IRR=1.IR)
         103    FORMAT(10X.F10.4.8X.F10.4.10X.F10.6.12X.F10.6)
                GO TO 98
          79    PRINT104
         104    FORMAT(///.10X.'PRESTRESSED COL - 5 TENOONS'.//.10X.'BENDING MOMEN
               1T'.8X.'CURVATURE'.11X.'DEFLECTION'.10X.'STEEL MOMENT'.///)
                PRINT105.(ZM2(IRR).ZP2(IRR).ZD2(IRR).ZS2(IRR).IRR=2.I)
         105    FORMAT(10X.F10.4.10X.F10.6.10X.F10.6.10X.F10.4)
                PRINT106
         106    FORMAT(///.10X.'STRESS IN'.13X.'STRESS IN'.11X.'STRESS IN'.11X.'EX
               #TREME FIBRE'.5X.'EXTREME FIBRE')
                PRINT107
         107    FORMAT(10X.'COMP.TENOON'.11X.'CENTRAL TENOON'.6X.'TENS.TENOON'.9X
               #.'STRAIN(COMP.)'.5X.'STRAIN(TENS.)'.//)
                PRINT108.(FORC(K.IRR).FORM(K.IRR).FORT(K.IRR).STC(K.IRR).STT(K.IR
               1R).IRR=1.IR)
         108    FORMAT(10X.F10.4.10X.F10.4.10X.F10.4.10X.F10.6.10X.F10.6)
          98    CONTINUE
          75    CONTINUE
                CALL CALC03(ZP1.ZM1.16.-1.8.0.6.0.0.0.0.0.0008.0.0.50.0.1.1.0.0)
                CALL CALC03(ZP1.ZS1.16.0.8.0.6.0.0.0.0.0.0008.0.0.50.0.1.2.0.0)
                CALL CALC03(ZP2.ZM2.16.10.8.0.6.0.0.0.0.0.0008.0.0.50.0.1.2.0.0)
                CALL CALC03(ZP2.ZS2.16.0.8.0.6.0.0.0.0.0.0008.0.0.50.0.1.2.0.0)
                CALL CALC03(ZP3.ZM3.16.10.8.0.6.0.0.0.0.0.0008.0.0.50.0.1.3.0.0)
                CALL CALC03(ZP3.ZS3.16.0.8.0.6.0.0.0.0.0.0008.0.0.50.0.1.2.0.0)
                CALL CALC03(ZP4.ZM4.16.10.8.0.6.0.0.0.0.0.0008.0.0.50.0.1.4.0.0)
                CALL CALC03(ZP4.ZS4.16.0.8.0.6.0.0.0.0.0.0008.0.0.50.0.1.2.0.0)
                CALL CALC03(ZP5.ZM5.16.10.8.0.6.0.0.0.0.0.0008.0.0.50.0.1.5.0.0)
                CALL CALC03(ZP5.ZS5.16.0.8.0.6.0.0.0.0.0.0008.0.0.50.0.1.2.0.0)
                CALL CALC03(ZP6.ZM6.16.10.8.0.6.0.0.0.0.0.0008.0.0.50.0.1.6.0.0)
                CALL CALC03(ZP6.ZS6.16.0.8.0.6.0.0.0.0.0.0008.0.0.50.0.1.3.0.0)
                CALL CALC03(ZD1.ZM1.16.10.8.0.6.0.0.0.0.0.25.0.0.50.0.1.1.0.0)
                CALL CALC03(ZD2.ZM2.16.10.8.0.6.0.0.0.0.0.25.0.0.50.0.1.2.0.0)
                CALL CALC03(ZD3.ZM3.16.10.8.0.6.0.0.0.0.0.25.0.0.50.0.1.3.0.0)
                CALL CALC03(ZD4.ZM4.16.10.8.0.6.0.0.0.0.0.25.0.0.50.0.1.4.0.0)
```

```
      CALL CALC03(ZD5,ZM5,16,10,8,0.6,0.0,0.0.25,0.0.50,0.1,5,0.0)
      CALL CALC03(ZD6,ZM6,16,10,8,0.6,0.0,0.0.25,0.0.50,0.1,6,0.0)
      MOVE=10
      CALL PLTEND(10.0)
      STOP
      END
```

```
FORTRAN IV G LEVEL  21                 MAIN                DATE = 91333           19/09/11
                  C
                  C
                  C
 0001                   FUNCTION PRST(EPR.FPR.EPPR.FYP.NI)
                  C
                  C
                  C     THIS SUBPROGRAMME CALCULATES PRESTRESSED TENDON STRESS (KSI) FOR A
                  C     PARTICULAR STRAIN
                  C
                  C
 0002                   IMPLICIT REAL*8 (A-H.O-Y)
 0003                   DIMENSION FPR(20).EPPR(20)
 0004                   COMMON/AREA6/YMPR.EYS.ITYP
 0005                   K=2
 0006                   IF(EPR)31.32.32
 0007              31   EPR=-EPR
 0008                   K=1
 0009              32   IF(EPR-EYS)33.34.34
 0010              34   PRST=FYP*(-1.0)**K
 0011                   RETURN
 0012              33   IF(ITYP.EQ.1) GO TO 37
 0013                   DO 35 N=2.NI
 0014                   IF(EPPR(N)-EPR)35.35.36
 0015              35   CONTINUE
 0016              36   PRST=(-1.)**K*(FPR(N)-(FPR(N)-FPR(N-1))*(EPPR(N)-EPR)/
                       *(EPPR(N)-EPPR(N-1)))
 0017                   GO TO 38
 0018              37   PRST=((-1.)**K)*YMPR*EPR
 0019              38   RETURN
 0020                   END
```

```
FORTRAN IV G LEVEL  21                 MAIN              DATE = 81333          19/30/11
                C
                C
                C
                      FUNCTION FCI(EAL,FCU,E0)
                C
                C
                C     THIS SUBPROGRAMME CALCULATES CONCRETE STRESS (KSI) FOR A PARTICULAR STRAIN
                C
                C
                      IMPLICIT REAL*8(A-H,O-Y)
                      DIMENSION FC(7),EC(7)
                      ECON=EAL
                      IF(EAL)37,38,38
                   37 FCI=0.0
                      GO TO 39
                   38 IF(ECON.GE.E0) GO TO 40
                      FCI=FCU*((2*(ECON/E0))-((ECON/E0)**2))
                      GO TO 39
                   40 FCI=FCU
                   39 RETURN
                      END
```

```
FORTRAN IV G LEVEL  21                    MAIN                    DATE = 81333          19/09/11
                 C
                 C
                 C
 0001                    FUNCTION FSTL3(EI9,SE,EA,FS,EPS,EPL,N2,FSC,ESC)
                 C
                 C
                 C       THIS SUBPROGRAMME CALCULATES THE STRESS OF STEEL TUBE FOR A
                 C       PARTICULAR STRAIN (KSI)
                 C
                 C
 0002                    IMPLICIT REAL*8(A-H,O-Y)
 0003                    INTEGER TYPE,TYPC
 0004                    COMMON/AREA6/TYPE,TYPC
 0005                    DIMENSION FS(25),EPS(25),FSC(25),ESC(25)
 0006                    KI=1
 0007                    IF(EI9)41,41,42
 0008              42    KI=2
 0009                    EIT=EI9
 0010                    GO TO 43
 0011              41    EIT=-EI9
 0012              43    IF(EIT-EPL) 44,45,45
 0013              45    FSTL3=SE*(-1.0)**KI
 0014                    RETURN
 0015              44    IF(TYPE.EQ.1) GO TO 55
 0016                    IF(TYPC.EQ.1) GO TO 65
 0017                    IF(KI.EQ.1) GO TO 60
 0018              65    DO 46 N=2,N2
 0019                    IF(EPS(N)-EIT)46,46,47
 0020              46    CONTINUE
 0021              47    FSTL3=(-1.)**KI*(FS(N)-(FS(N)-FS(N-1))*(EPS(N)-EIT)/(EPS(N)-EPS
                        *(N-1)))
 0022                    GO TO 56
 0023              55    FSTL3=((-1.)**KI)*EA*EIT
 0024                    RETURN
 0025              60    DO 61 I=2,N2
 0026                    IF(ESC(I)-EIT)61,61,62
 0027              61    CONTINUE
 0028              62    FSTL3=(-1.)**KI*(FSC(I)-(FSC(I)-FSC(I-1))*(ESC(I)-EIT)/(ESC(I)-
                        *ESC(I-1)))
 0029              56    RETURN
 0030                    END
```

```
C
C
C
      SUBROUTINE COMPIL(R.C.XPI.XMI.IM.IR.TL.XS2.E)
C
C
C     THIS SUBROUTINE CALCULATES TOTAL FORCE IN CONCRETE AND STEEL
C     STRIPS AND INCLUDES PRESTRESSING FORCES
C
C
      IMPLICIT REAL*8(A-H.O-Y)
      COMMON/AREA1/DD1.DD2.THK.KK
      COMMON/AREA2/SE.EA.FCU.PU.PL.FPP(20).EPPP(20).FST(25).EPS(25).EPL
     *.N1.N2.N3
      COMMON/AREA3/STRC.STRT.STRM.FSC(25).ESC(25).ECE
      COMMON/AREA4/PR1.PR2.PR3.ACL
      COMMON/AREA5/APR.FPS.ESE.E0
      COMMON/AREA7/FPSC.FPST.FPSM.ESEC.ESET.ESEM
      COMMON/AREA9/ECC.ECM.ECT
      COMMON/AREA10/FYP
      COMMON/AREA11/V1(20).EM1(20).RHO1(20).DKN1(20)
      COMMON/AREA12/H
      DIMENSION    ASI(30).ACI(20).E(30).X(101).Y(101)
      H=(TL/2.0)/KK
      EY=SE/EA
      DIAO=DD1
      DIAI=DD2
      XS1=0.0
      XC1=0.0
      XS2=0.0
      XC2=0.0
      RO=DD1/2
      RI=DD2/2
      DO 51 L=1.30
      STI=(DIAO-DIAI)/10.0
      CTI=DIAI/20.0
      IF(L.GT.25) GO TO 49
      IF(L.LE.5) GO TO 49
      CDI=DIAI/2.-CTI*(L-5)
      GI=CDI+CTI/2.
      E(L)=(C-(DIAO/2.)+CDI)*R
      LL=L-5
      EAL=E(L)
      ACI(LL)=(RI**2)*DARCOS(CDI/RI)-(CDI*DSQRT(RI**2-CDI**2))
      ASI(L)=(RO**2)*DARCOS(CDI/RO)-(CDI*DSQRT(RO**2-CDI**2))-ACI(LL)
      FC=FCI(EAL.FCU.E0)
      FS=FSTL3(EAL.SE.EA.FST.EPS.EPL.N2.FSC.ESC)
      IF(LL.EQ.1) GO TO 50
      XS1=XS1+FS*(ASI(L)-ASI(L-1))
      XC1=XC1+FC*(ACI(LL)-ACI(LL-1))
      XS2=XS2+FS*(ASI(L)-ASI(L-1))*GI
      XC2=XC2+FC*(ACI(LL)-ACI(LL-1))*GI
      GO TO 51
   50 XS1=XS1+FS*(ASI((L)-ASI(L-1))
      XC1=XC1+FC*ACI(LL)
      XS2=XS2+FS*(ASI(L)-ASI(L-1))*GI
      XC2=XC2+FC*(ACI(LL)*GI)
      GO TO 51
   49 IF(L.GT.25) GO TO 52
      CDI=DIAO/2.-(L*STI)
      GO TO 53
   52 CDI=DIAO/2.-(5*STI)-(20*CTI)-((L-25)*STI)
      ASI(L)=(RO**2)*DARCOS(CDI/RO)-(CDI*DSQRT(RO**2-CDI**2))-ACI(20)
      E(L)=(C-(DIAO/2.)+CDI)*R
      EAL=E(L)
      FS=FSTL3(EAL.SE.EA.FST.EPS.EPL.N2.FSC.ESC)
      GI=CDI+STI/2.
      XS1=XS1+FS*(ASI(L)-ASI(L-1))
      XS2=XS2+FS*(ASI(L)-ASI(L-1))*GI
      GO TO 51
   53 GI=CDI+STI/2.
      ASI(L)=(RO**2)*DARCOS(CDI/RO)-(CDI*DSQRT(RO**2-CDI**2))
      E(L)=(C-(DIAO/2.)+CDI)*R
      EAL=E(L)
      FS=FSTL3(EAL.SE.EA.FST.EPS.EPL.N2.FSC.ESC)
      IF(L.EQ.1) GO TO 54
      XS1=XS1+FS*(ASI(L)-ASI(L-1))
      XS2=XS2+FS*(ASI(L)-ASI(L-1))*GI
```

```
      GO TO 51
   54 XS1=XS1+FS*ASI(L)
      XS2=XS2+FS*ASI(L)*GI
   51 CONTINUE
      XP=XS1+XC1
      XM=XS2+XC2
   48 CONTINUE
      IF(IM.EQ.100)  GO TO 55
      CALL COSINE(XP,XM,R,C,TL)
      CALL CAL1(DDT,DDC,DDM,R,C,XM,RHO1,V1,EM1,DKN1,TL)
      ECC=DDC
      ECT=DDT
      ECM=DDM
      AC=.795*(DD2**2)
      AS=.795*((DD1**2)-(DD2**2))
      ATR=AS*6+AC
      ARM=DD2/2.-PR1
      IF(IM.EQ.1) GO TO 56
      IF(IM.EQ.2) GO TO 57
      IF(IM.EQ.3) GO TO 58
      IF(IM.EQ.4) GO TO 59
      FPS=(FPSC*2)+(FPST*2)+FPSM
      ECE=ECOMP(EO,FPS,APR,ATR,FCU)
      EPRC=ESEC-(ECC-ECE)
      EPRT=ESET-(ECT-ECE)
      EPRM=ESEM-(ECM-ECE)
      STRM=PRST(EPRM,FPR,EPPR,FYP,N1)
      STRC=PRST(EPRC,FPR,EPPR,FYP,N1)
      STRT=PRST(EPRT,FPR,EPPR,FYP,N1)
      XPC=APR*STRC*2
      XPT=APR*STRT*2
      XPM=APR*STRM
      XP1=XP-XPC-XPT-XPM
      XM1=XM-(XPC*ARM)+(XPT*ARM)
      GO TO 60
   58 FPS=(FPSC*2)+(FPST*2)
      ECE=ECOMP(EO,FPS,APR,ATR,FCU)
      EPRC=ESEC-(ECC-ECE)
      EPRT=ESET-(ECT-ECE)
      STRC=PRST(EPRC,FPR,EPPR,FYP,N1)
      STRT=PRST(EPRT,FPR,EPPR,FYP,N1)
      XPC=APR*STRC*2
      XPT=APR*STRT*2.
      XP1=XP-XPC-XPT
      XM1=XM-(XPC*ARM)+(XPT*ARM)
      GO TO 60
   59 FPS=FPSC+FPST+FPSM
      ECE=ECOMP(EO,FPS,APR,ATR,FCU)
      EPRC=ESEC-(ECC-ECE)
      EPRT=ESET-(ECT-ECE)
      EPRM=ESEM-(ECM-ECE)
      STRC=PRST(EPRC,FPR,EPPR,FYP,N1)
      STRT=PRST(EPRT,FPR,EPPR,FYP,N1)
      STRM=PRST(EPRM,FPR,EPPR,FYP,N1)
      XPC=APR*STRC
      XPT=APR*STRT
      XPM=APR*STRM
      XP1=XP-XPC-XPT-XPM
      XM1=XM-(XPC*ARM)+(XPT*ARM)
      GO TO 60
   57 FPS=FPSC+FPST
      ECE=ECOMP(EO,FPS,APR,ATR,FCU)
      EPRC=ESEC-(ECC-ECE)
      EPRT=ESET-(ECT-ECE)
      STRC=PRST(EPRC,FPR,EPPR,FYP,N1)
      STRT=PRST(EPRT,FPR,EPPR,FYP,N1)
      XPC=APR*STRC
      XPT=APR*STRT
      XP1=XP-XPC-XPT
      XM1=XM-(XPC*ARM)+(XPT*ARM)
      GO TO 60
   56 FPS=FPSM
      ECE=ECOMP(EO,FPS,APR,ATR,FCU)
      EPRM=ESEM-(ECM-ECE)
      STRM=PRST(EPRM,FPR,EPPR,FYP,N1)
      XPM=APR*STRM
      XP1=XP-XPM
      XM1=XM
```

```
FORTRAN IV G LEVEL  21                    COMPIL              DATE = 51333            19/09/11

                GO TO 60
          60    CONTINUE
                RETURN
          55    XPI=XP
                XMI=XM
                RETURN
                END
```

```
FORTRAN IV G LEVEL  21                  MAIN               DATE = 81333         19/09/11
      C
      C
      C
            SUBROUTINE DFLECT (EXPL,XYM,DTA,R,C,KK,ENOM,TL,IM,IR,V,EM,DKN,RHO)
      C
      C
      C     THIS SUBROUTINE CALCULATES THE DEFLECTION SHAPE BY FINITE DIFFERENCE
      C     METHOD
      C
      C
            IMPLICIT REAL*8(A-H,O-Y)
            DIMENSION RHO(20),V(20),EM(20),DKN(20),E(30),VD(20)
            COMMON/AREA1/H
            RHOO=R
            DO 51 N=1,KK
            IF(N.EQ.1)GO TO 62
            IF(N.EQ.2) GO TO 63
            V(N)=(RHO(N-1)*(H**2))-V(N-2)+(2*V(N-1))
            GO TO 64
       63   V(2)=(RHO(N-1)*(H**2))+(2*V(N-1))
       64   EM(N)=XYM-(EXPL*V(N))
            GO TO 65
       62   V(1)=0.5*((H**2)*RHOO)
            EM(1)=XYM-(EXPL*V(1))
            RHO9=RHOO
            EA1=R*C
            GO TO 66
       65   CONTINUE
            RHO9=RHO(N-1)
       66   PPKD=EXPL
            EMN=EM(N)
            YO=XYM/PPKD
            CALL SURFI(RHO9,EAI,RHOI,PPKD,EMN,XYM,R,IM,IR,TL,DKI)
            DKN(N)=DKI
            RHO(N)=RHOI
       51   CONTINUE
            DTA=V(KK)
            ENOM=EM(KK)
            DO 100 I=1,KK
            VD(I)=DTA-V(I)
      100   CONTINUE
            RETURN
            END
```

```
FORTRAN IV G LEVEL  21                MAIN                DATE = 91333          19/09/18
                C
                C
                C
                      SUBROUTINE GURFI(RHO9,E4I,RHOI,PPKD,EMN,XYM,R,IM,IR,TL,OKI)
                C
                C
                C     THIS NUMERICAL METHOD DETERMINES THE STRAIN DISTRIBUTION
                C     ALONG THE COLUMN LENGTH
                C
                C
                      IMPLICIT REAL*8(A-H,O-Y)
                      DIMENSION E(20)
                      RHO3=RHO9/2.
                      ECM3=E4I/2.
                      OK3=ECM3/RHO3
                      CALL COMPIL(RHO3,OK3,PP3,AM3,IM,IR,TL,XS2,E)
                      RHOI=RHO3
                      E4I=ECM3
                      DO 67 I=1,15
                      ALP=0.00001
                      BET=0.000000001
                      DPHI=(ALP*RHOI)+BET
                      DE4=(ALP*E4I)+BET
                      RHOI=RHOI+DPHI
                      ECM1=E4I
                      OK1=ECM1/RHOI
                      CALL COMPIL(RHOI,OK1,PP1,AM1,IM,IR,TL,XS2,E)
                      A4=(PP1-PP3)/DPHI
                      C4=(AM1-AM3)/DPHI
                      ECM2=E4I+DE4
                      RHO2=RHOI
                      OK2=ECM2/RHO2
                      CALL COMPIL(RHO2,OK2,PP2,AM2,IM,IR,TL,XS2,E)
                      B4=(PP2-PP3)/DE4
                      D4=(AM2-AM3)/DE4
                      DELE4=(EMN-AM3-((PPKD-PP3)*(C4/A4)))/(D4-(C4*(B4/A4)))
                      DELPI=(PPKD-PP3-(B4*DELE4))/A4
                      RHOI=RHOI+DELPI
                      E4I=E4I+DELE4
                      OKI=E4I/RHOI
                      CALL COMPIL(RHOI,OKI,PPI,AMI,IM,IR,TL,XS2,E)
                      IF(DABS(PPI-PPKD).LE.0.03) GO TO 56
                      GO TO 59
                56    IF(DABS(AMI-EMN).LE.0.03) GO TO 70
                59    CONTINUE
                      PP3=PPI
                      AM3=AMI
                67    CONTINUE
                70    CONTINUE
                      RETURN
                      END
```

```
FORTRAN IV G LEVEL  21                MAIN                DATE = 81333          19/09/11
              C
              C
              C
                    SUBROUTINE CAL1(DDT.DDC.DDM.R.C.XM.RHO.V.EM.DKN.TL)
              C
              C
              C     THIS SUBROUTINE CALCULATES THE CHANGE OF STRIN IN PRESTRESSED TENDONS
              C
              C
                    IMPLICIT REAL*8(A-H.O-Y)
                    DIMENSION RHO(20),V(20).EM(20).DKN(20).EEM(20).EIN(20).DK(20).DI
                   *(20)
                    COMMON/AREA13/VV(20).RRHO(20)
                    COMMON/AREA12/H
                    COMMON/AREA1/DD1.DD2.THK.KK
                    COMMON/AREA4/PR1.PR2.PR3.ACL
                    SUM1=0.0
                    SUM2=0.0
                    SUM3=0.0
                    CALL NUE(R.C.XM.RHO.V.EM.DKN.EEM.EIN.DK.DI)
                    KR=KK+1
                    DO   72 L=5.KR
                    S11=RRHO(L)
                    S3=DK(L)
                    S4=S3-PR1
                    S5=S3-PR3
                    S6=S3-PR2
                    SUM=S11*S4
                    SOM=S11*S5
                    SIM=S11*S6
                    SUM1=SUM1+SUM
                    SUM2=SUM2+SOM
                    SUM3=SUM3+SIM
               72   CONTINUE
                    DDC=SUM1/((KR-5)+1)
                    DDT=SUM2/((KR-5)+1)
                    DDM=SUM3/((KR-5)+1)
                    RETURN
                    END
```

```
FORTRAN IV G LEVEL  21                  MAIN                DATE = 81333        19/09/11

      C
      C
      C
            SUBROUTINE NUE(R.C.XM.RHO.V.EM.DKN.EEM.EIN.DK.DI)
      C
      C
      C     THIS SUBROUTINE CALCULATES THE STIFFNESS ALONG THE COLUMN LENGTH
      C
      C
            IMPLICIT REAL*8(A-H.O-Y)
            DIMENSION RHO(20).V(20).EM(20).DKN(20).EEM(20).EIN(20).DK(20).
           *DI(20)
            COMMON/AREA13/VV(20).RRHO(20)
            COMMON/AREA12/H
            COMMON/AREA1/DD1.DD2.THK.KK
            KR=KK+1
            VV(14)=0.0
            EEM(14)=XM
            RRHO(14)=R
            DI(1)=0.0
            DK(14)=C
            EIN(14)=XM/R
            DO 75 II=2.KR
            VV(II-1)=V(13)-V(14-(II-1))
            EEM(II-1)=EM(14-(II-1))
            RRHO(II-1)=RHO(14-(II-1))
            DI(II)=(II-1)*H
            DK(II-1)=DKN(14-(II-1))
            EIN(II-1)=EEM(II-1)/RRHO(II-1)
         75 CONTINUE
            RETURN
            END
```

```
FORTRAN IV G LEVEL  21                     MAIN              DATE = 91333          19/09/11
              C
              C
              C
                    SUBROUTINE COSINE(XP,XM,R,C,TL)
              C
              C
              C     THIS PROGRAMME CALCULATES APPROXIMATE DEFLECTIONS FOR
              C     ANALYSING THE FORCES IN PRESTRESSING TENDONS
              C
              C
                    IMPLICIT REAL*8(A-H,O-Y)
                    DIMENSION Y(20)
                    COMMON/AREA11/V1(20),EM1(20),RHO1(20),DKN1(20)
                    COMMON/AREA12/H
                    EPO=XM/XP
                    ECNA=-DCOS(DSQRT((R*(TL**2))/(4.*EPO)))*EPO
                    AL=DSQRT(((3.14**2)*EPO)/R)
                    DO 75  I=1,13
                    Y(I)=EPO*DCOS((3.14*I*H)/AL)
                    V1(I)=EPO-Y(I)
                    EM1(I)=XP*Y(I)
                    RHO1(I)=((3.14**2)/(AL**2))*EPO*DCOS((3.14*I*H)/AL)
                    DKN1(I)=C
               75   CONTINUE
                    RETURN
                    END
```

```
FORTRAN IV G LEVEL  21                ECOMP               DATE = 81333          19/09/11

 0001            FUNCTION ECOMP(E0,FPS,APR,ATR,FCU)
 0002            IMPLICIT REAL*8(A-H,O-Z)
 0003            ECOMP=((E0*2)-DSQRT(((E0*2.)**2)-(4.*(((FPS*APR)/(ATR*FCU))*(E0**
                1 2)))))/2.
 0004            RETURN
 0005            END
```

BIBLIOGRAPHY

1. Kloppel, K.V., and Goder, W.D., "Traglastversuche mit Ausbetonierten Stahlrohren and Aufstellung einer Bemessungsformel," Teil I & II, Der Stahlbau, 26 Jahrgang, Heft 1, Berlin, January, 1957, pp. 1-50.

2. Gardner, N.J., and Jacobson, E.R., "Structural Behaviour of Concrete-Filled Steel Tubes," Journal of American Concrete Institute, Title No. 64-38, July, 1967, pp. 404-412.

3. Richart, F.E., Brandtzaeg, A., and Brown, R.L., "A Study of the Failure of Concrete Under Combined Compressive Stresses," Bulletin No. 185, Engineering Experiment Station, University of Illinois, Urbana, 1928.

4. Furlong, R., "Strength of Steel-Encased Concrete Beam-Columns," Journal of the Structural Division, ASCE, October, 1967, pp. 113-124, Discussion April, 1969, Jan., 1969, Aug., 1968, March 1968 and Oct., 1968.

5. Furlong, R., "Design of Steel-Encased Concrete Beam-Columns," Journal of Structural Division, Proc. ASCE, Jan., 1968, pp. 267-281.

6. Gardner, N.J., "Use of Spiral Welded Steel Tubes in Pipe Columns," Journal of American Concrete Institute, Nov., 1968, pp. 937-942.

7. Neogi, P.K., Sen , H.K., and Chapman, J.C., "Concrete-Filled Tubular Steel Columns Under Eccentric Loading," The Structural Engineer, No. 5, Vol. 47, May 1969, pp. 187-195.

8. Knowles, R.B., and Park, R., "Strength of Concrete-Filled Steel Tubular Columns," Journal of Structural Division, ASCE, Dec., 1969, pp. 2565-2586.

9. Knowles, R.B., and Park, R., "Axial Load Design for Concrete-Filled Steel Tubes," Journal of Structural Division, ASCE, Oct., 1970, pp. 2126-2151, Disc., Feb., 1972, pp. 504.

10. Gardner, N.J., "Design of Pipe Columns," Transactions of the Engineering Institute of Canada, Vol. 13, No. A-3, March 1970, pp. I-VI.

11. Chen, W.F., and Rentschler, G.P., "Ultimate Strength of Concrete-Filled Steel Tubular Beam-Columns," Regional Conference on Tall Buildings, ASCE-IABSE Joint Committee, Madrid, Spain, pp. 161-180, September 17-19, (1973).

12. Chen, W.F., and Chen, C.H., "Analysis of Concrete-Filled Steel Tubular Beam-Columns," International Association for Bridge and Structural Engineering, Vol. 33-11, pp. 37-52, September, 1973.

13. Tomii, M., Matsui, C., and Sakino, K., "Concrete-Filled Steel Tube Structures," National Conference on the Planning and Design of Tall Buildings, Aug.,1973, Tokyo, Japan.

14. Yamada, M., "Cyclic Bending of Concrete-Filled Steel Tube Beam-Columns," National Conference on the Planning and Design of Tall Buildings, Aug., 1973, Tokyo, Japan.

15. Bridge, R.Q., "Concrete-Filled Steel Tubular Beam-Columns," Civil Engg. Transactions, The Institution of Engineers, Australia, 1976.

16. Ghosh, R.S., "Strengthening of Slender Hollow Steel Columns by Filling with Concrete," Canadian Journal of Civil Engineering, Vol. 4, No. 2, June, 1977, pp. 127-133.

17. Tomii, M., Yoshimura, K., and Moroshita, Y., "Experimental Studies on Concrete-Filled and Tubular Columns under Concentric Loading," International Colloquium on Stability of Structures under Static and Dynamic Loads, Proc., Washington, D.C., May 17-19, 1977, Published by ASCE, New York, N.Y., 1977, pp. 718-741.

18. d'Huart, J., "Design of Concrete Filled HSS Columns," International Symposium on Hollow Structural Sections, Toronto, Canada, May 25, 1977, pp. 1-18.

19. Ramamurty, L.N., and Srinivasan, C.N., "Behaviour of Concrete-Infilled Tubular Columns," Institution of Engineers (India), Civil Engg., Vol. 58, May, 1978, pp. 309-316.

20. Virdi, K.S., and Dowling, P.J., "Bond Strength in Concrete-Filled Steel Tubes," IABSE, March, 1980.

21. Brady, F.J., Cran, J.A., and Keen, R.G., "Hollow Structural Sections, The State of the Art," Canadian Society of Civil Engineers Conference, Fredericton, N.B., Canada, 1981.

22. ______________, "Stelco Design Manual," Stelco, Inc., Hamilton, Ontario, Canada, 1981.

23. Breckenridge, R.A., "A Study of the Characteristics of Prestressed Concrete Columns," Report 18-6, Engineering Center, University of Southern California, Los Angeles, Calif., April 1953.

24. Ozell, A.M., and Jernigan, A.M., "Some Studies on the Behaviour of Prestressed Concrete Columns," University of Florida, Technical Progress Report No. 3, July, 1956, Florida Engg., and Industrial Experiment Station.

25. Zia, P., "Ultimate Strength of Slender Prestressed Columns," Technical Paper Series No. 131, Florida Engg. and Industrial Experiment Station, University of Florida, Gainesville, Fla., July, 1957.

26. Lin, T.Y., and Itaya, R., "A Prestressed Concrete Column Under Eccentric Loading," Journal of Prestressed Concrete Institute, V. 2, Dec. 1957.

27. Brown, K.J., "The Ultimate Load Carrying Capacity of Prestressed Concrete Columns Under Direct and Eccentric Loading," Civil Engineering and Public Works Review (U.K.), Papers No. 705, 706, 707, Apr., May and June, 1965.

28. Hall, A.S., "Buckling of Prestressed Columns," Construction Review (U.K.), June, 1963, pp. 27-33.

29. Itaya, R., "Design and Uses of Prestressed Concrete Columns," Journal of Prestressed Concrete Institute, Vol. 10, No. 3, June, 1965.

30. Aroni, Samuel, "The Strength of Slender Prestressed Concrete Columns," Journal of the Prestressed Concrete Institute (PCIJ) Vol. 13, No. 2, April, 1968, pp. 19-33.

31. Zia, P., and Moreadith, F.L., "Ultimate Load Capacity of Prestressed Concrete Columns," Journal of the American Concrete Institute, Vol. 63, No. 7, July, 1966, pp. 767-788.

32. Zia, P., and Guillermo, E.C., "Combined Bending and Axial Load in Prestressed Concrete Columns," Journal of the Prestressed Concrete Institute, Vol. 12, No. 3, June, 1967, pp. 52-59.

33. Anderson, A.R., and Moustafa, S.E., "Ultimate Strength of Prestressed Concrete Piles and Columns," Journal of American Concrete Institute, Title No. 67-37, August, 1970, pp. 620-635.

34. Mikhailov, V.V., "Design of Slender Prestressed Concrete Columns Based on Stability Criteria," PCIJ, Sept.-Oct. 1972, pp. 49-55.

35. Nathan, N.D., "Slenderness of Prestressed Concrete Beam-Columns," PCIJ, Nov.-Dec., 1972, pp. 45-57.

36. Al-Rawi Ghassan, A., "Circular Prestressed Concrete Columns Subject to Concentric Forces, Bending Moments, and Torsion," Ph.D. Thesis, The Univ. of Oklahoma, 1971.

37. Lohr, W.S., "Concrete Encased in Steel Shells Proposed," Engineering News - Record, Vol. 113, December 13, 1934, pp. 760-762.

38. Barnard, P.R., "Researches into the Complete Stress-Strain Curve for Concrete," Mag. of Conc. Research, Vol. 16, No. 49, December, 1964.

39. Hognestad, E.A., "A Study of Combined Bending and Axial Load in Reinforced Concrete Members," Bulletin No. 399, University of Illinois Engineering Experiment Station, Urbana, Illinois, 1951.

40. Gurfinkel, G., and Robinson, A., "Determination of Strain Distribution and Curvature in a Reinforced Concrete to Bending Moment and Longitudinal Load," Journal of American Concrete Institute, Title No. 64-37, July, 1967, pp. 398-402.

41. Newmark, N.M., "Numerical Procedures for Computing Deflections, Moments and Buckling Loads," Journal of Structural Division, ASCE, Transactions, May, 1942.

42. ________________, "Design and Control of Concrete Mixtures," Canadian Portland Cement Association, Engg. Bulletin, Metric Edition, 1979.

VITA AUCTORIS

MOKKARALA VENKATA PRAKASH

The author was born on March 15, 1957, in Vizianagaram, India. In 1973, he completed his secondary school education and joined the Department of Civil Engineering, Andhra University, Visakhapatnam (INDIA). In 1978, he graduated from Andhra University with a degree of Bachelor of Civil Engineering. Then he spent more than one year working as a Design Engineer with Tata Consulting Engineers, Bombay.

In 1979, he joined the Master's program in Civil Engineering Department, University of Windsor, Windsor, Ontario, Canada.